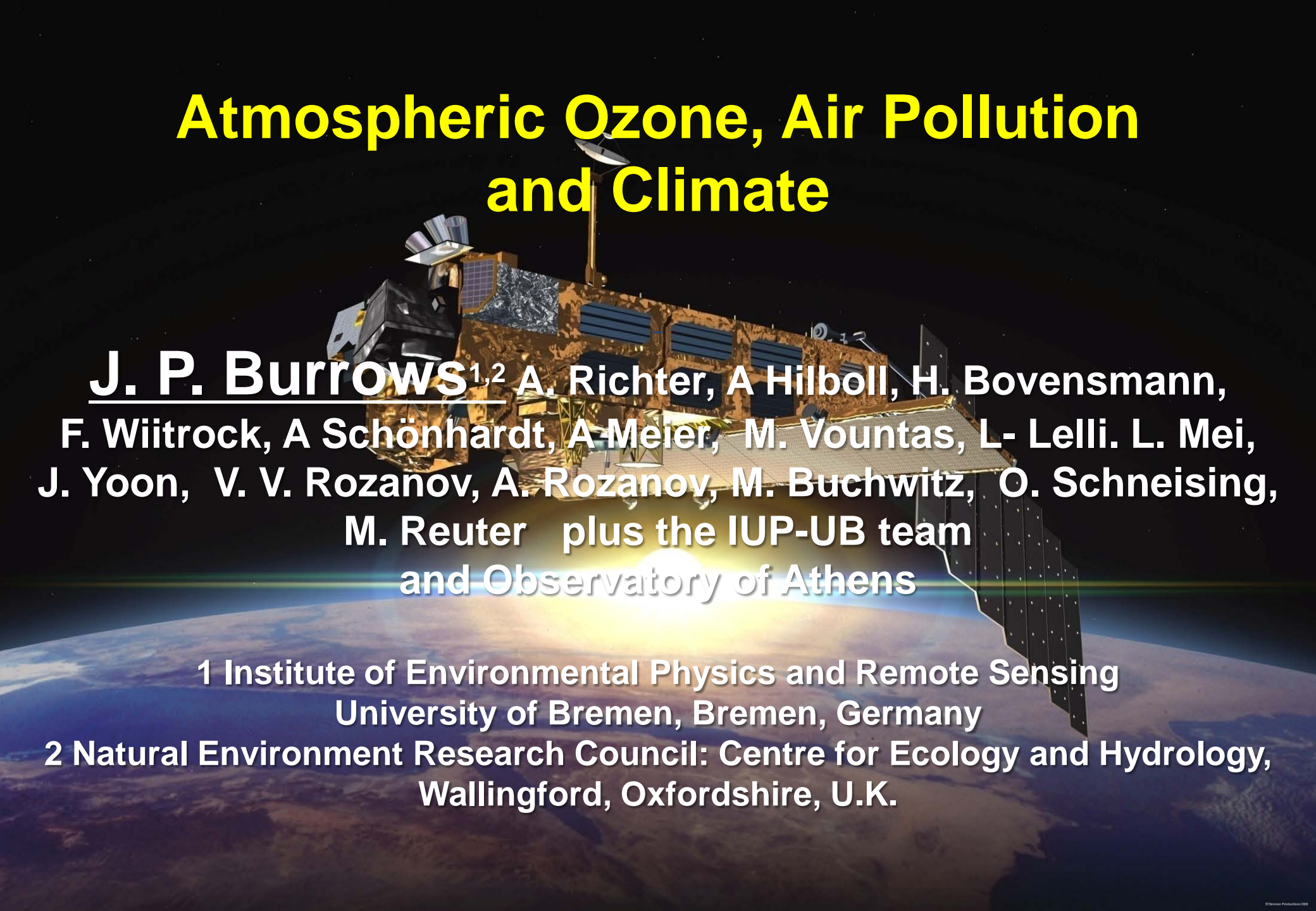


Atmospheric Ozone, Air Pollution and Climate

A detailed illustration of a satellite in orbit above the Earth. The satellite is a complex structure with various instruments, solar panels, and antennas. The Earth's surface is visible below, showing continents and oceans. The sun is positioned behind the satellite, creating a bright glow and lens flare effects across the scene.

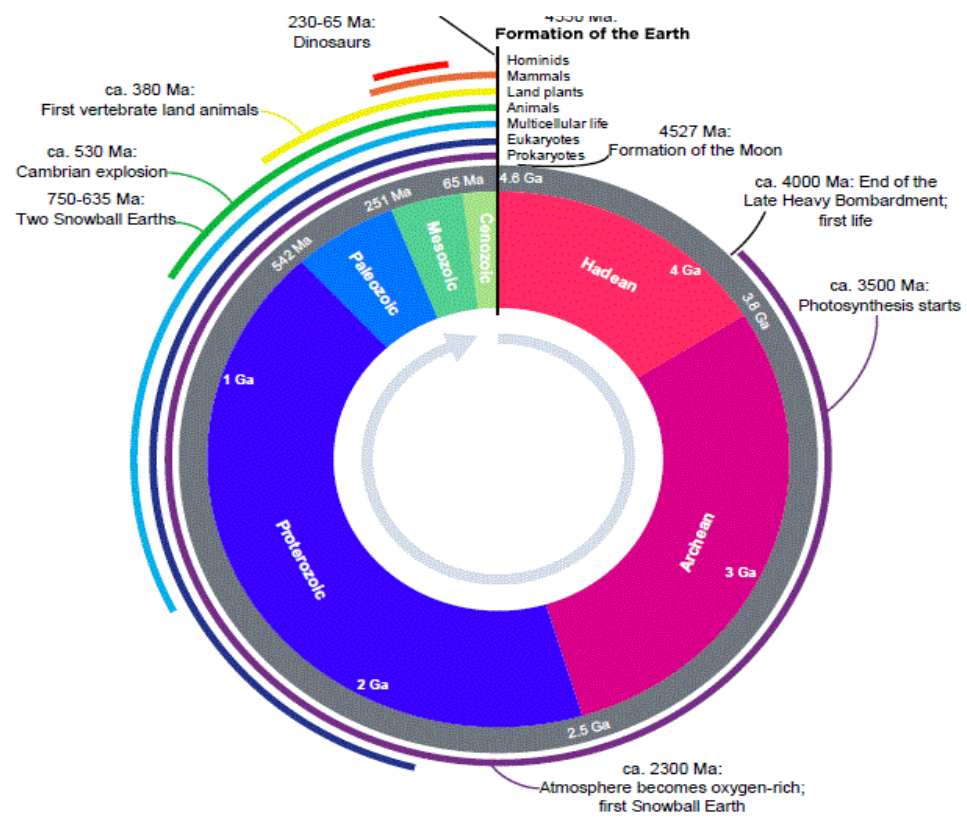
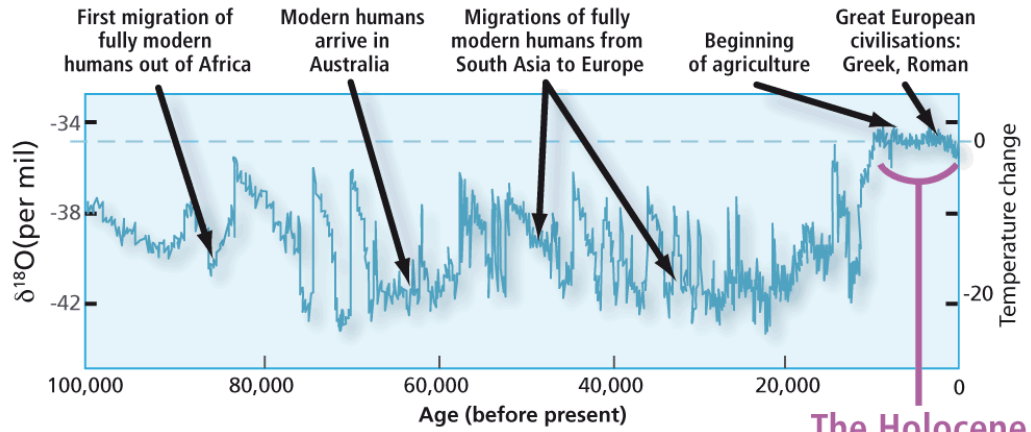
J. P. Burrows^{1,2} A. Richter, A Hilboll, H. Bovensmann,
F. Witrock, A Schönhardt, A Meier, M. Vountas, L. Lelli, L. Mei,
J. Yoon, V. V. Rozanov, A. Rozanov, M. Buchwitz, O. Schneising,
M. Reuter plus the IUP-UB team
and Observatory of Athens

1 Institute of Environmental Physics and Remote Sensing
University of Bremen, Bremen, Germany

2 Natural Environment Research Council: Centre for Ecology and Hydrology,
Wallingford, Oxfordshire, U.K.

Geological Time Scales

EON	ERA	PERIOD	EPOCH	Ma		
Phanerozoic	Cenozoic	Quaternary	Holocene		0.011	
			Pleistocene	Late	0.8	
				Early	2.4	
		Tertiary	Neogene	Pliocene		3.6
				Late	5.3	
				Early	11.2	
			Paleogene	Miocene		16.4
				Late	23.0	
				Early	28.5	
		Eocene	Late	34.0		
			Middle	41.3		
			Early	49.0		
		Paleocene	Late	55.8		
			Early	61.0		
			Early	65.5		
	Mesozoic	Cretaceous	Late	99.6		
			Early	145		
		Jurassic	Late	161		
			Middle	176		
		Triassic	Early	200		
			Late	228		
	Paleozoic	Permian	Middle	245		
			Early	251		
		Pennsylvanian	Late	260		
			Middle	271		
		Mississippian	Early	299		
			Late	306		
		Devonian	Early	311		
			Middle	318		
		Silurian	Late	326		
			Early	345		
		Ordovician	Middle	359		
			Early	385		
	Cambrian	Late	397			
		Early	416			
Proterozoic	Neoproterozoic (Z)	Late	419			
		Middle	423			
		Early	428			
Archean	Mesoproterozoic (Y)	Late	444			
		Middle	488			
		Early	501			
Hadaean	Paleoproterozoic (X)	Late	513			
		Middle	542			
		Early	1000			
Precambrian	Proterozoic	Late	1600			
		Early	2500			
Precambrian	Archean	Late	3200			
		Early	4000			

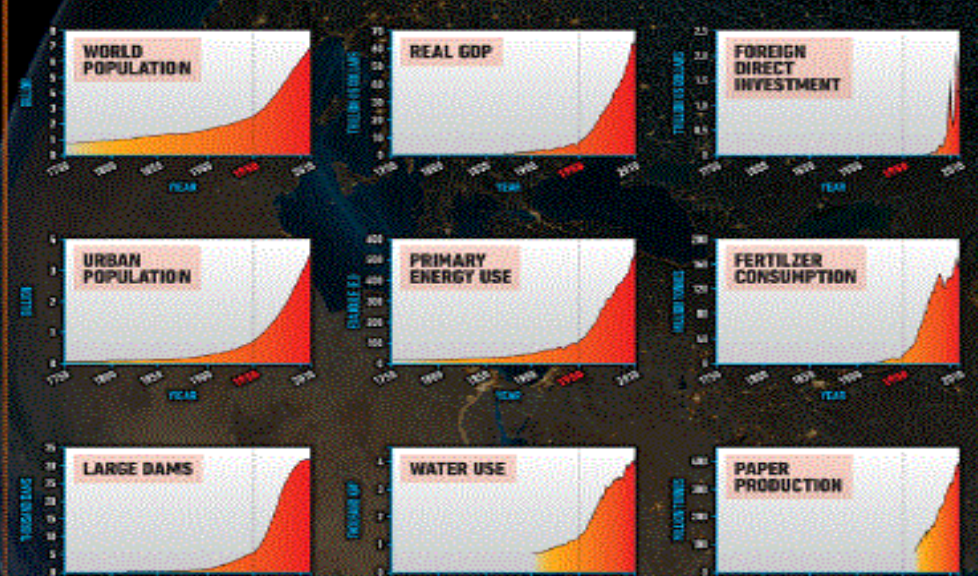


The Anthropocene

THE GREAT ACCELERATION

In September 2015 the nations of the world will meet to agree on Sustainable Development Indicators will be essential to assess progress

SOCIO-ECONOMIC TRENDS



EARTH SYSTEM TRENDS

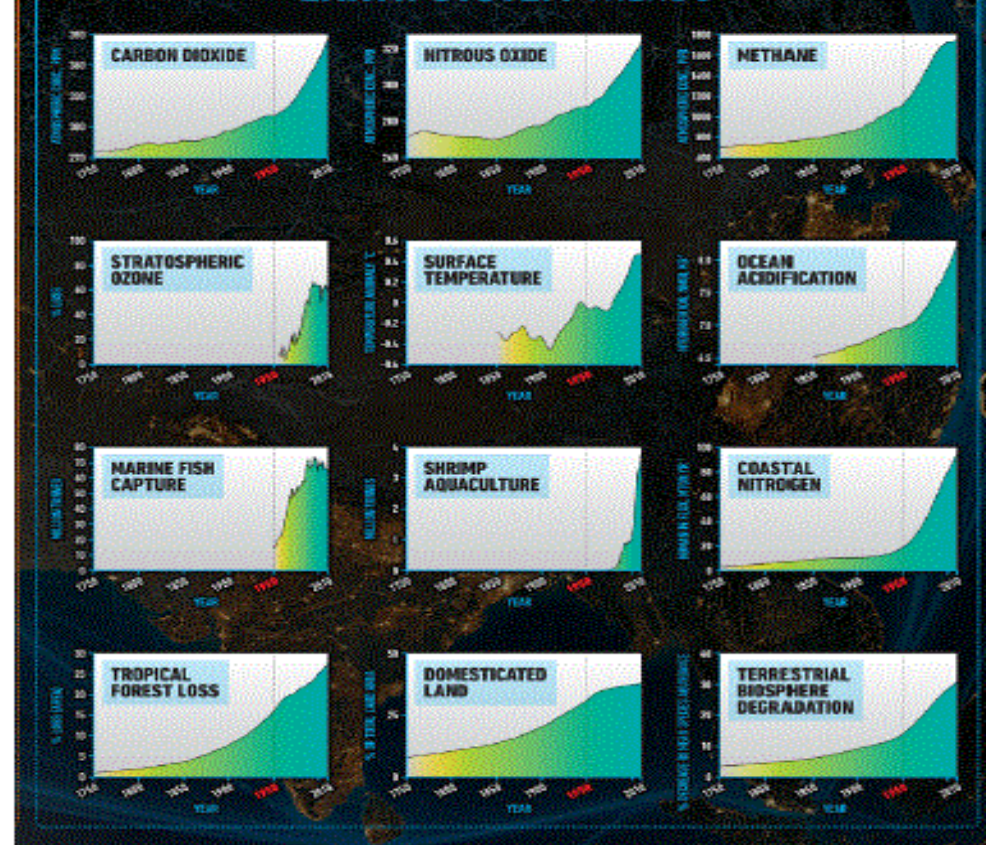


Figure 2: Twelve Earth system trends from 1750 to present.

Why observe the atmosphere from space?

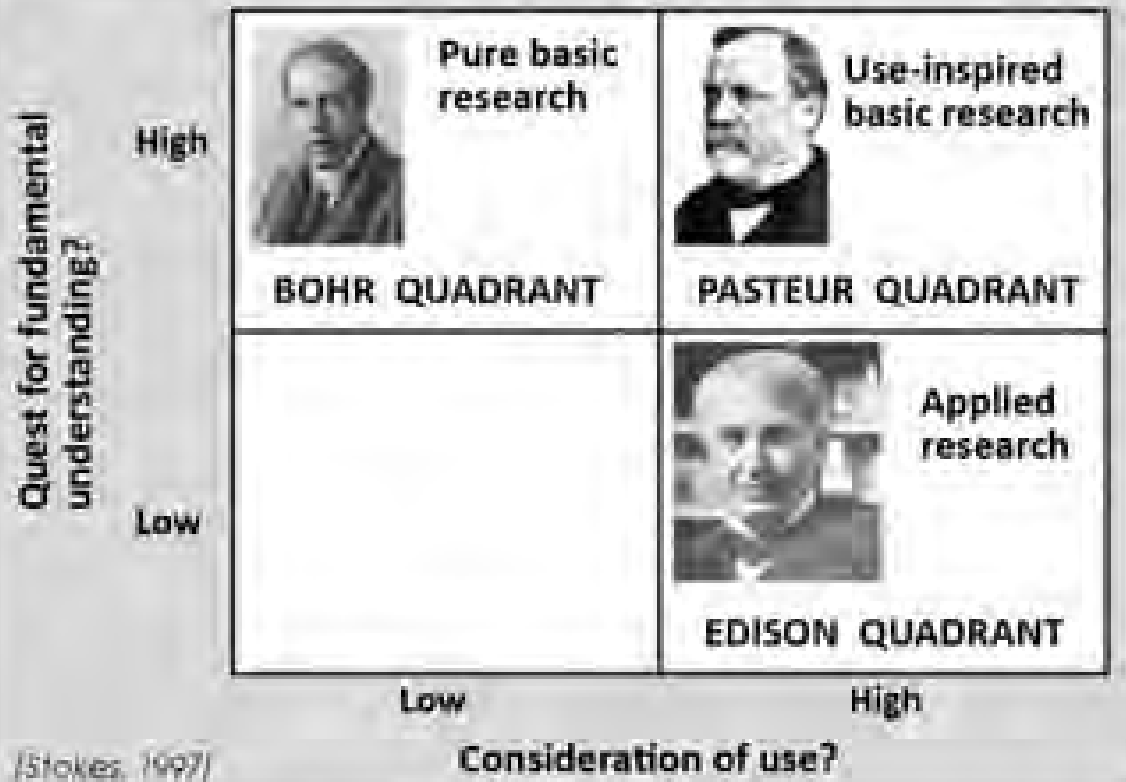
Earth has entered
and P. J. Crutzen

From the Neolithic
rose from 4M to
Dramatic changes
emissions since
Energy supplied
=> Release of

- ⇒ Global transport and land use change
- ⇒ Climate Change
- ⇒ Global destruction

- ⇒ It is **impossible**
- ⇒ Environmental/Climate
- ⇒ Evidence based

PASTEUR'S QUADRANT



USE-INSPIRED RESEARCH: to pursue fundamental understanding but motivated by a question of use

Figure 1

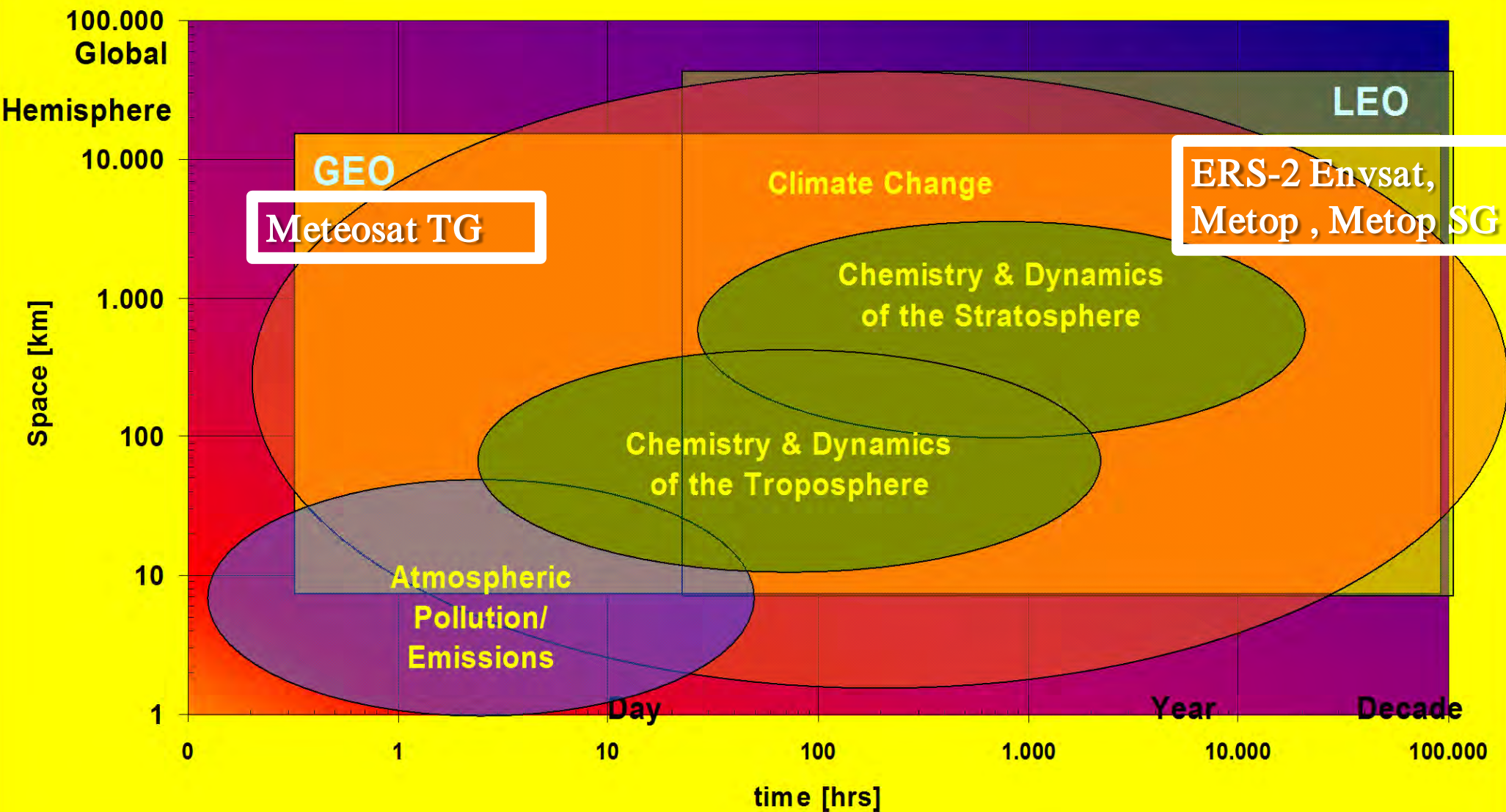
Stoermerging!



image: NASA

not measured!!

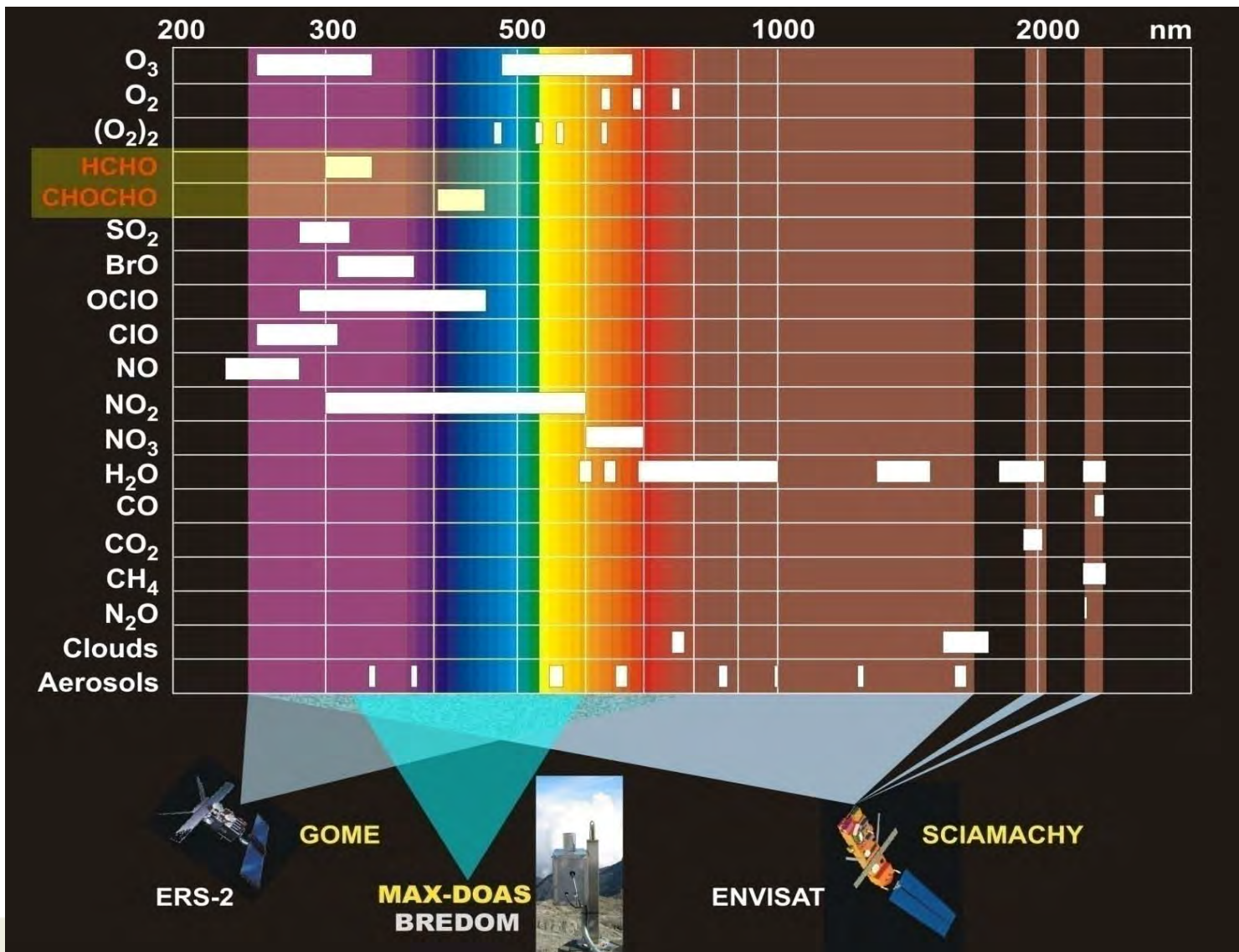
Spatial and Temporal Scales relevant for measurements from LEO and GEO



European LEO and GEO Passive Remote Sensing of trace constituents in the Anthropocene - Some Relevant History

- 1984-1988** Development and Submission to ESA for POEM/ Envisat AO, of SCIAMACHY (SCanning Imaging Absorption spectroMeter for Atmospheric CHartography) concept Burrows et al – hunting light
- 1988** Proposal of SCIA-mini for ERS-2 later descoped to GOME
- 1989** Selection of SCIAMACHY for ENVISAT
- 1990** Selection of GOME for ERS-2
- 1995** Launch of GOME 20.04.1995
- 1998** Proposal of GeoSCIA IUP/IFE-UB to ESA EEM-1
- 2002** Proposal of GeoSCIA++ UV-VIS-NIR-SWIR-TIR/Ligthning/firto ESA EEM-2
- 2002** Launch of SCIAMACHY on ENVISAT 28.02 2002
- 2002** Proposal of GeoTROPE UV-VIS-NIR-SWIR-TIR to ESA EEM-3
- 2004/5** Proposal of GeoSCIA-R and GeoSCIA-Lite
- 2006** EUMESAT Post Metop Committee recommends GOME-2 follow on UVNS
- 2006** Methane and carbon dioxide Mapper MaMap 01– Aircraft - UB
- 2006** EU Copernicus funds UVNS/Sentinel 5 Metop Second Generation
- 2006** Launch of GOME-2 on MetOp A
- 2008** CarbonSat and CarbonSat Constellation studies at UB - SCIA Heritage
- 2010** CarbonSat selected for ESA EE8 Phase AB1 Studies
- 2011** Start of SCIA-ISS studies UB NICT / Decommssioning of ERS-2
- 2012** Loss of Envisat 9th April
- 2012** Launch of GOME-2 on Metop-B 17th September
- 2013** Sentinel 5 agreed for Metop Second Generation 2020- 2034
- 2015** September ESA decision either CarbonSat or FLEX for ESA EE8????

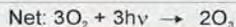
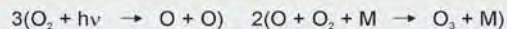
SCIAMACHY: Target Molecules



Ozone Production & Catalytic Destruction



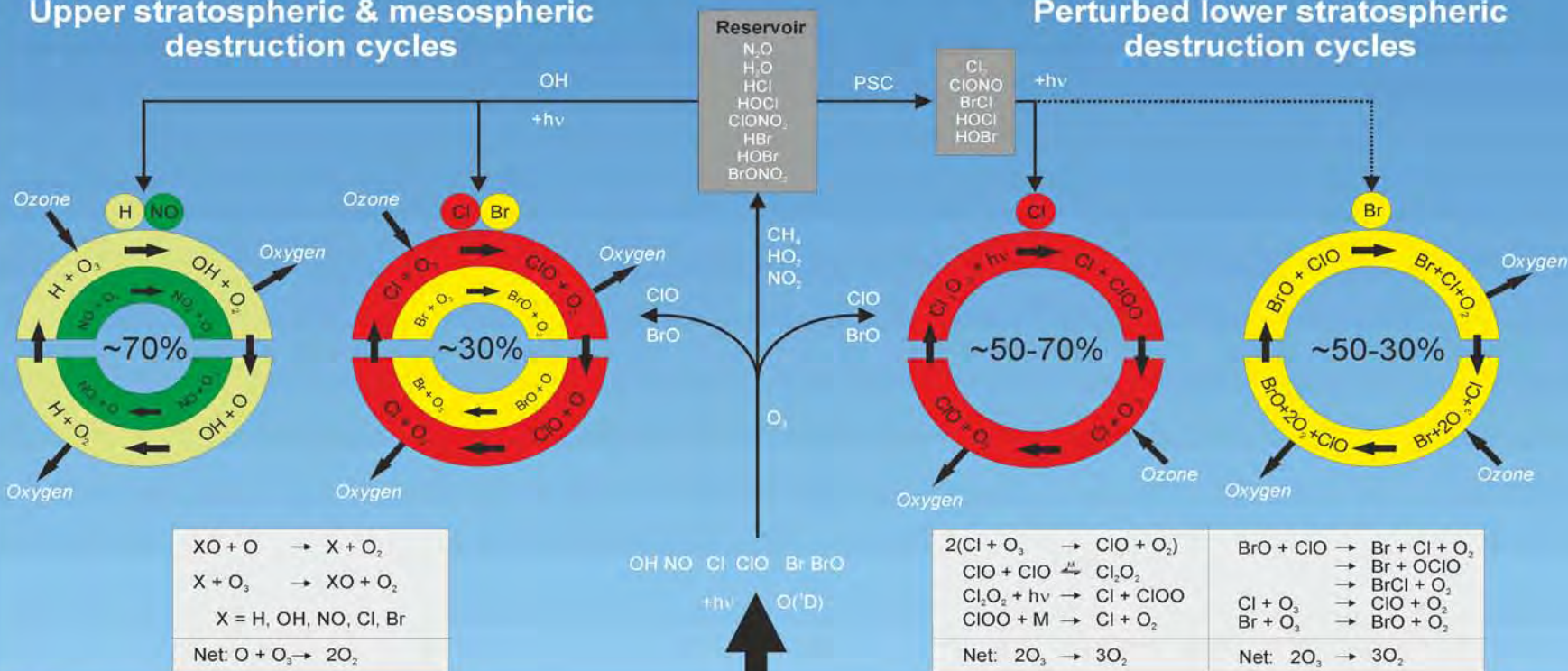
Ozone Production



Upper stratospheric & mesospheric destruction cycles

Perturbed lower stratospheric destruction cycles

Stratosphere



Tropopause

Troposphere

Chemistry

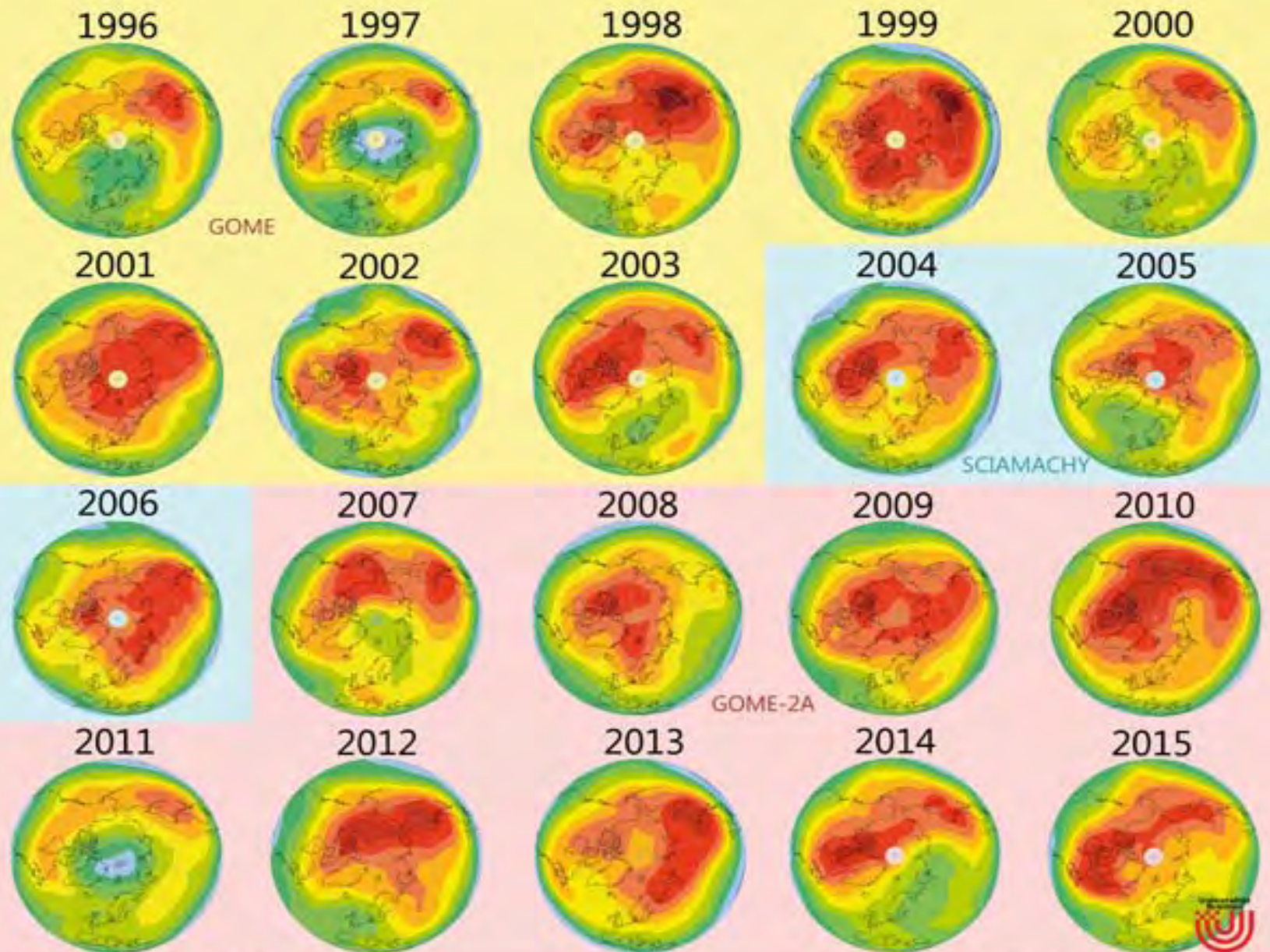
Dynamics

Transport Trop.-Strat. Exchange

CFC, Halons
H₂O, N₂O

Tropospheric Emission
(natural & anthropogenic)



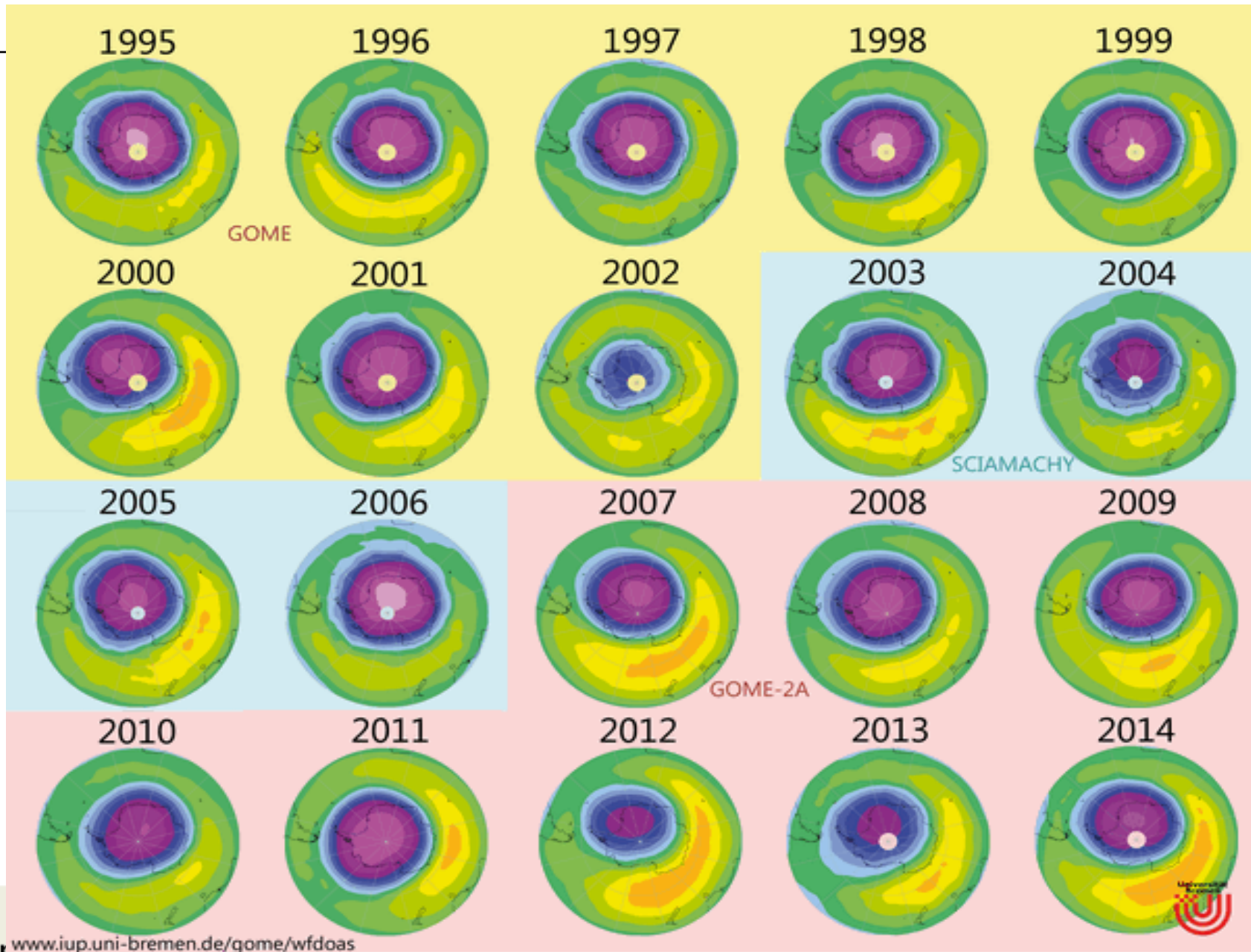


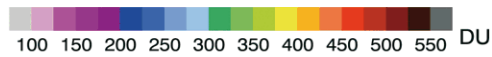
www.iup.uni-bremen.de/gome/wfdoas



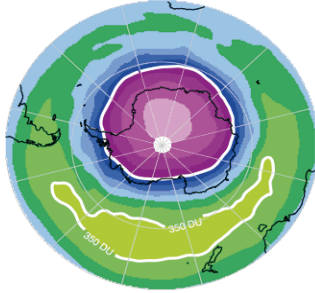
NH March total ozone
GOME/-2 & SCIAMACHY



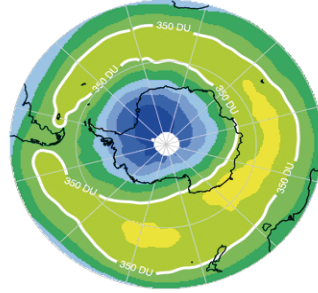




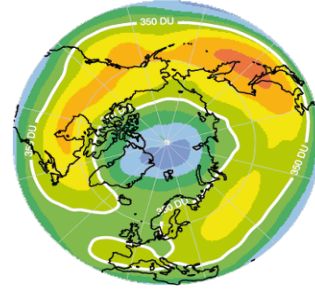
Oct. 2006



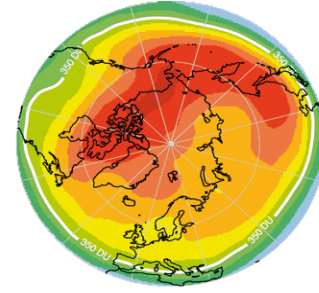
Oct. 2002



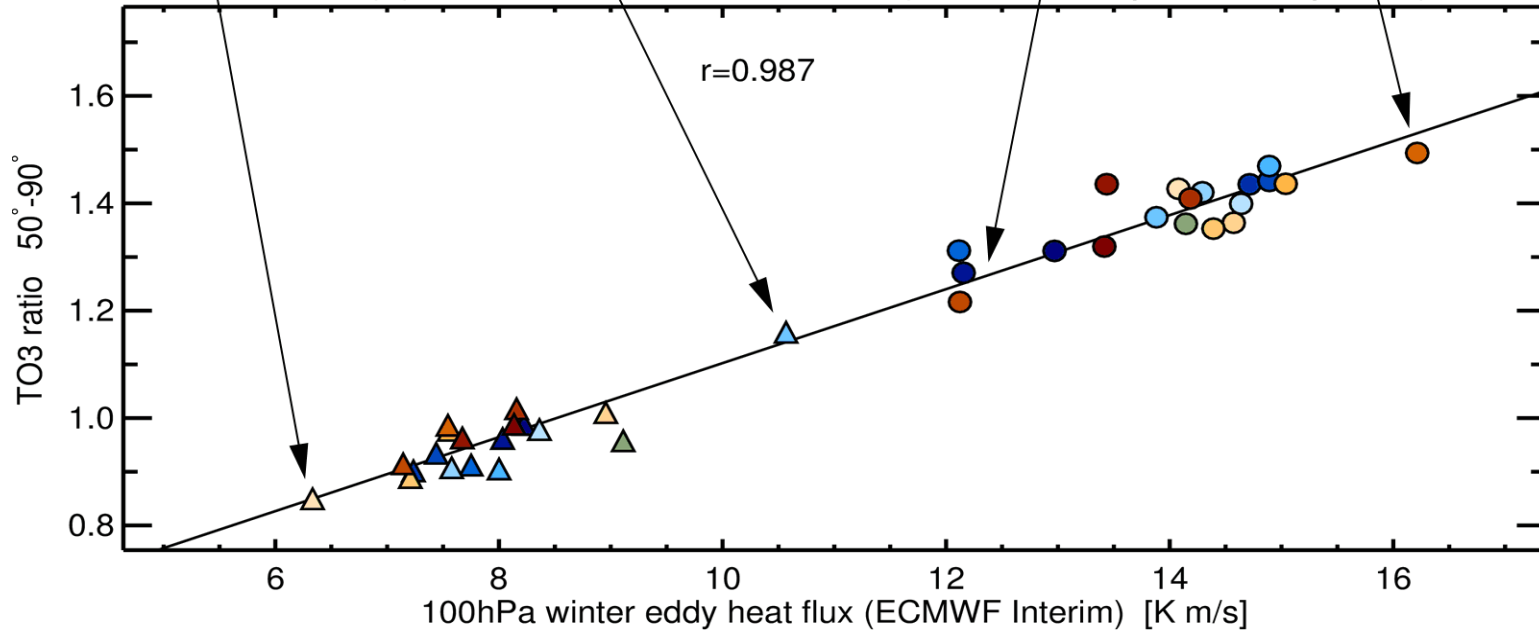
Mar. 2011



Mar. 2010



GOME(2)/SCIAMACHY TO3 ratios (NH: Mar/Sep, SH: Sep/Mar)



1996 1997 1998 1999
 2000 2001 2002 2003
 2004 2005 2006 2007
 2008 2009 2010 2011
 2012 2013 2014

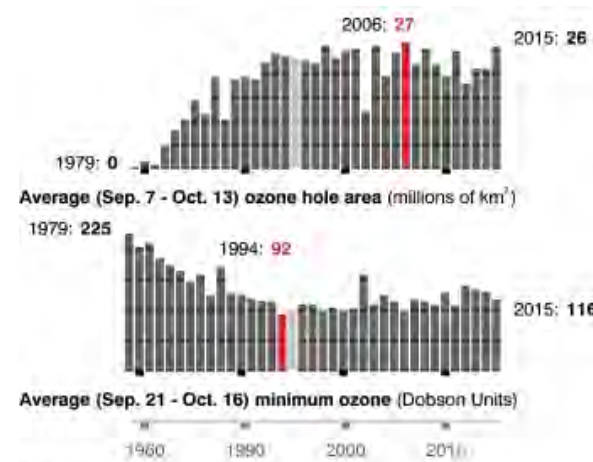
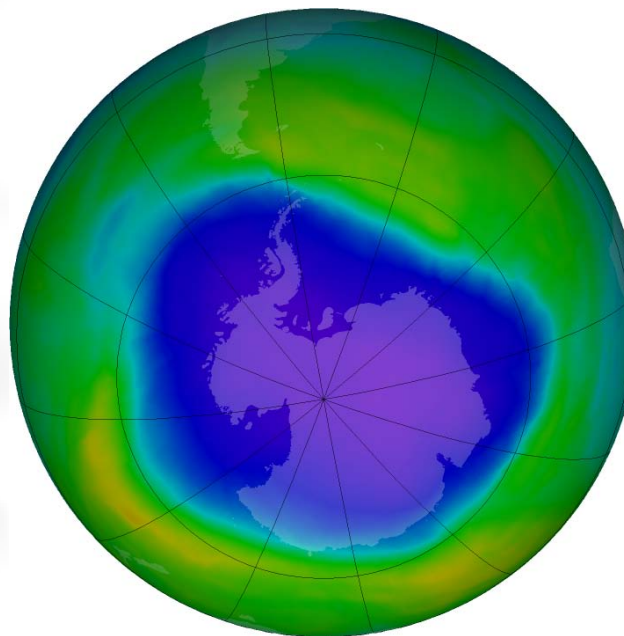
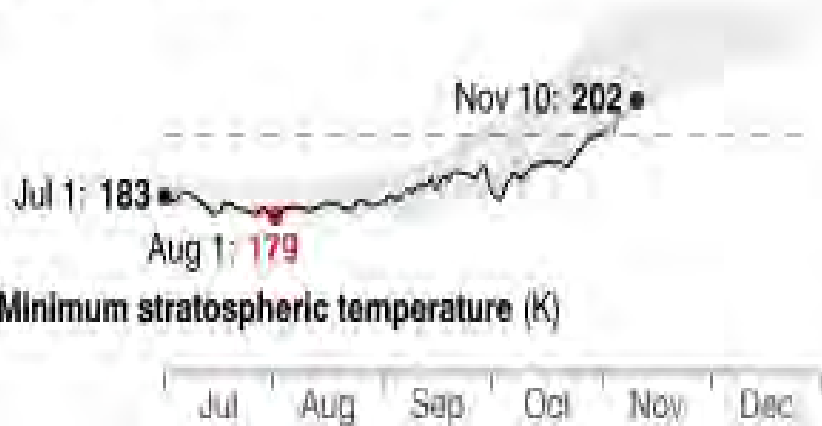
1995/1996 1996/1997 1997/1998 1998/1999
 1999/2000 2000/2001 2001/2002 2002/2003
 2003/2004 2004/2005 2005/2006 2006/2007
 2007/2008 2008/2009 2009/2010 2010/2011
 2011/2012 2012/2013 2013/2014

Update Weber et al. 2011, WMO 2014

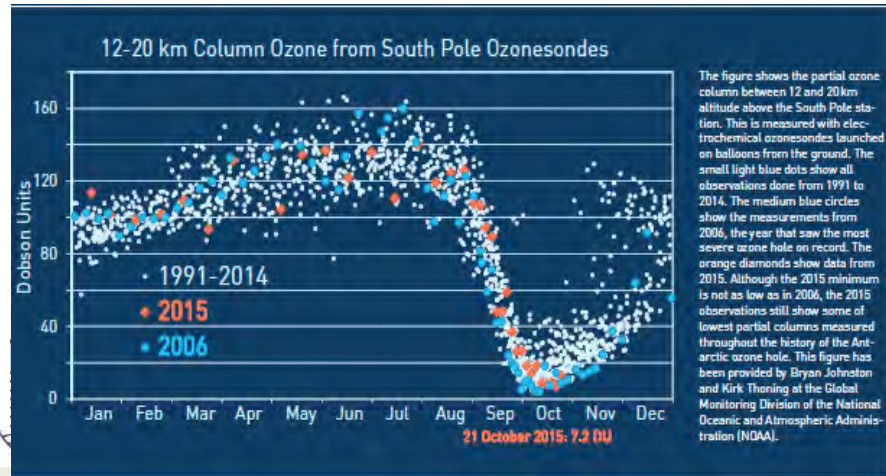


Ozone hole above Antarctica 2015

30 October 2015



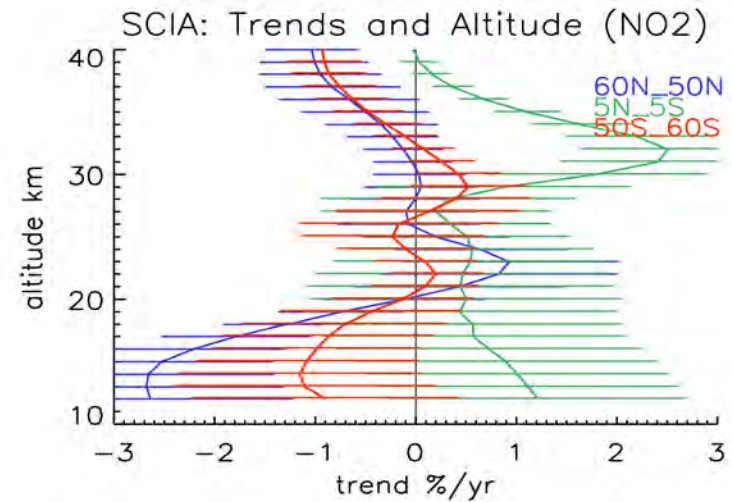
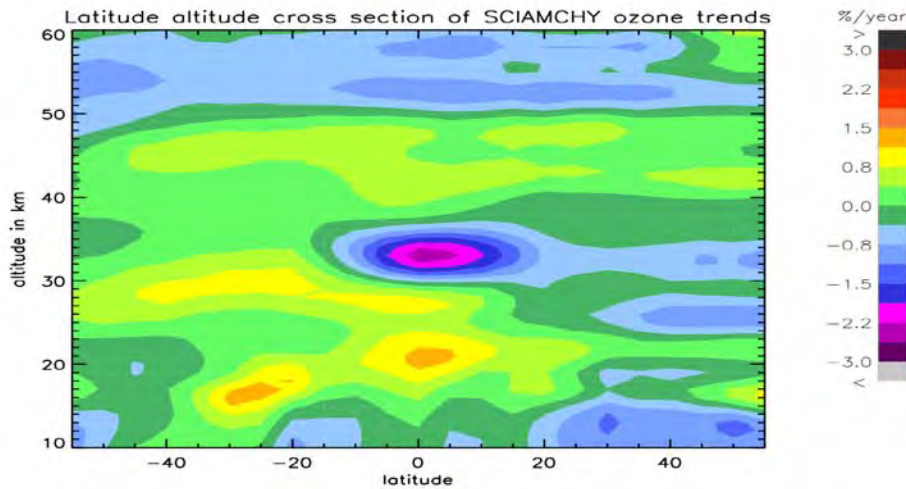
Note: No data were acquired during the 1995 season



The figure shows the partial ozone column between 12 and 20 km altitude above the South Pole station. This is measured with electrochemical ozonesondes launched on balloons from the ground. The small light blue dots show all observations done from 1991 to 2014. The medium blue circles show the measurements from 2006, the year that saw the most severe ozone hole on record. The orange diamonds show data from 2015. Although the 2015 minimum is not as low as in 2006, the 2015 observations still show some of the lowest partial columns measured throughout the history of the Antarctic ozone hole. This figure has been provided by Bryan Johnston and Kirk Thoning at the Global Monitoring Division of the National Oceanic and Atmospheric Administration (NOAA).

Latitude-altitude dependence of ozone trends

Impact of SST / T-hiatus on BDC



- minimum in the tropical 30-35 km range related slowing BDC and changing NO_x
Gebhardt et al 2012 OQS and ACP 2013 and Aschmann et al ACP 2014

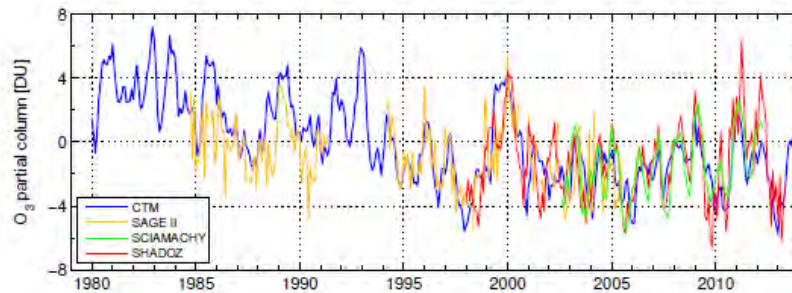


Fig. 2. Observed and simulated tropical (20°N–20°S) LS O₃ partial columns (17–21 km). Anomalies are deviations from the modelled 1980–2013 averages.

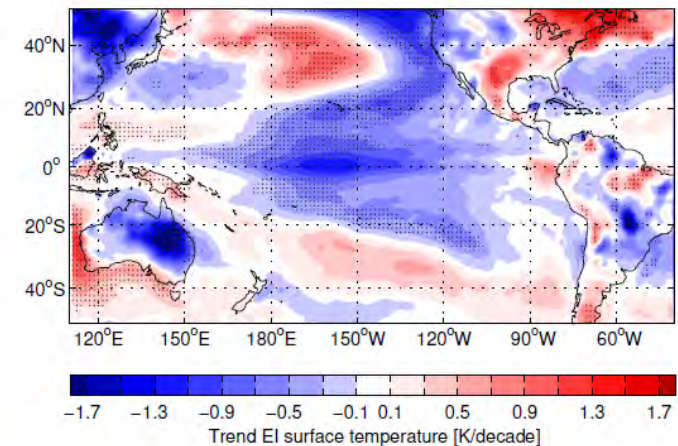
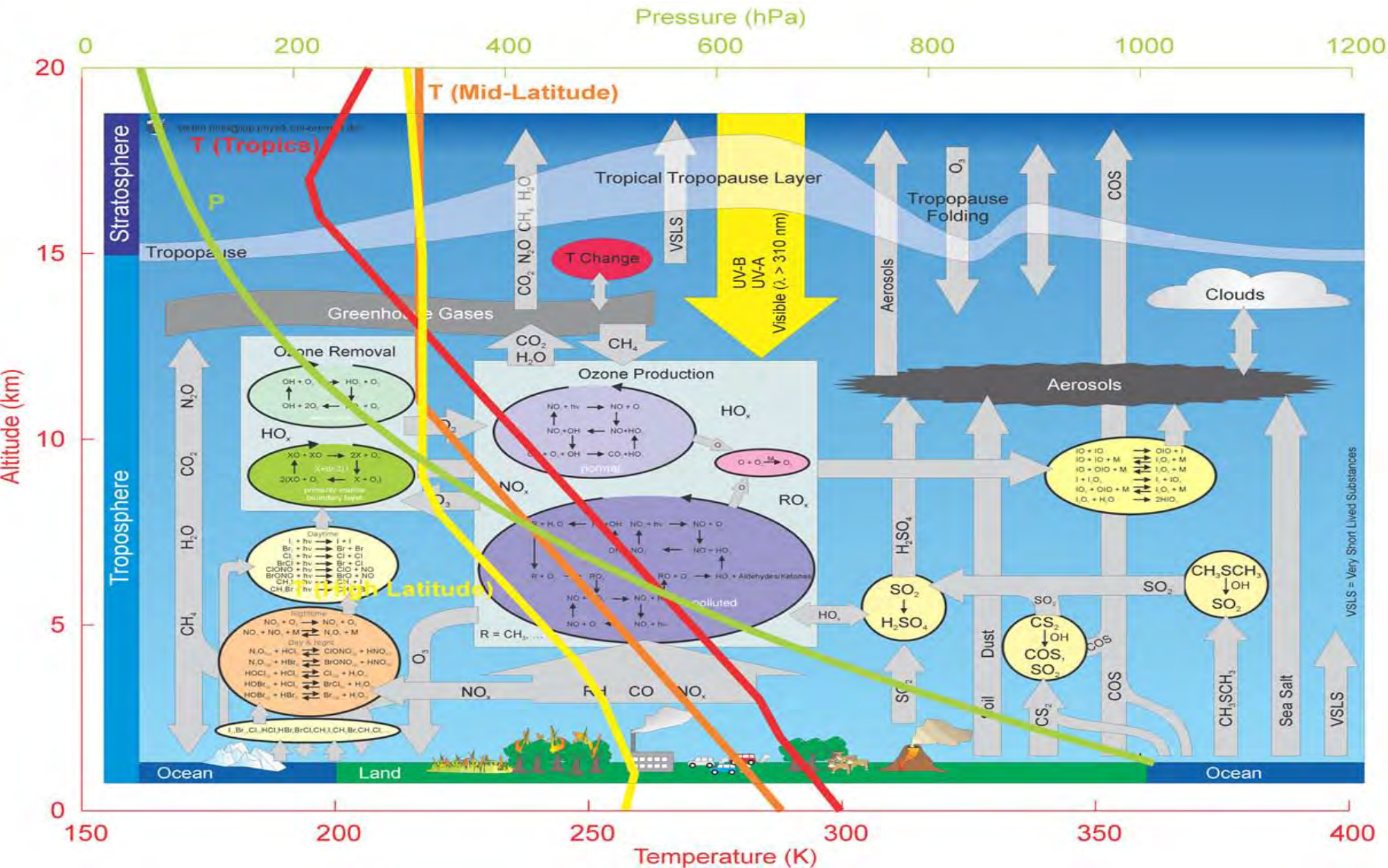


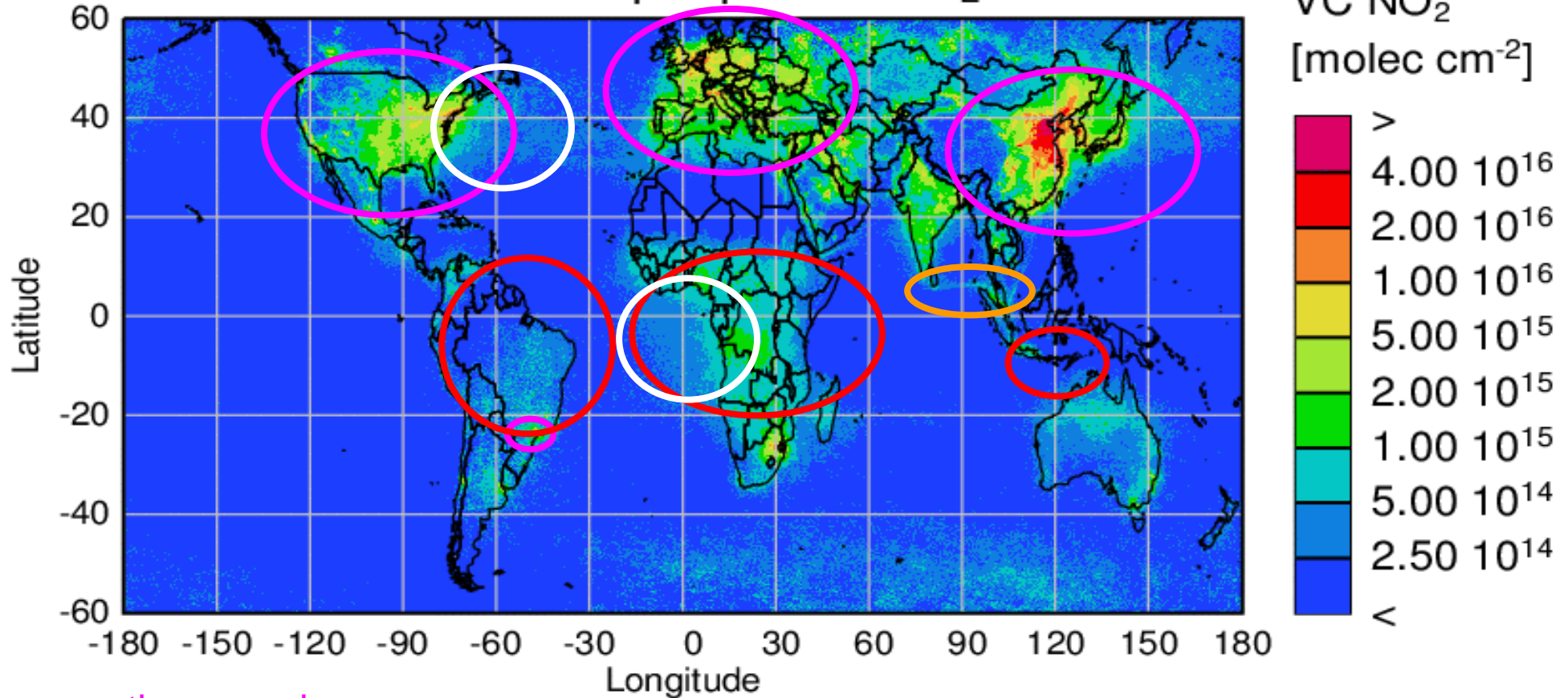
Fig. 5. Linear trends of El surface temperature from 2002–2013. Stippling indicates where the trend exceeds the 95% confidence threshold. Setup adapted from Kosaka and Xie (2013).

Some Key Processes in Global Tropospheric Chemistry/ Chemical Weather ~ 2014



Tropospheric NO₂ and Sources?

SCIAMACHY tropospheric NO₂ 2011



anthropogenic
pollution

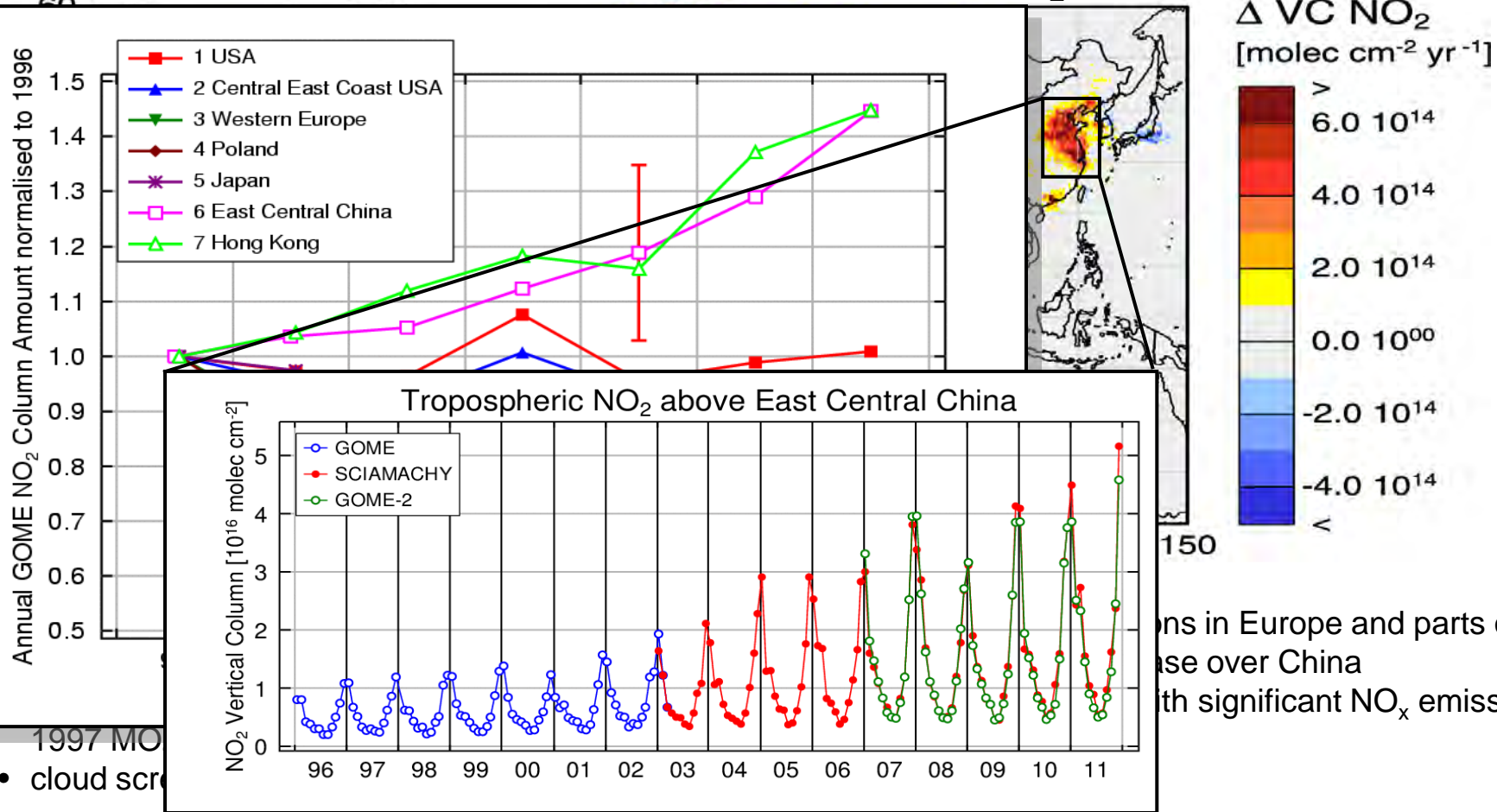
biomass burning

ships

transport

Satellite NO₂ Trends: The Global View 1995-

GOME annual changes in tropospheric NO₂

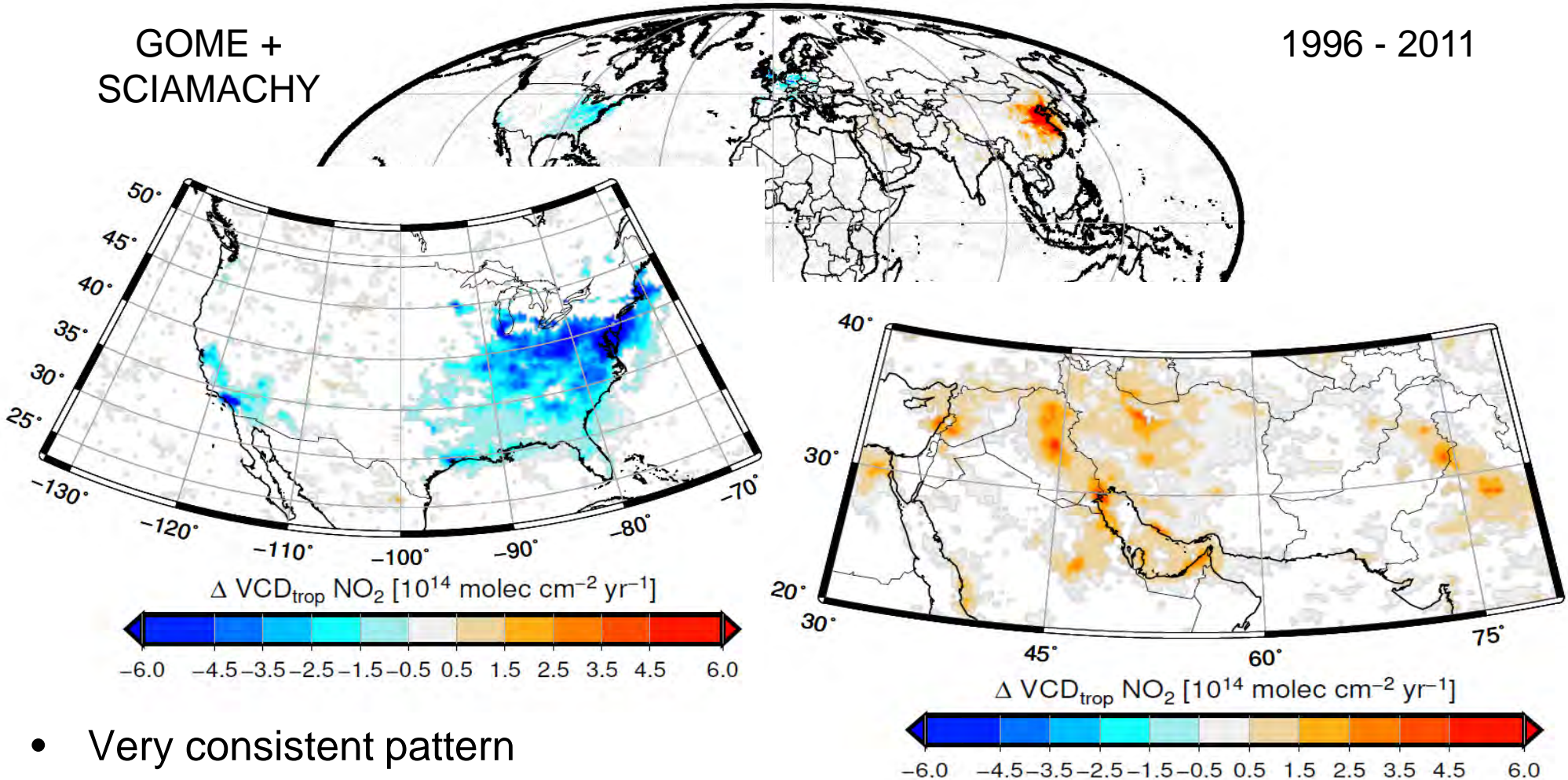


A. Richter et al., Increase in tropospheric nitrogen dioxide over China observed from space, *Nature*, 437 2005

The spatial distribution of satellite NO₂ trends

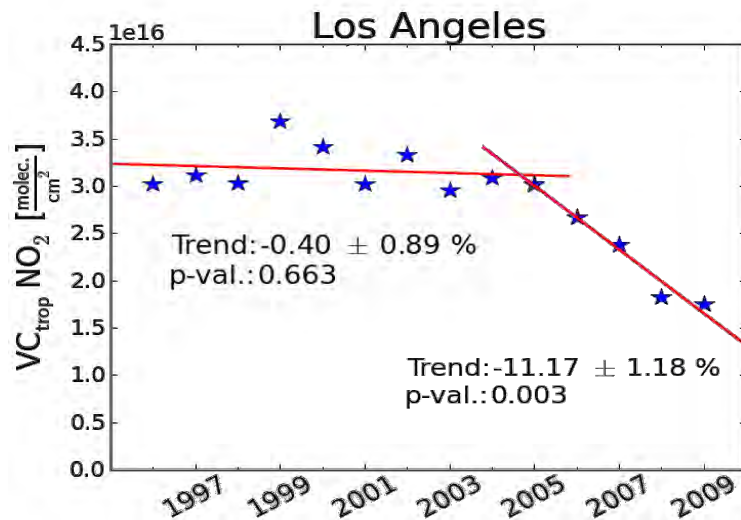
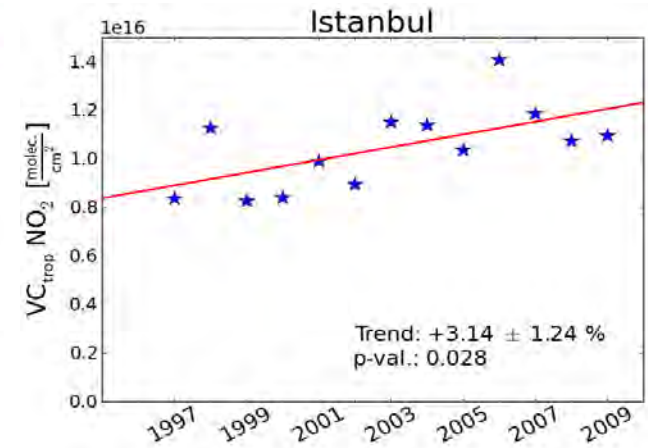
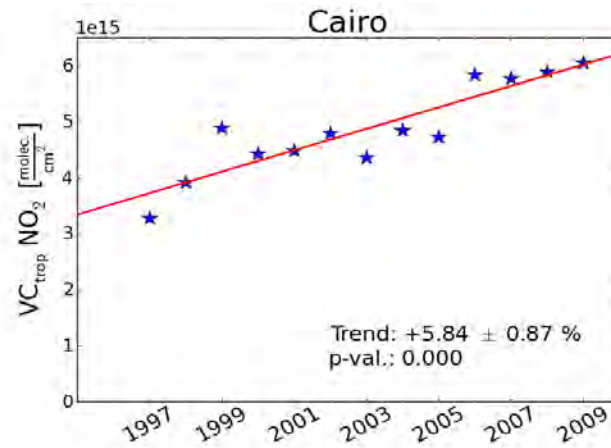
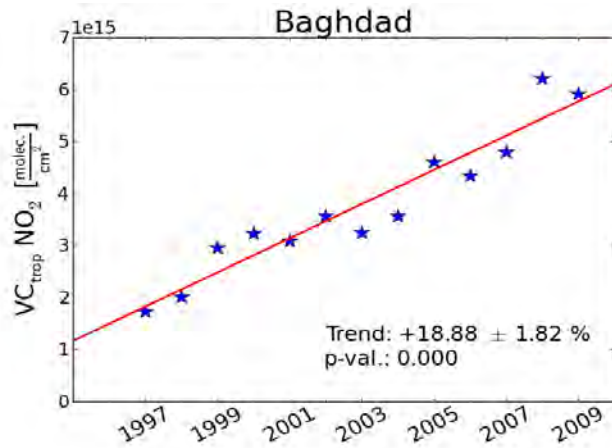
GOME +
SCIAMACHY

1996 - 2011



- Very consistent pattern
- Many cities can be identified

NO₂ Trends over some Megacities/Urban Agglomerations

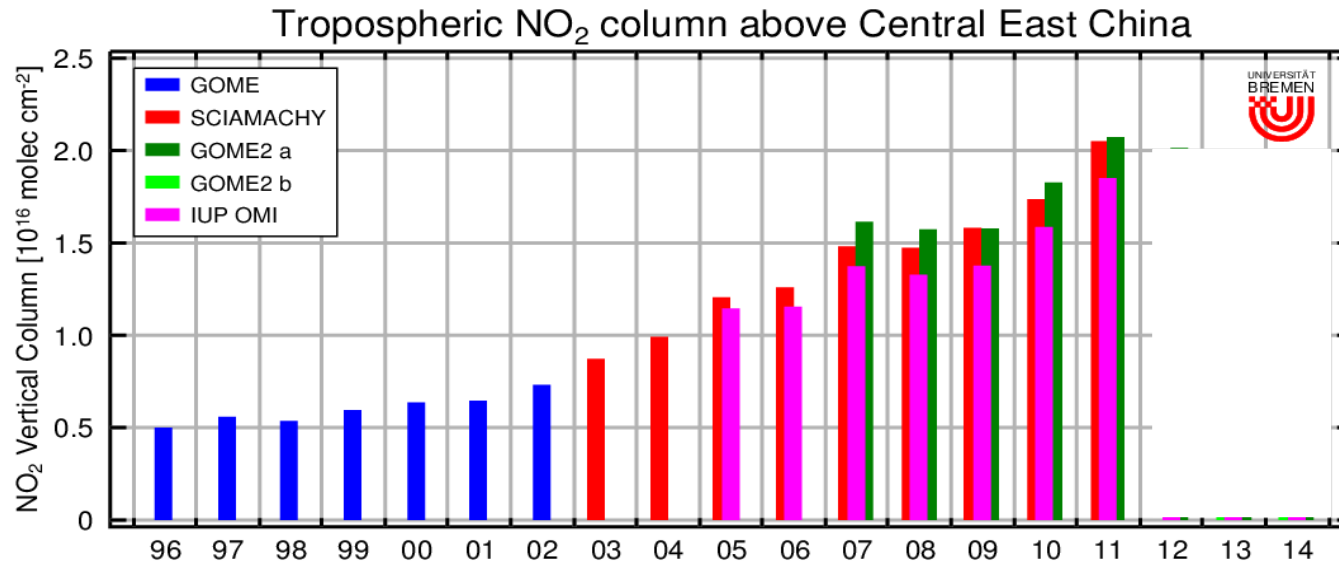


NO₂ levels are changing in cities throughout the world.

Contributing factors are

- Urbanisation
- Population growth
- Increase in standard of living
- changes in fuels used
- Improvements in emission controls

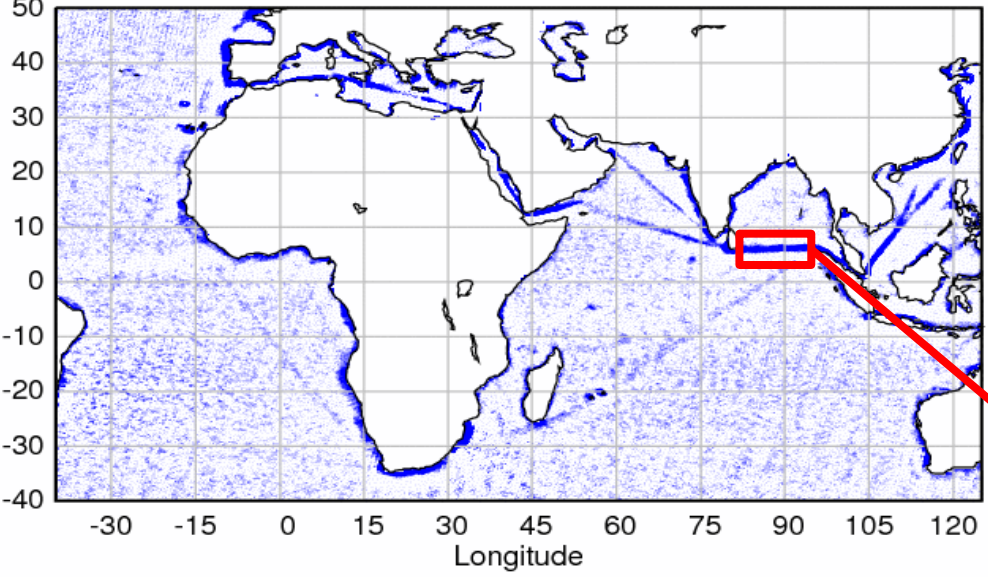
Recent NO₂ Trends above China



- Until 2011, there was continuous increase in NO₂
- After two years of stagnation, 2014 saw a large decrease
 - ⇒ economic slow down?
 - ⇒ Improved technology?
 - ⇒ Switch in fuels used?
 - ⇒ Other factors?

NO_x Emissions from Shipping

GOME-2 shipping NO₂ January 2007 - October 2010



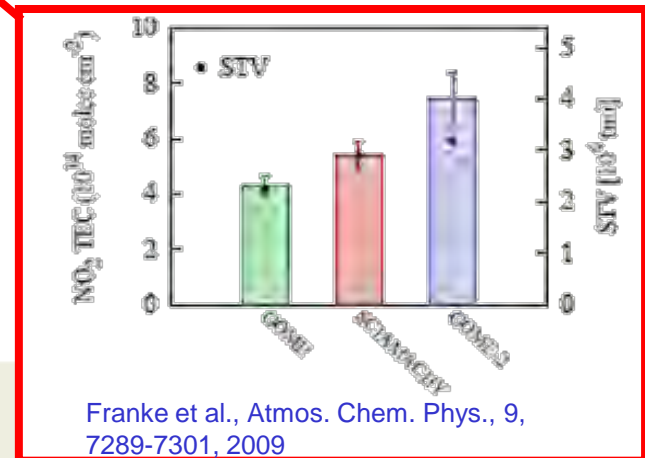
Ship emissions:

- large source of NO_x, SO_x and aerosols
- relevant input into marine boundary layer
- well defined NO₂ patterns in Red Sea and Indian Ocean in GOME-2 data
- consistent with pattern of shipping

With estimate of NO₂ lifetime, NO_x emissions can be estimated => agreement within error bars.

But: error bars mainly from lifetime)

A. Richter et al., Satellite Measurements of NO₂ from International Shipping Emissions, *Geophys. Res. Lett.*, 31, L23110, doi:10.1029/2004GL020822, 2004
 A. Richter et al.: An improved NO₂ retrieval for the GOME-2 satellite instrument, *Atmos. Meas. Tech.*, 4, 1147-1159, doi:10.5194/amt-4-1147-2011, 2011



Franke et al., *Atmos. Chem. Phys.*, 9, 7289-7301, 2009

Latest Aircraft Instrument IUP UB - AirMap instrument

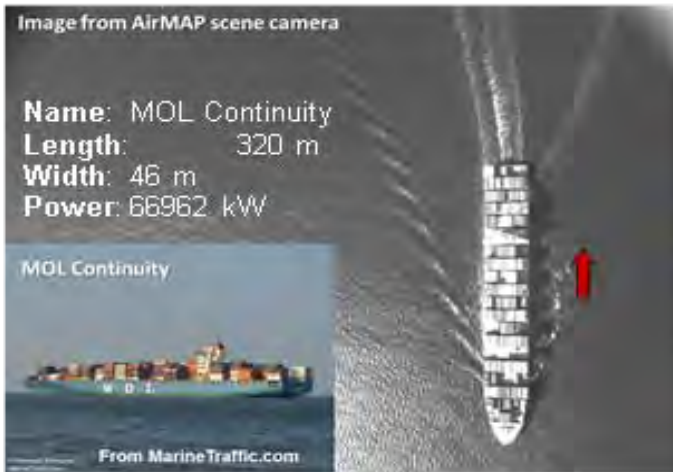
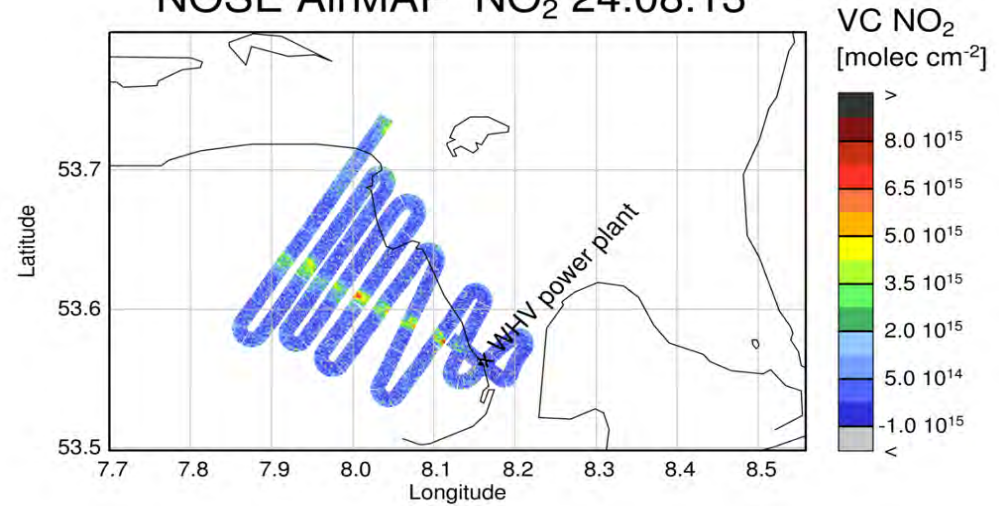


- Push-broom imager
 - 48° field of view
 - Swath ~ flight altitude
 - Acton 300i spectrometer
 - Princeton frame transfer CCD
 - Fibre optics
 - Only narrow spectral range
 - Video camera, GPS
 - At typical
 - flight altitude (3000m)
 - aircraft speed (60m/s)
 - Integration time (0.5s)
- ⇒ 35 pixels @ **80 x 30 m²**

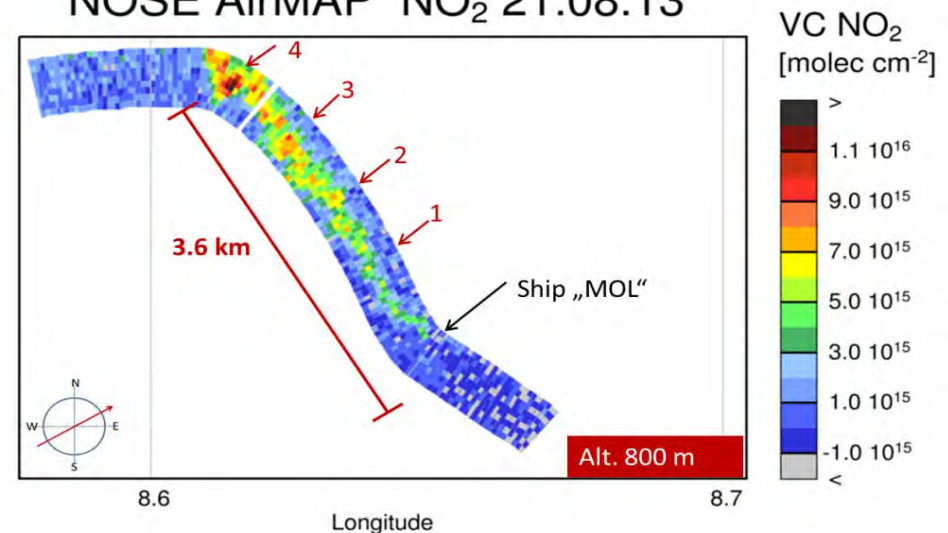
Some Recent AirMap targets – Northern Germany and Shipping



NOSE AirMAP NO₂ 24.08.13

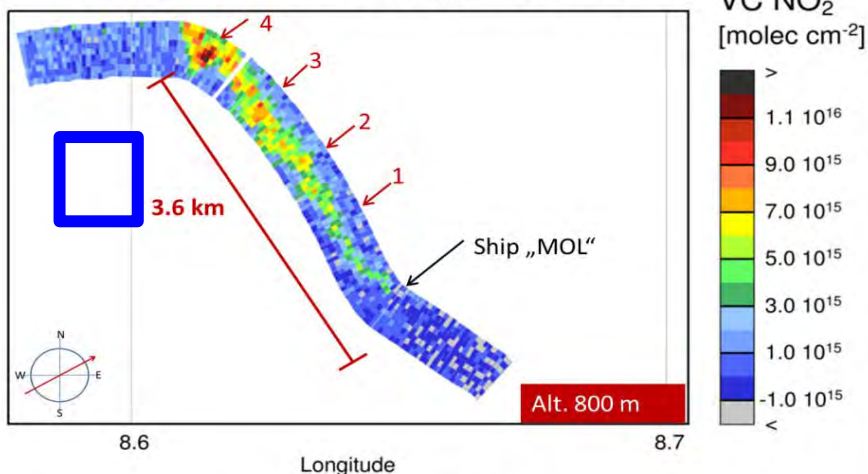


NOSE AirMAP NO₂ 21.08.13

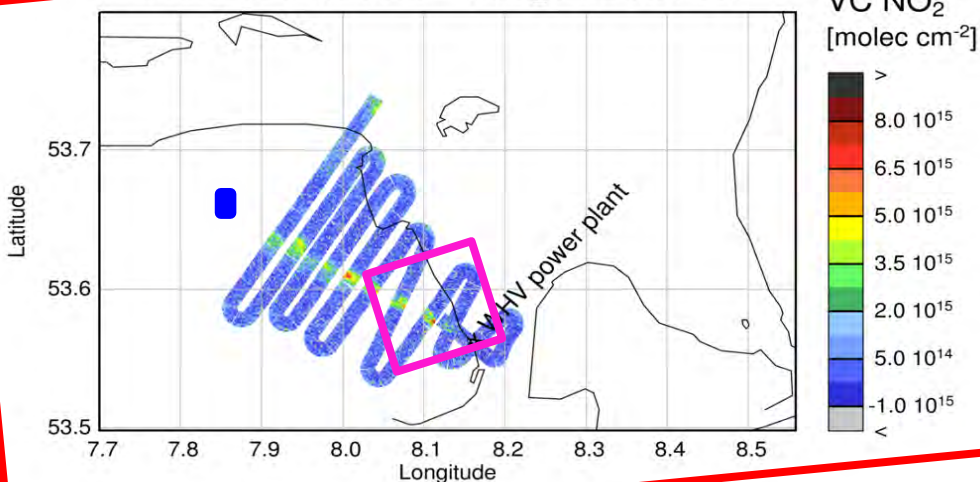


Spatial resolution – the evolution to meet the needs of tropospheric chemistry spatial and temporal scales?

NOSE AirMAP NO₂ 21.08.13



NOSE AirMAP NO₂ 24.08.13



Spatial resolution of satellite instruments is improving:

• GOME G3	40 x 320 km ²	1995-2011
• GOME HR	40 x 80 km ²	1995-2011
• SCIAMACHY	30 x 60 km ²	2002-2012
• GOME-2 G1	40 x 80 km ²	2007-2012
• GOME-2 HR	40 x 20 km ²	2007-2021+
• GOM-2 Tandem	40x40 km ²	2012-2021 +
• OMI	13 x 24 km ²	2004-
• S5P	7.5 x 7.5 km ²	2017-2023+
• S5	7 x 7 km ²	2017-2034+
• S4	8 x 8 km ²	2019-2034
• SCA-ISS/ UVScope	1x1 km ²	2020

New challenges:

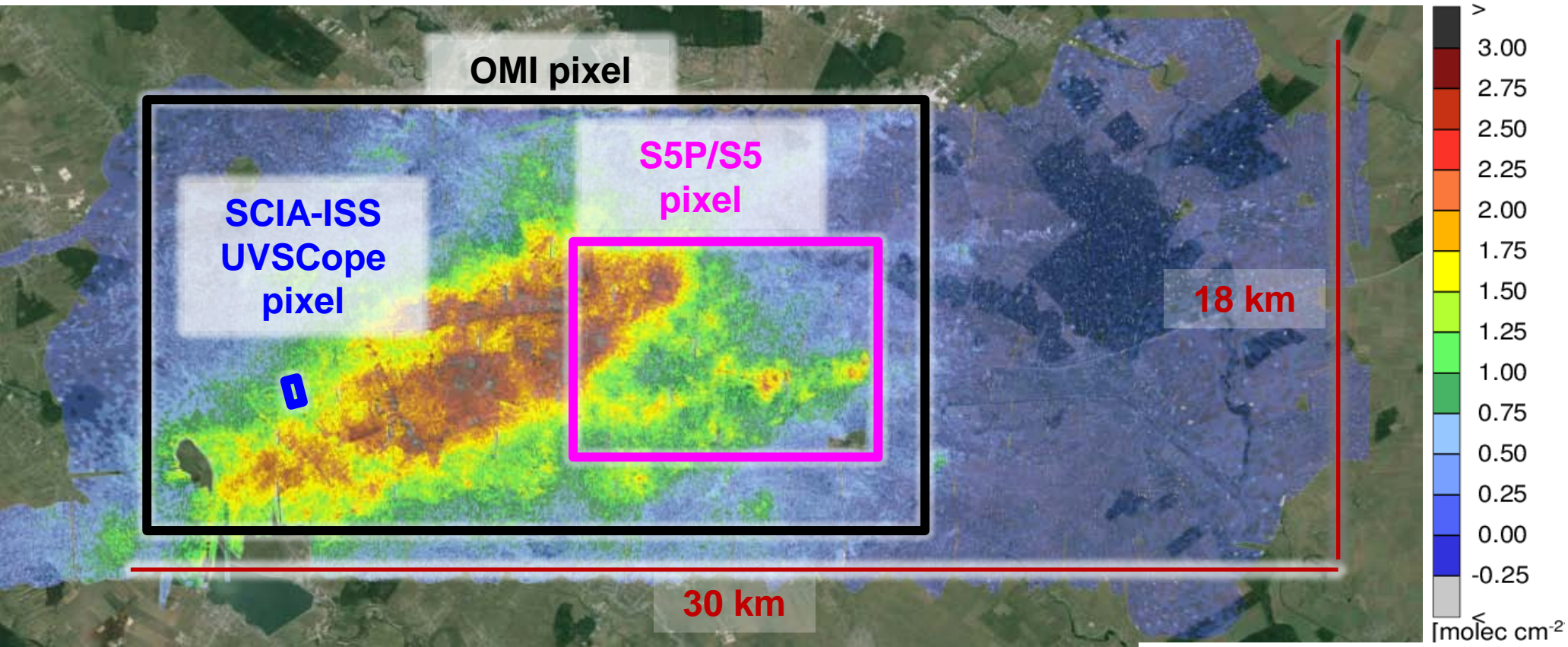
- Data have more variability
- 3d effects in radiative transfer become relevant



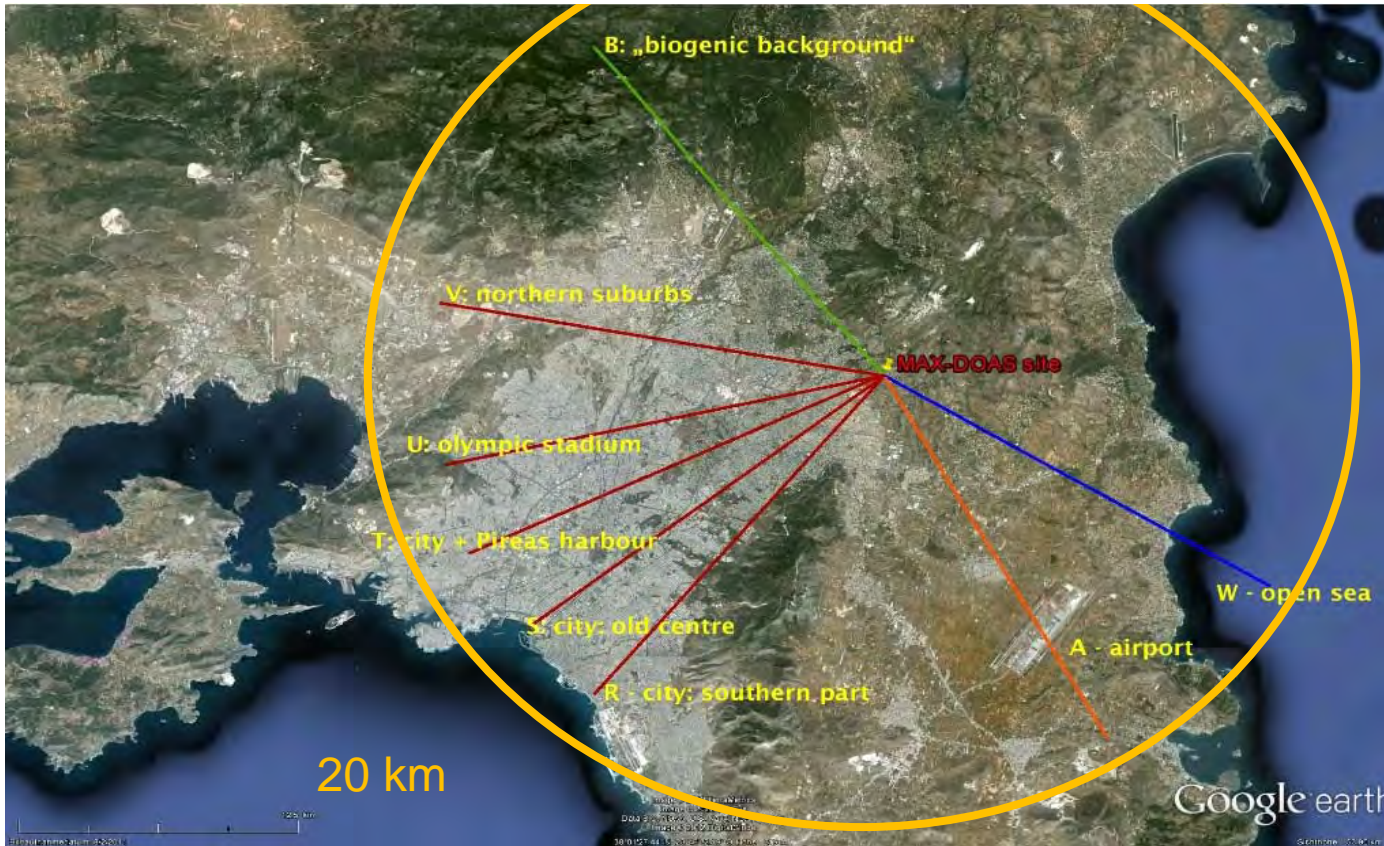
AirMap: Bucharest VC NO₂ 08.09.2014

- ESA Campaign
- Composite of the results from the flights on 14 Large values
- Low wind speed ($\approx 0 - 1$ m/s), alternating directions

NO₂ VC
10¹⁶ molec cm⁻²

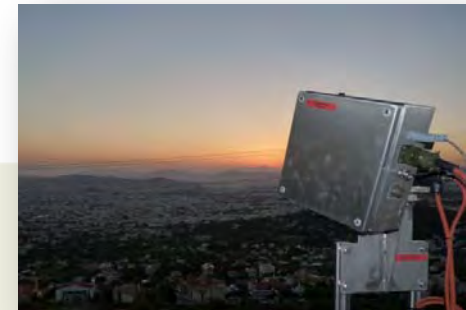


MAX-DOAS Measurements in Athens

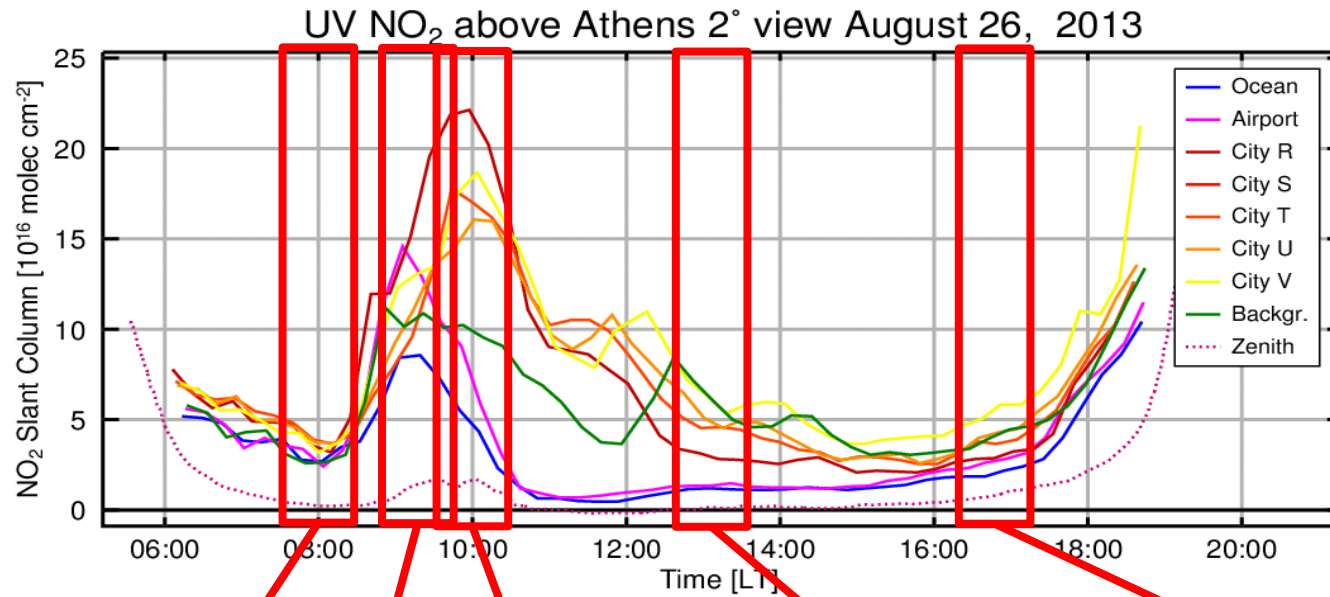


- Oct 2012 – now
- 330 – 500 nm
- 8 viewing azimuths
 - Ocean
 - Airport
 - City x 5
 - Background
- $-1^\circ \dots 30^\circ$ elevation + zenith
- 15 minutes cycle
- Closest zenith reference

- 3.2 million inhabitants
- Emissions from industry and transportation
- Intense photochemistry
- Affected by fires and Sahara dust events



Spatial Gradients City Pollution



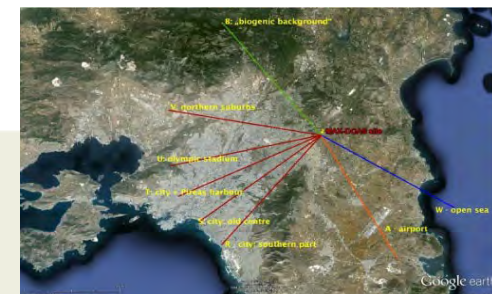
All directions lowest values

Maximum clean regions

Maximum city

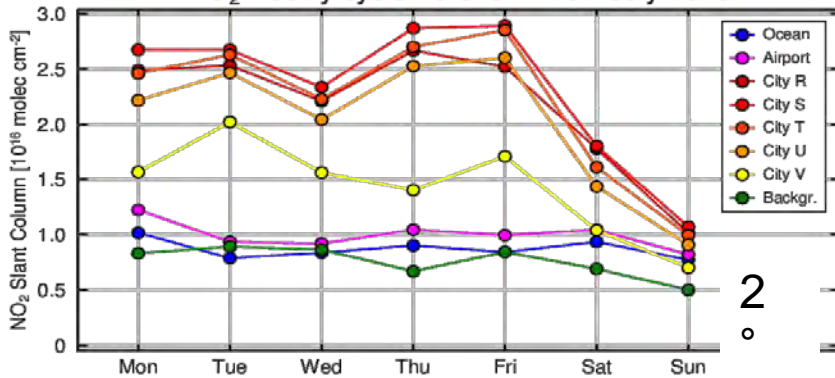
Biogenic Background direction largest

Residential area direction highest



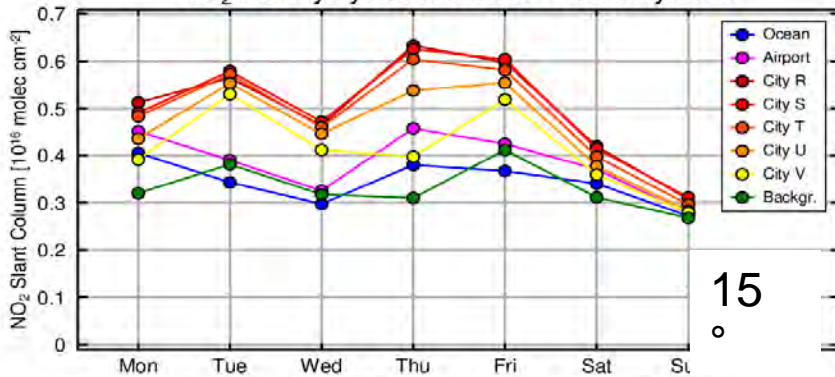
Weekly Cycle in NO₂ for Athens

NO₂ weekly cycle Athens 2° view July 2013



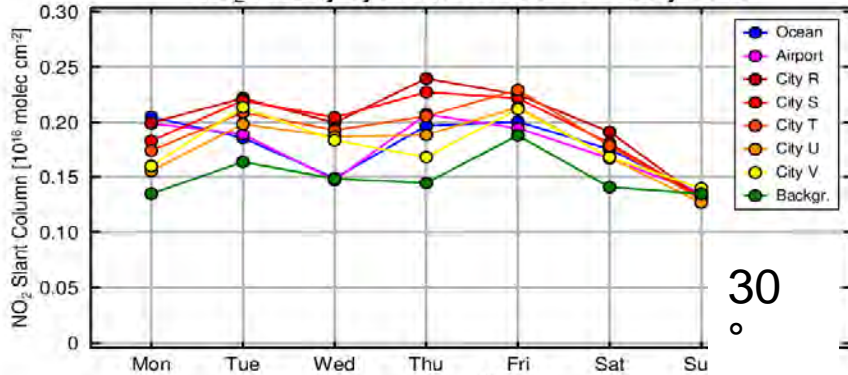
2°

NO₂ weekly cycle Athens 15° view July 2013



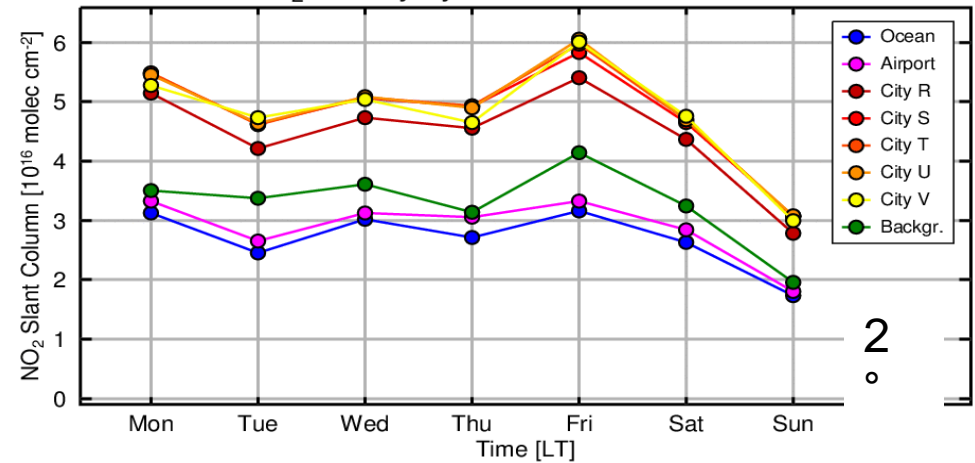
15°

NO₂ weekly cycle Athens 30° view July 2013



30°

NO₂ weekly cycle Athens 2° view 2013

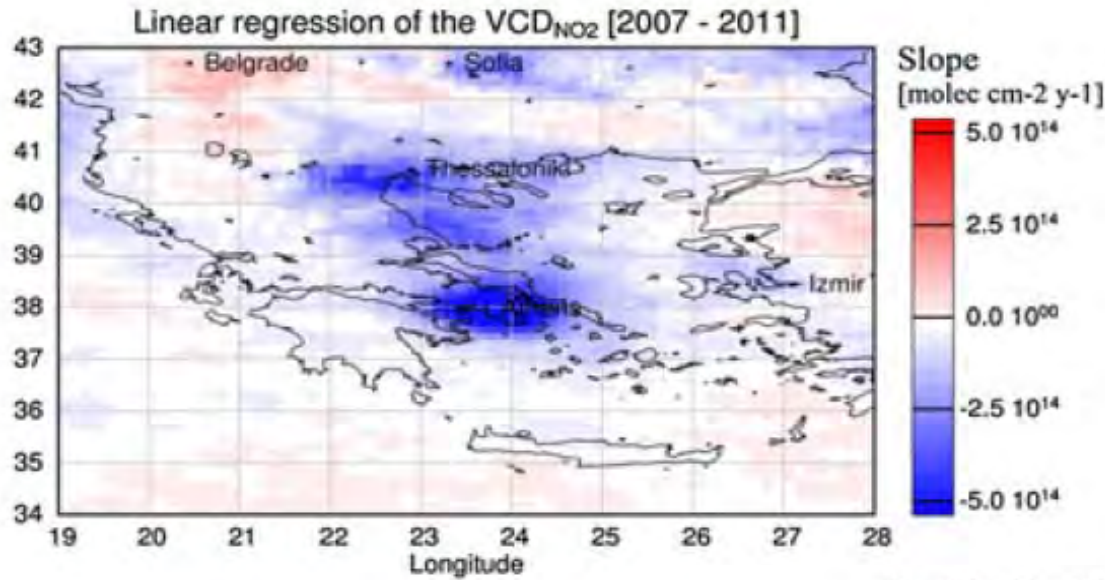


2°

- Very clear weekly cycle
- Most pronounced over city directions
- Most pronounced in lowest elevation angles
- Best seen during summer break

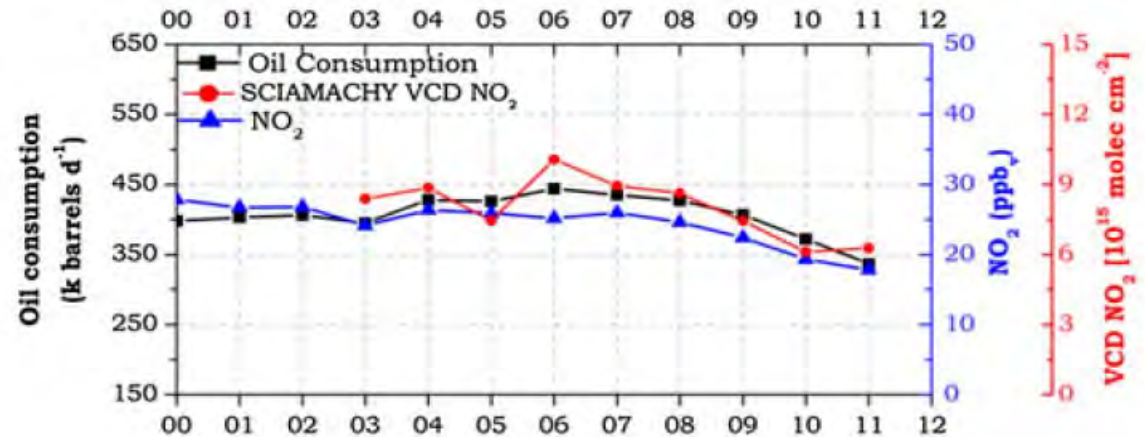


NO₂ Trends above Europe

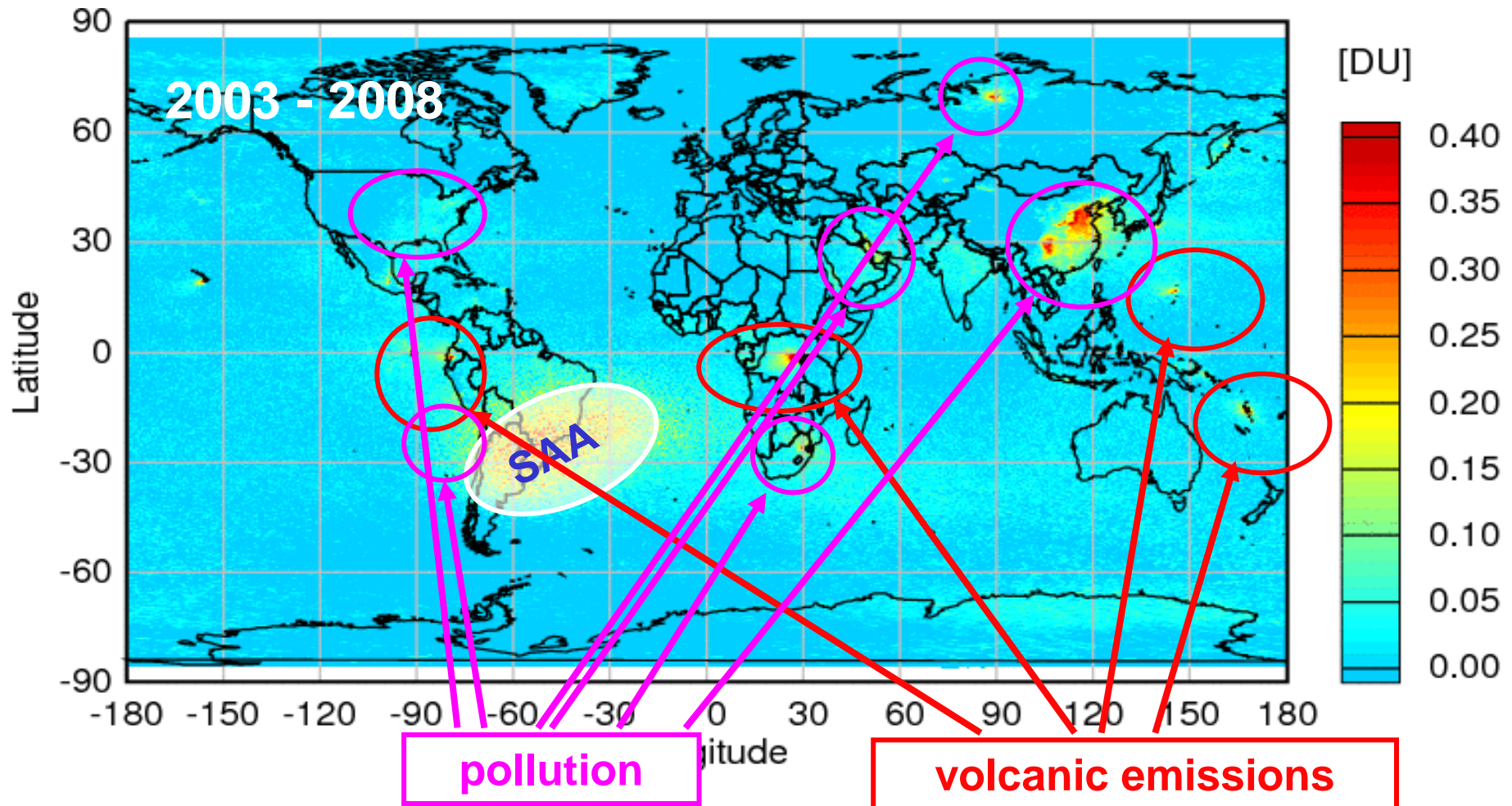


- Decreasing NO₂ trend over Greek cities from 2007 – 2011
- Both in satellite and surface data
- Link to oil consumption
- Effect of economic crisis

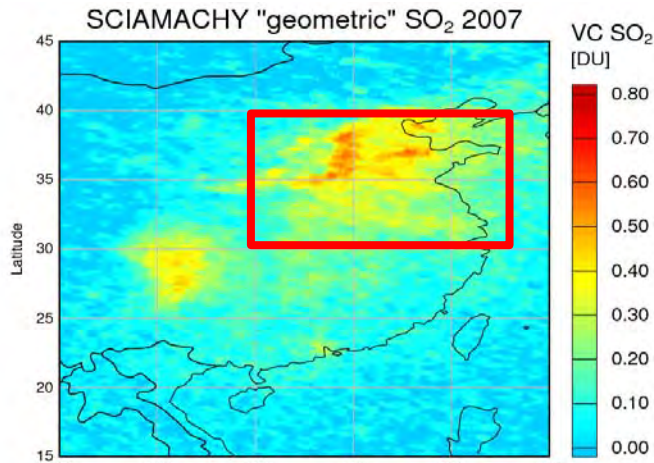
Vrekoussis, M. et al., Economic crisis detected from space: Air quality observations over Athens/Greece, Geophys. Res. L ett., 40, doi:10.1002/grl.50118., 2013



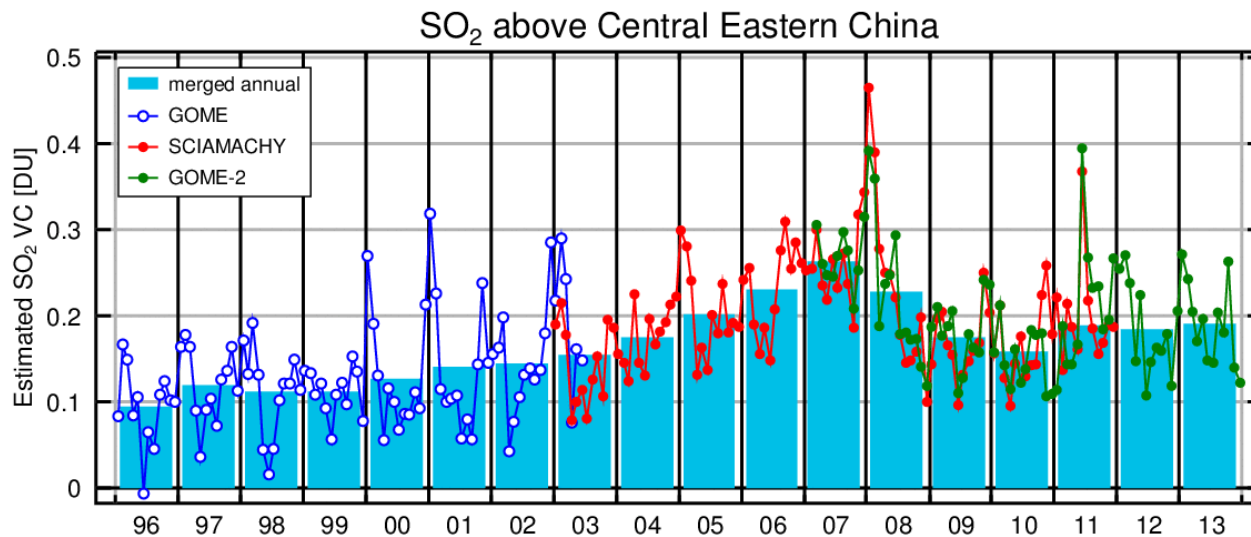
SCIAMACHY SO₂: The global Picture



SO₂ columns above China



- SO₂ increase in similar regions as NO₂ increase
- Main reason is increase in power generation using coal



- Legislation made flue gas desulphurisation mandatory after 2006
- Marked decrease in SO₂ but small upward trend since 2009 (industrial sources)

NMVOCs: HCHO and glyoxal

Sources:

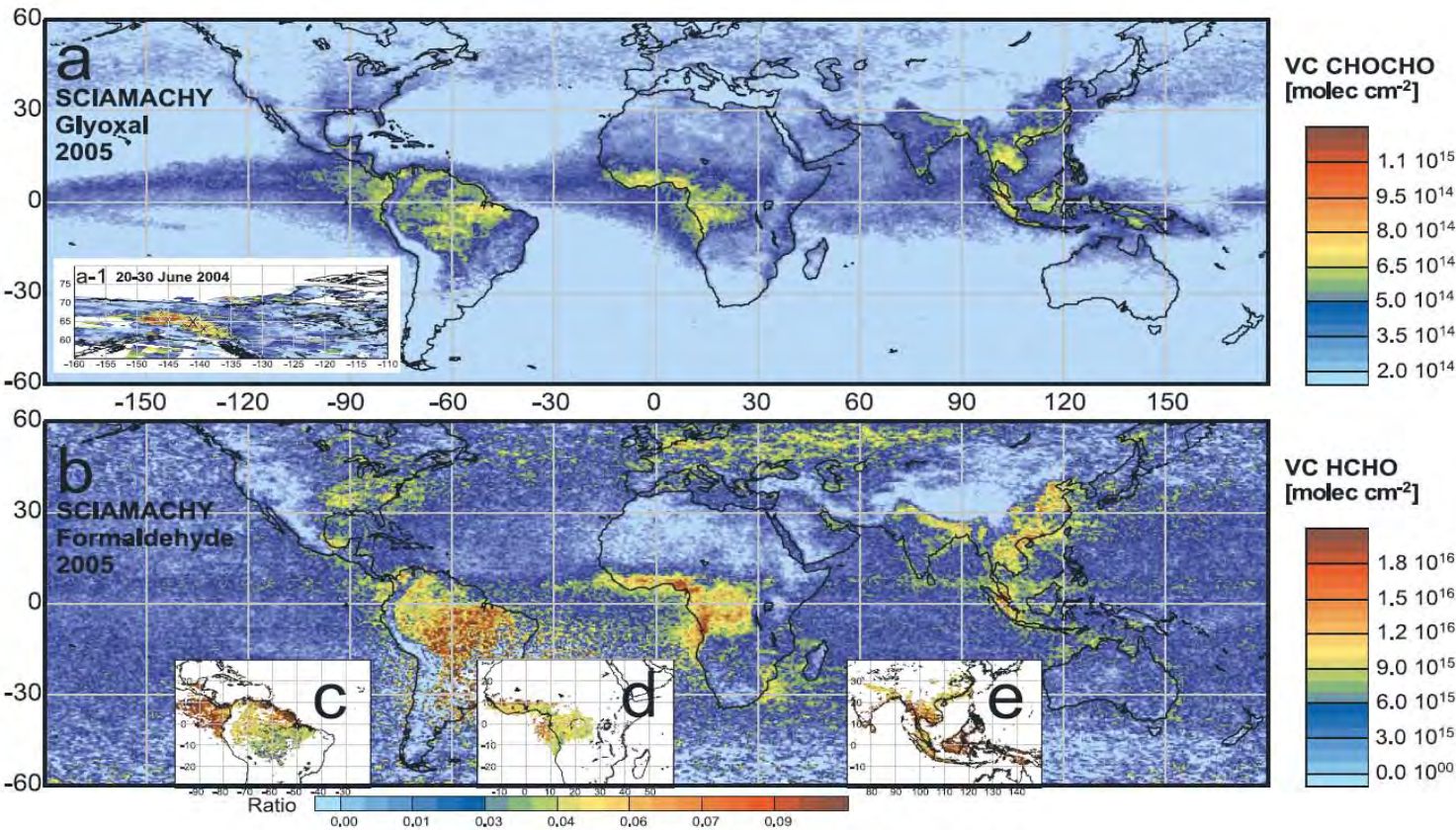
- Biogenic
- Fires
- Fossil fuel
- VOC oxidation

Sinks:

- Photolysis
- OH

Relevance:

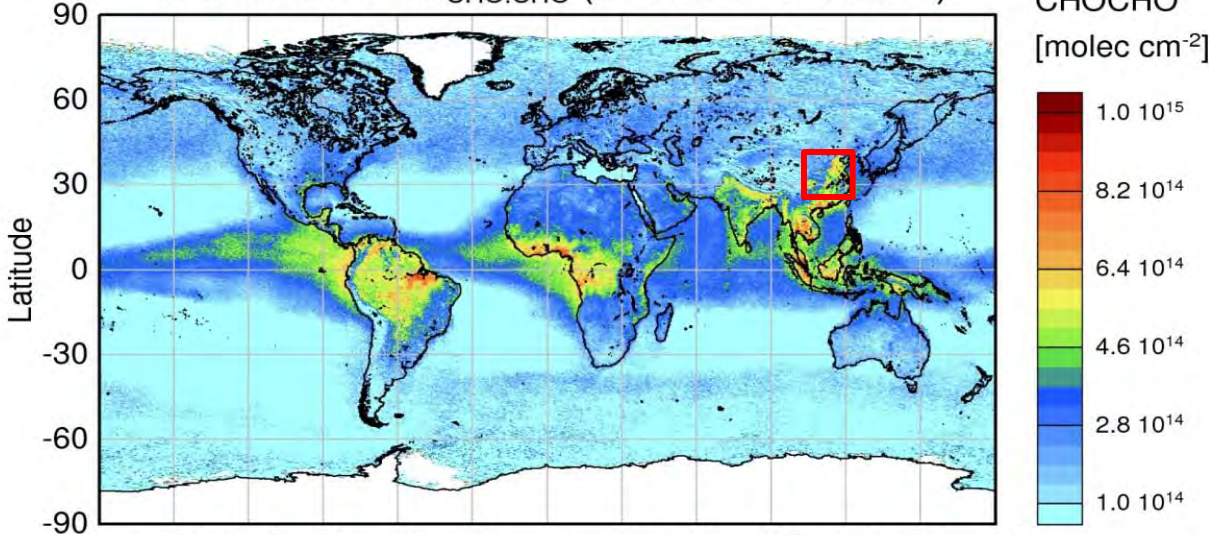
- O₃ production
- SOA



Wittrock, F., et al., (2006), Simultaneous global observations of glyoxal and formaldehyde from space, *Geophys. Res. Lett.*, 33, L16804, doi:10.1029/2006GL026310.

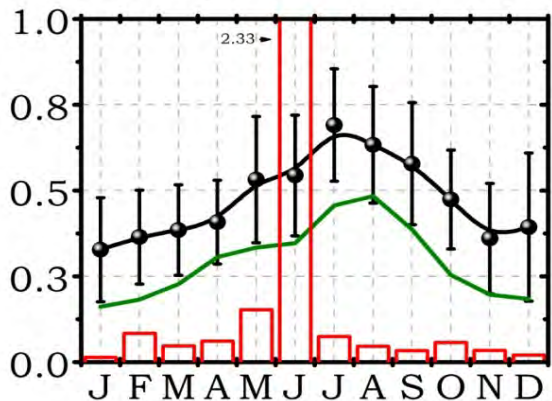
Glyoxal, CHO.CHO columns

SCIAMACHY VC_{CHO.CHO} (01.01.03 - 31.12.07)

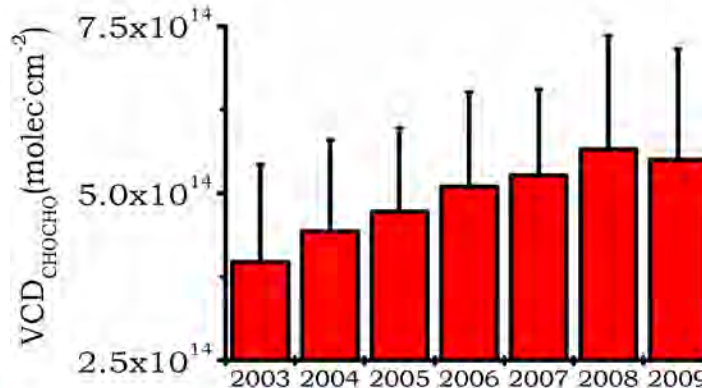


- Glyoxal is a VOC with little primary emission
- Main sources are oxidation of biogenic and anthropogenic VOCs, biomass burning
- Seasonality of glyoxal indicates mainly biogenic precursors
- Consistent upward trend over SCIAMACHY time series
- Additional anthropogenic emissions?
- Land use changes?
- More biomass burning?

Asia (northern China)



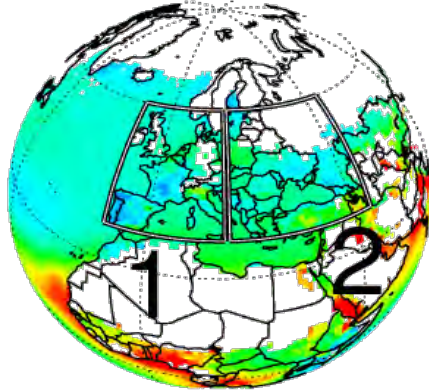
CHOCHO NDVI fire counts



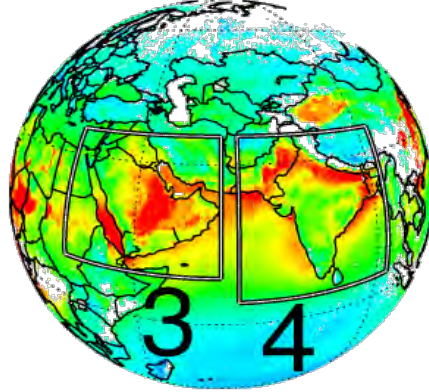
Vrekoussis, M., et al., Temporal and spatial variability of glyoxal as observed from space, *Atmos. Chem. Phys.*, 9, 4485-4504, 2009

Aerosols in the troposphere

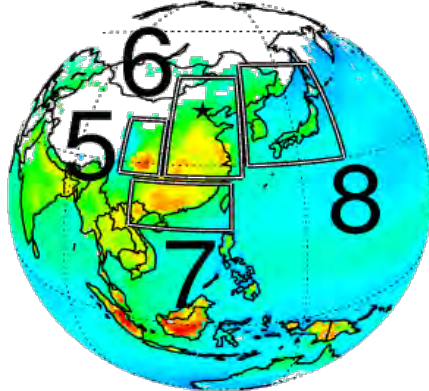
(a) MODIS (TERRA)



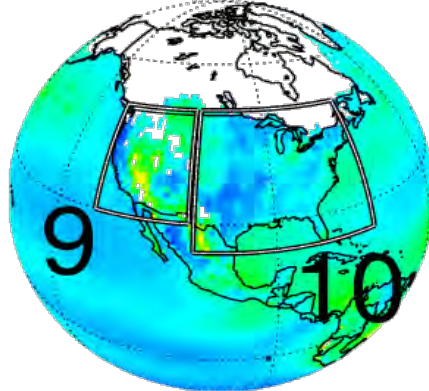
(b) MISR (TERRA)



(c) SeaWiFS (OrbView-2)



(d) MODIS (AQUA)



□ No Observation or Not Enough Data

Aerosol Optical Thickness (AOT) [unitless]



Sources

- Sea-salt
- Dust / sand
- Combustion / fires
- Secondary aerosols (SO_2 , HNO_3 , SOA, ...)

Sinks

- Wet & dry deposition

Relevance

- Health
- Scattering

Yoon, J., Changes in atmospheric aerosol loading retrieved from space based measurements during the past decade, *Atmos. Chem. Phys. Discuss.*, 13, 26001-26041, doi:10.5194/acpd-13-26001-2013, 2013.

Changes in aerosol AOT 2003-2008

2003 - 2008

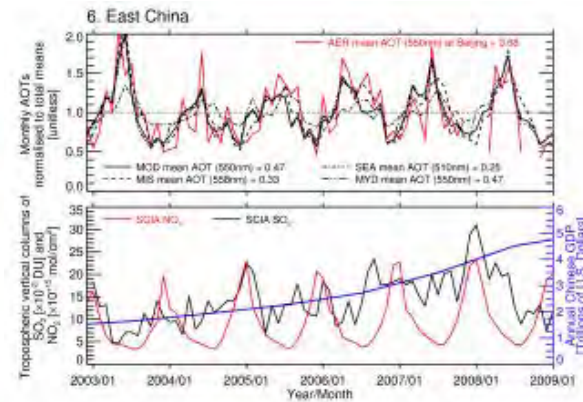
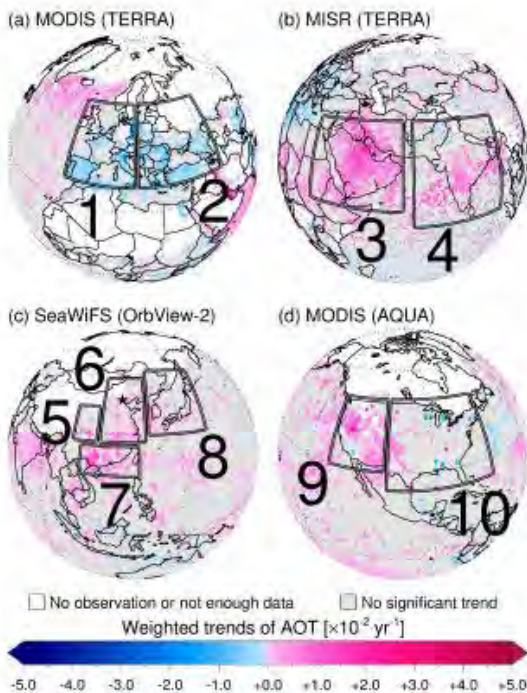
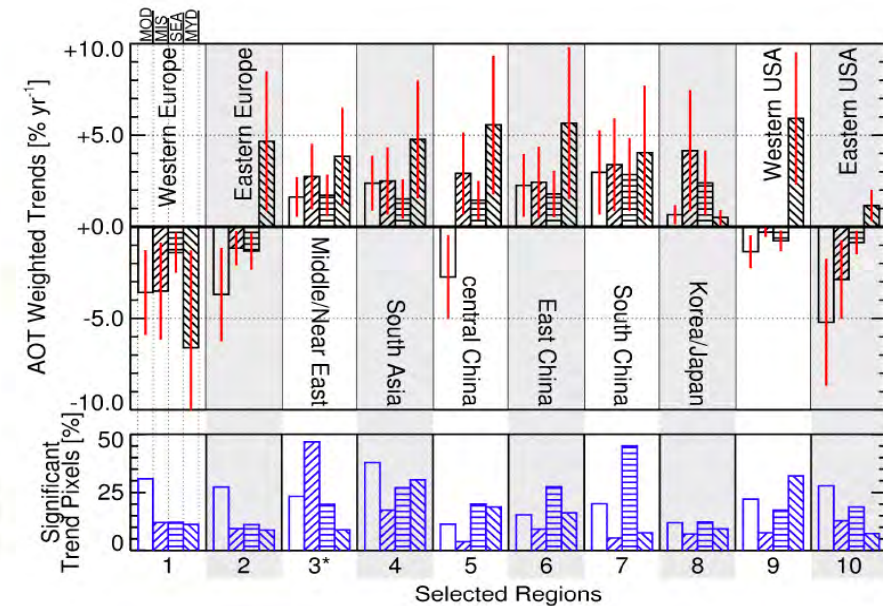


Figure 13. Time series of atmospheric AOTs normalized to their average mean values from the MODIS-Terra (MOD), MISR-Terra (MIS), SeaWiFS-OrbView-2 (SEA), MODIS-Aqua (MYD), and AERONET (AER) data sets; tropospheric nitrogen dioxide and sulfur dioxide columns from SCIAMACHY (SCIA) over eastern China (region 6); and Chinese GDP from 2003 to 2008.



- Downward trend in Western Europe and Eastern US
- Upward trend in Asia
- Some differences between instruments

Yoon, J., Changes in atmospheric aerosol loading retrieved from space based measurements during the past decade, Atmos. Chem. Phys. Discuss., 13, 26001-26041, doi:10.5194/acpd-13-26001-2013, 2013.

Changes in CTH using observations of O₂ A band and SACURA GOME- SCIAMACHY GOME-2

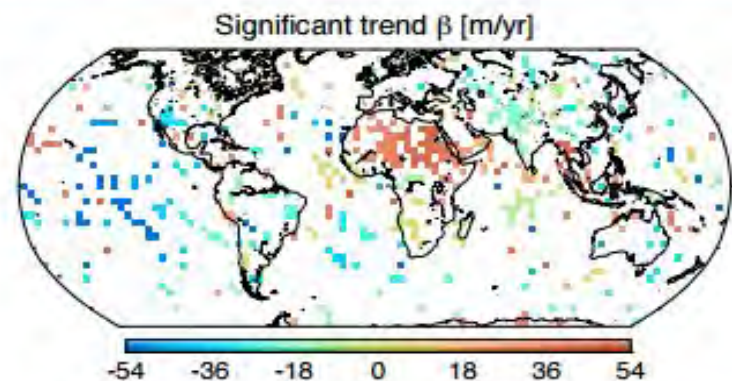


Figure 13. Global trend β in CTH anomaly, statistically significant at 95 % confidence level. Data are gridded onto a mesh of 2°-sided cells.

Table 4. Overview of zonal trends in CTH [m yr^{-1}], ENSO excluded, masking any data within the box 170–120° W, 5° N–5° S. Bootstrap resamples $n = 10^3$. The zonal values are not weighted by the respective land and water abundances.

	Belt		Land + water	Land	Water
With ENSO	Tropics	5° N–5° S	-4.34 ± 5.65	-1.56 ± 4.02	-5.15 ± 8.21
	Tropics	20° N–20° S	-2.16 ± 2.97	$+1.83 \pm 4.40$	-3.39 ± 5.32
	Mid-latitude	30–60° N	-2.17 ± 1.52	-2.85 ± 4.23	-1.52 ± 3.68
Without ENSO	Mid-latitude	30–60° S	-2.71 ± 2.59	-2.70 ± 9.25	-2.71 ± 2.47
	Tropics	5° N–5° S	-1.80 ± 6.00	-1.43 ± 5.05	-1.99 ± 8.52
	Tropics	20° N–20° S	$+0.53 \pm 3.53$	$+5.93 \pm 5.33$	-1.74 ± 4.36
	Mid-latitude	30–60° N	-2.11 ± 3.09	-2.72 ± 4.60	-1.53 ± 3.70
	Mid-latitude	30–60° S	-2.78 ± 2.54	-3.24 ± 8.77	-2.75 ± 2.35

Natural variability and instrument or algorithm error

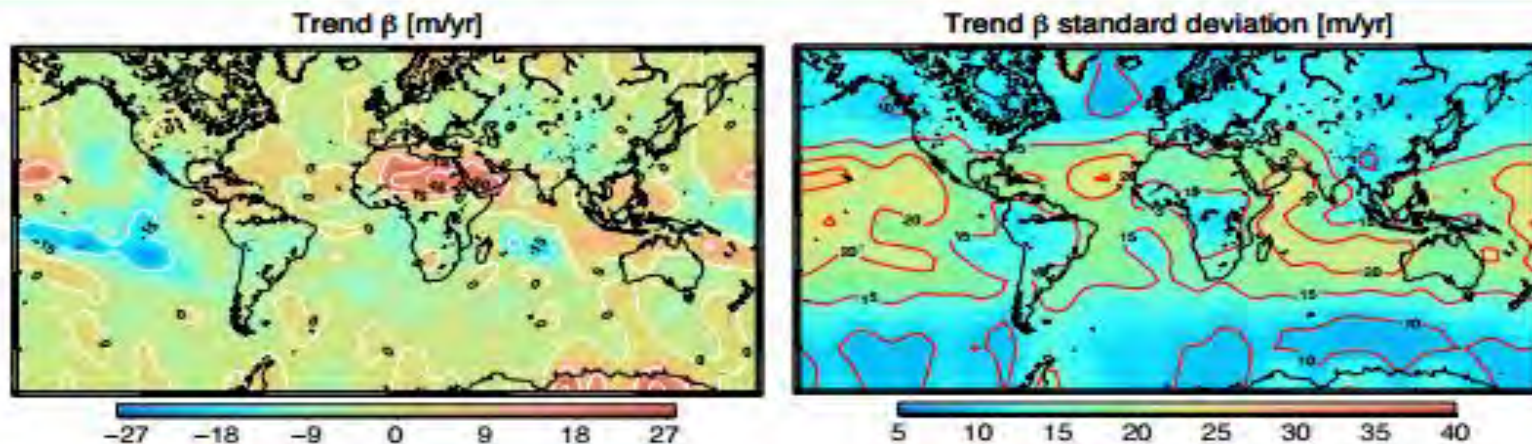
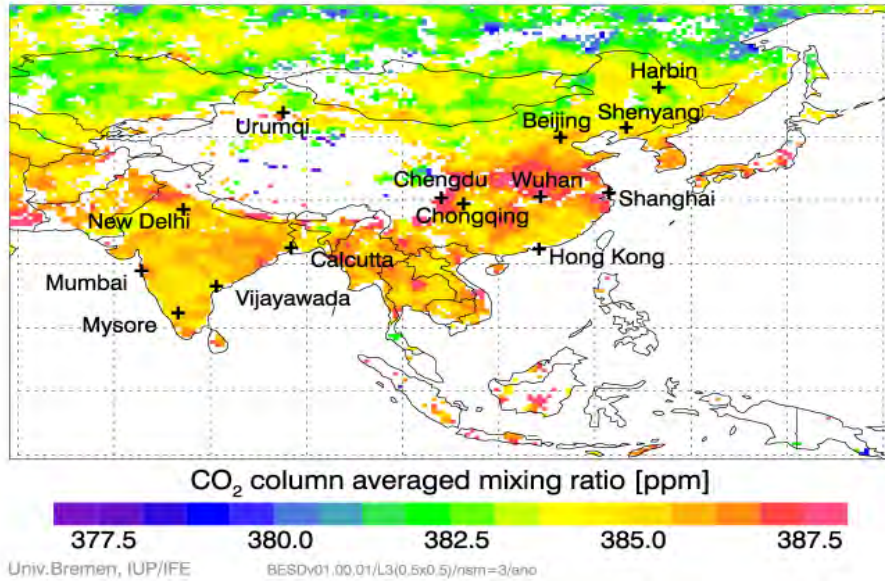


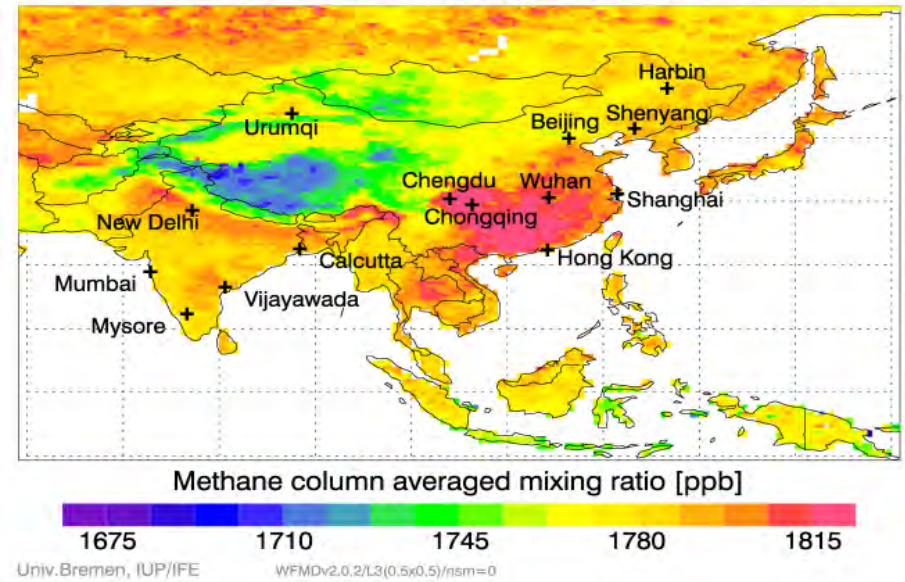
Figure 12. Global map of linear trend β in CTH (left) and standard deviation σ_β (right).

SCIAMACHY on ENVISAT: CO₂ & CH₄ from space

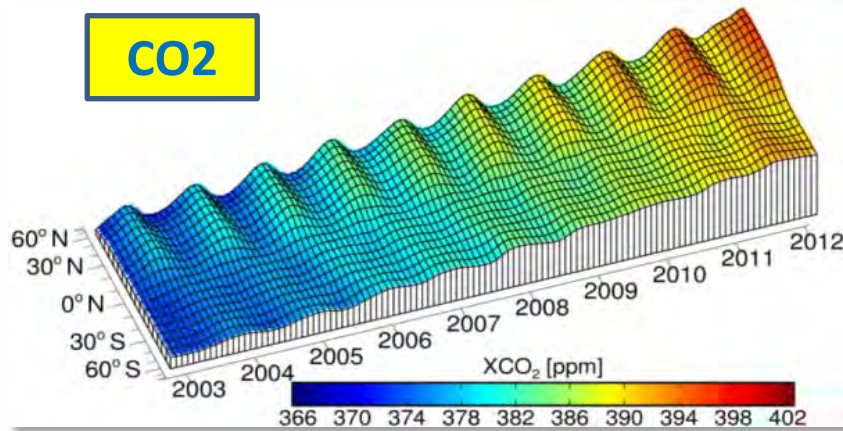
Carbon Dioxide SCIAMACHY/BESD 2006-2011



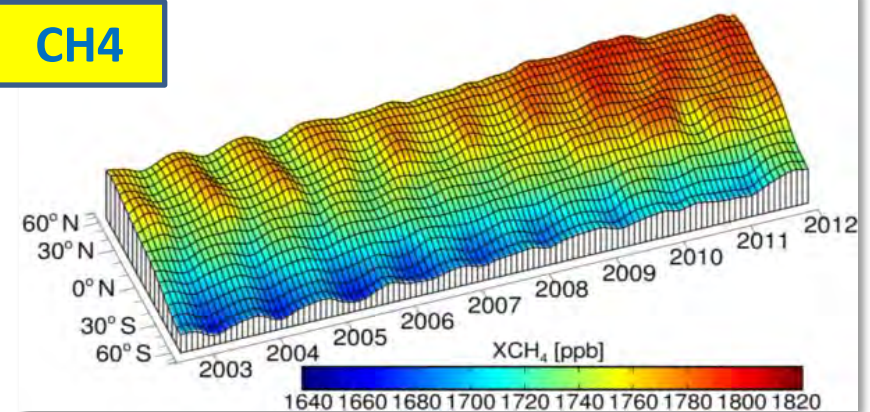
Methane SCIAMACHY/WFMD 2003-2005



CO₂



CH₄

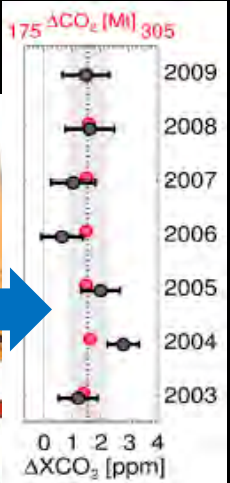
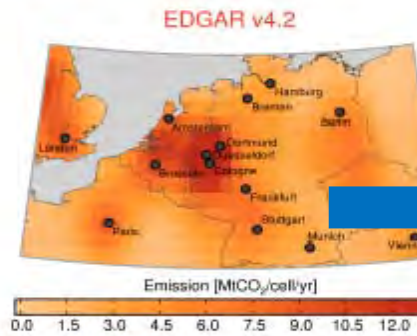
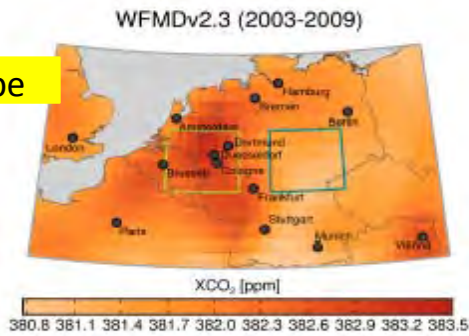


SCIAMACHY XCO₂: Anthropogenic source regions

Schneising et al., ACP, 2013

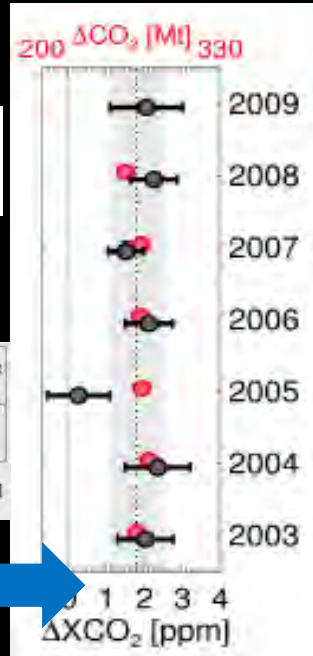
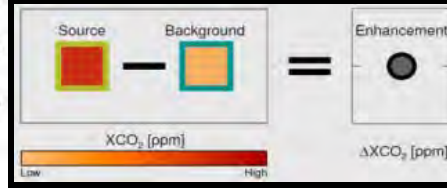
SCIAMACHY XCO₂ EDGAR CO₂ emissions

NW Europe

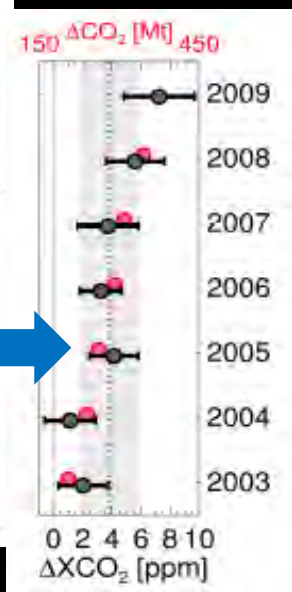
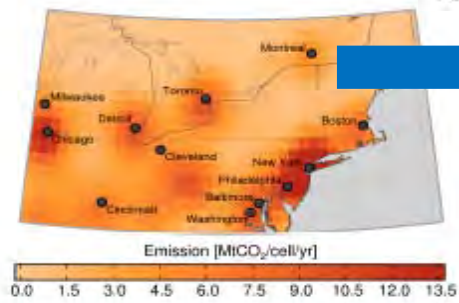
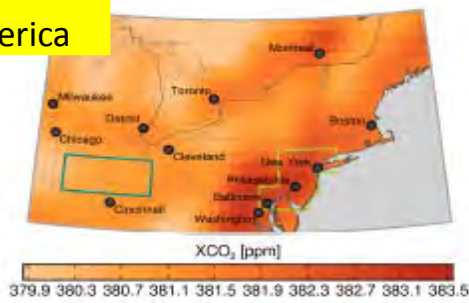


SCIAMACHY
EDGAR

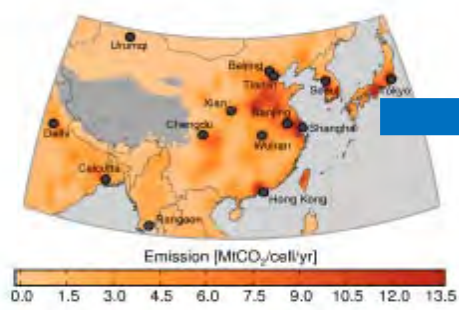
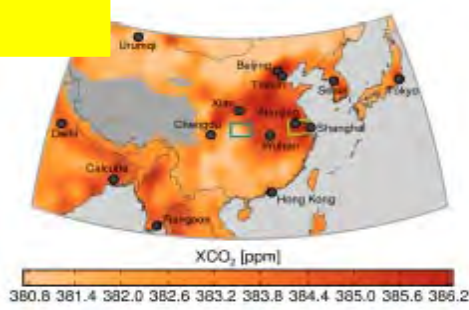
Regional enhancement =
Source - Background



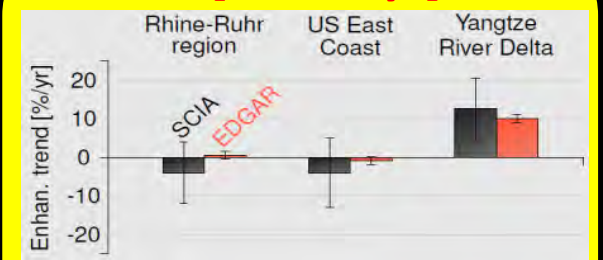
East N. America



China



Trend [%CO₂/yr]

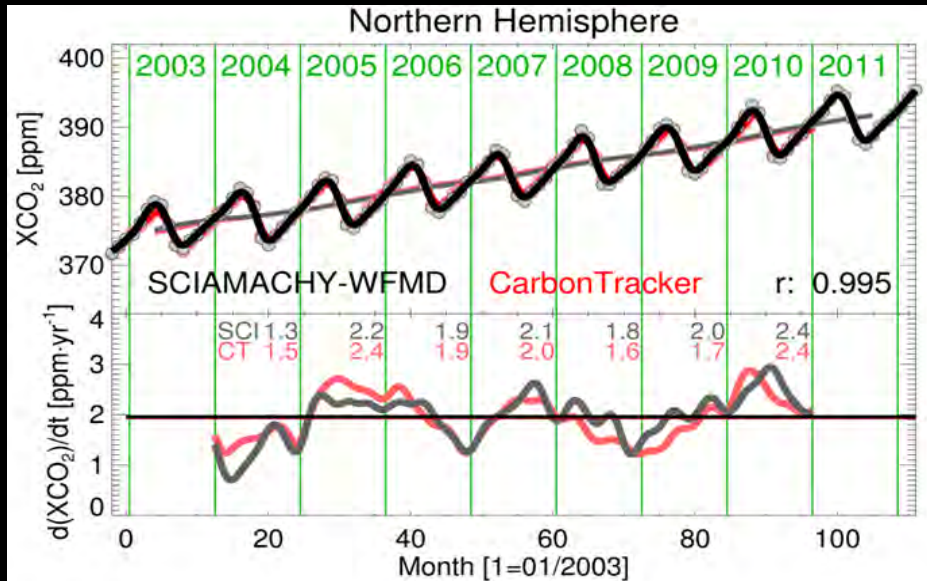


EDGAR are emissions
consistent with SCIAMACHY

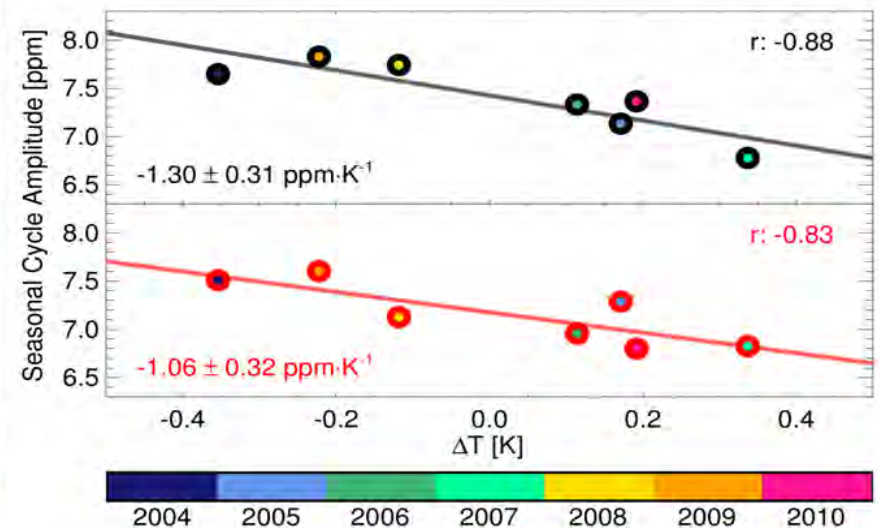
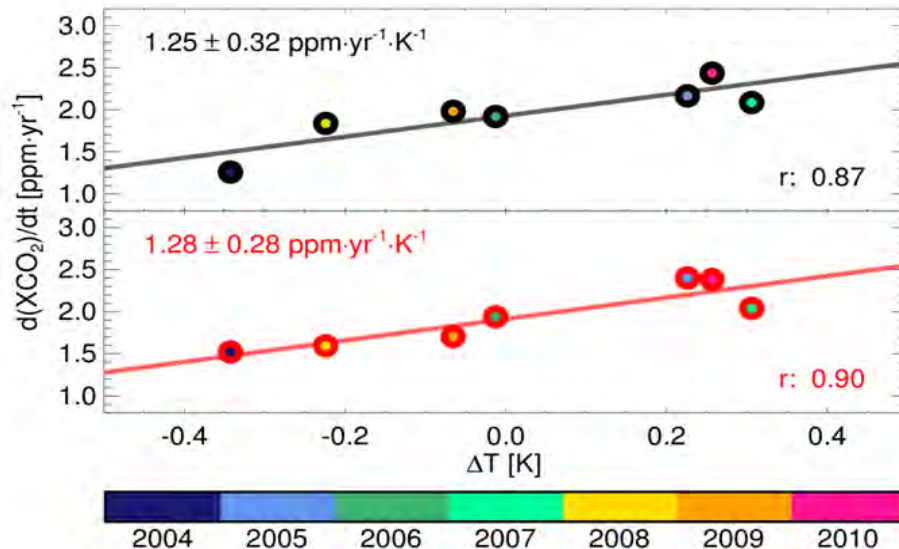
Highlight GHG

Temperature response of terrestrial carbon sink

(Schneising et al., 2014, ACP)



- Years with **higher surface temperatures** during the growing season are associated with **larger CO₂ growth rates** and **smaller seasonal cycle amplitudes** (reduced net carbon uptake by vegetation)
- **Temperature sensitivity:** 2.7 ± 0.7 GtC/yr/K
- **Positive carbon-climate feedback** unless the biosphere adapts its carbon storage under warming conditions in the longer term



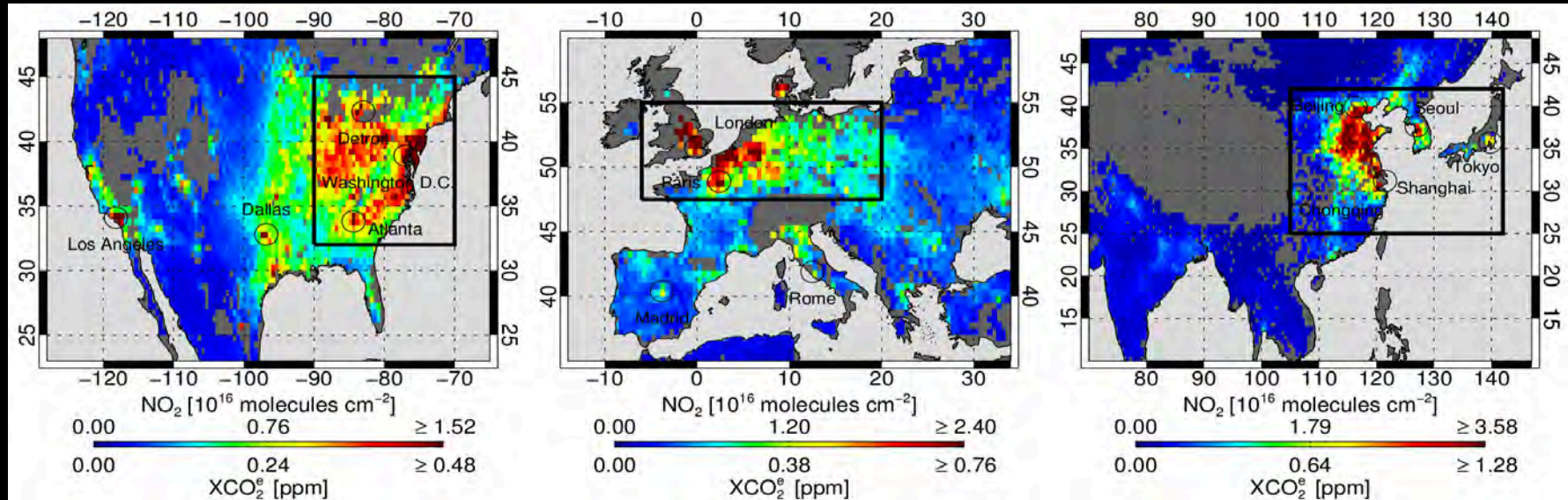
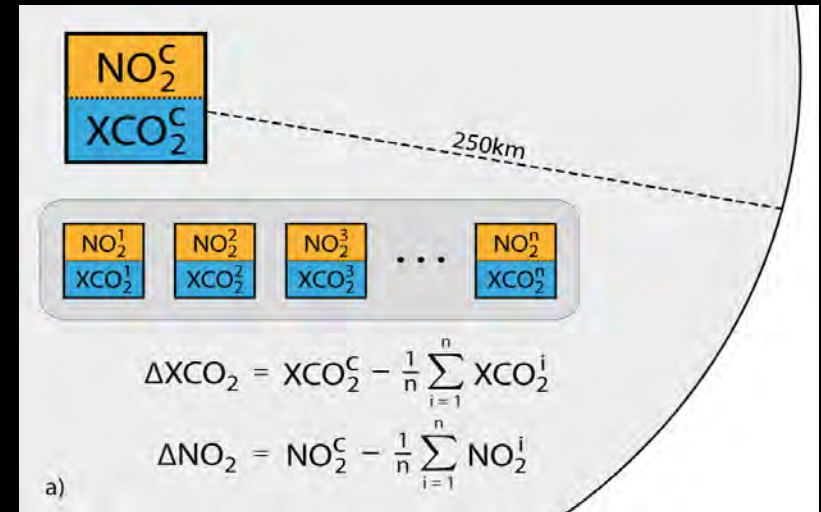
European Carbon Dioxide Surface Flux estimated from SCIAMACHY (and some GOSAT data)

European carbon uptake in gigatonnes of carbon in 2010

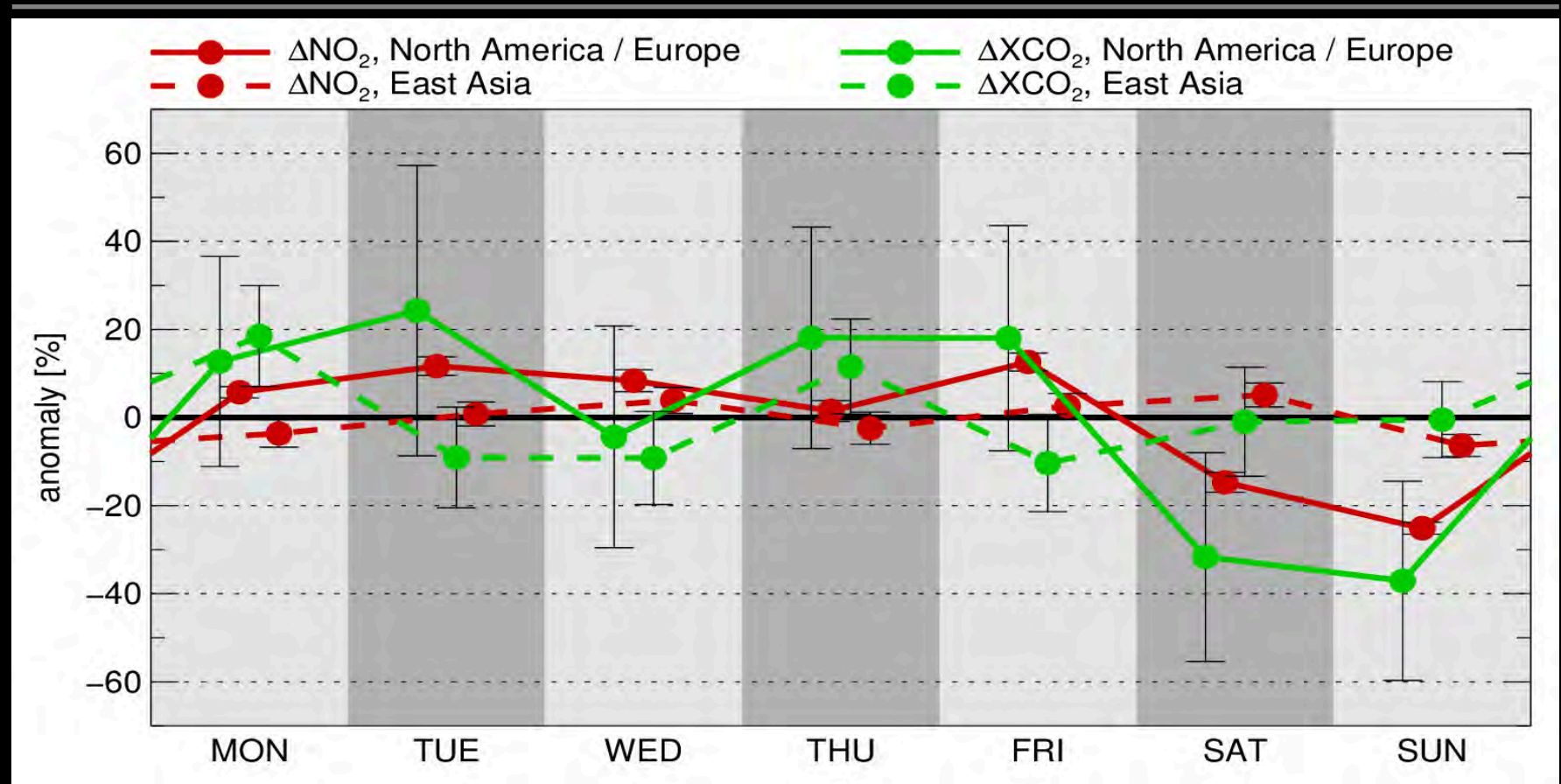


Anthropogenic CO₂ and NO_x emissions (Reuter et al., 2014, nat. geosci.)

- CO₂ and NO_x are **co-emitted** species in anthropogenic fossil fuel combustion processes.
- A **spatial high-pass filtering** method is used to derive co-located regional anomalies ΔXCO₂ and ΔNO₂.
- A **statistical relationship** between ΔXCO₂ and ΔNO₂ allows to conclude on **CO₂ with anthropogenic origin**.

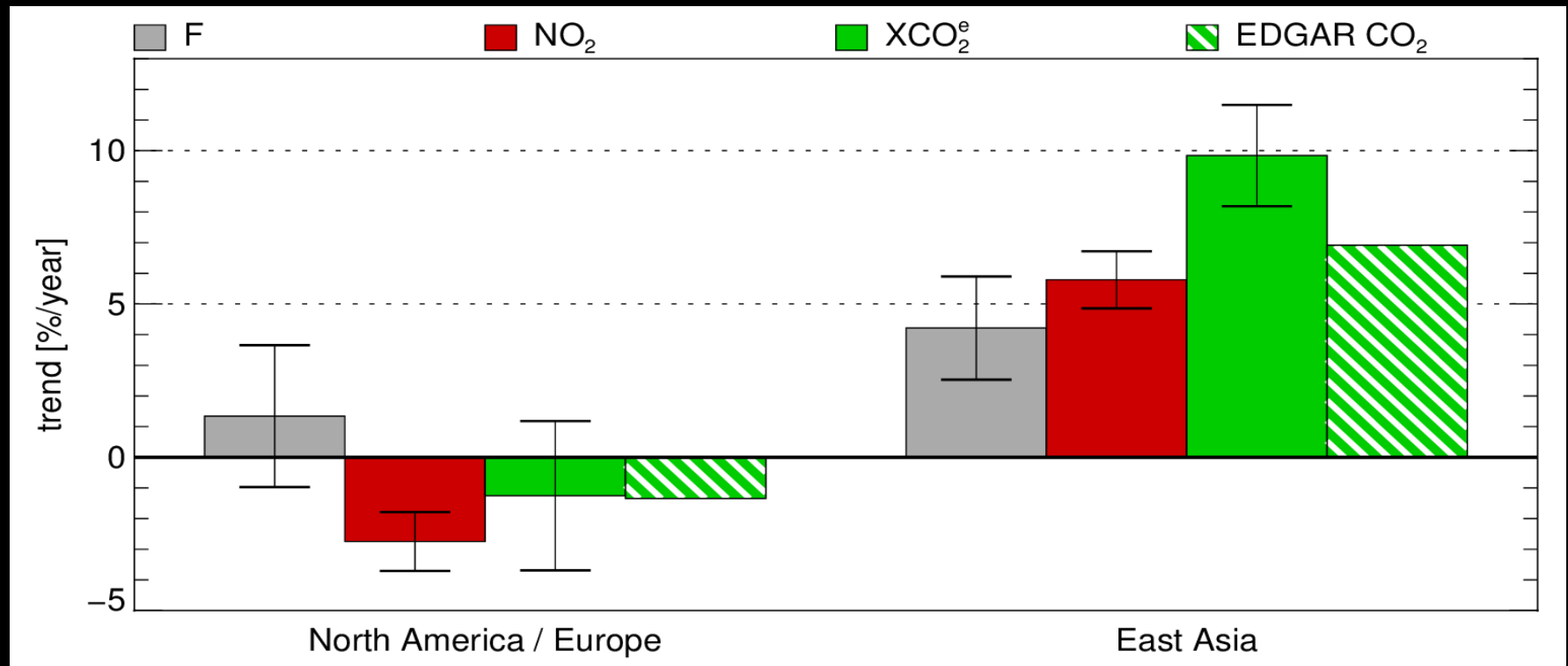


Anthropogenic CO₂ and NO_x emissions (Reuter et al., 2014, nat. geosci.)



- We find significantly **lower ΔXCO_2 levels at weekends** in North America and Europe but not in East Asia.
- The weekend effect of XCO₂ is a tiny signal and this is its **first detection from space**.
- It underlines that the analyzed CO₂ signals originate from **anthropogenic activities**.

Anthropogenic CO₂ and NO_x emissions (Reuter et al., 2014, nat. geosci.)

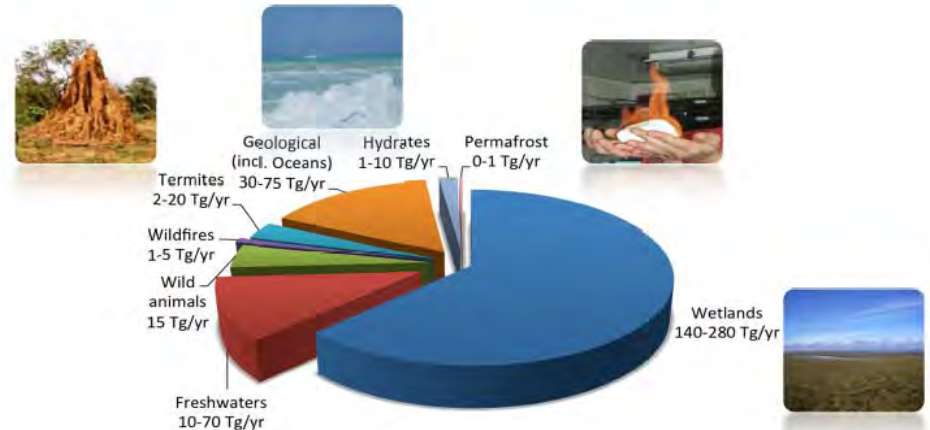


- **North America and Europe:** satellite data show a small **downward trend in emissions** of both, NO_x and CO₂ albeit associated with a large uncertainty.
- **East Asia:** CO₂ emissions increased on average at a rate of 9.8%/a but NO_x increased “only” by 5.8%/a, i.e., significantly less compared to CO₂ (**increasing CO₂-to-NO_x emission ratio F**).
- **Interpretation: technology** used in East Asia is **getting cleaner** thus emitting less toxic nitrogen gases per amount of fossil fuel burned.

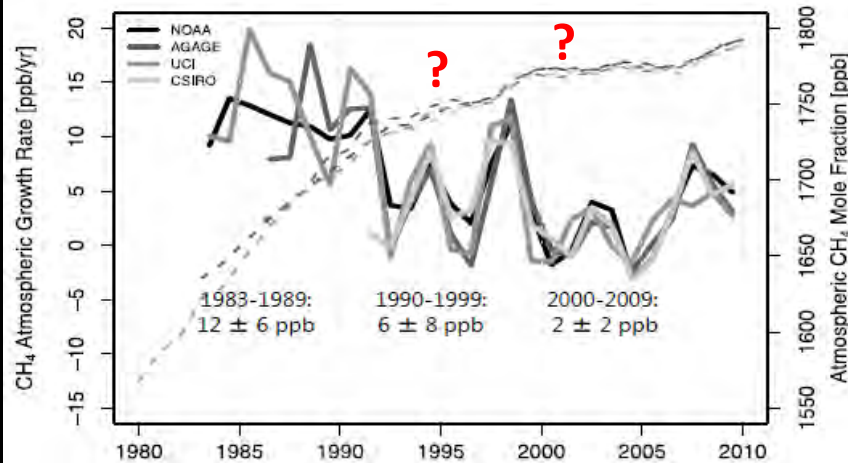
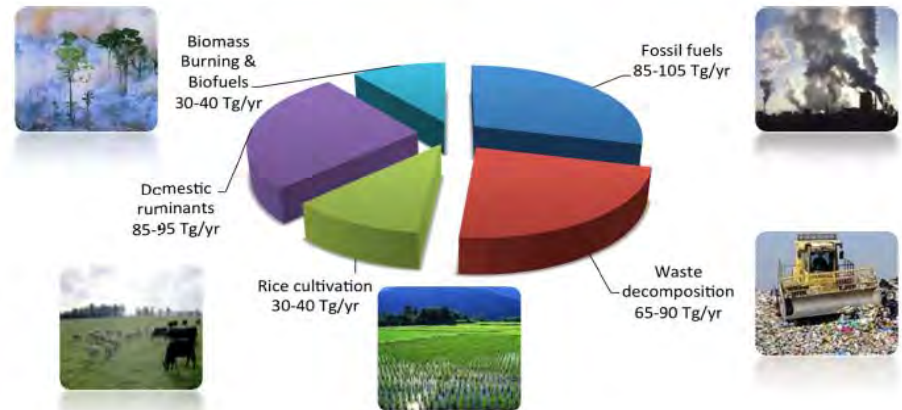
Methane

- Second most important anthropogenic GHG (directly after CO₂)
- Important precursor of O₃ in global tropospheric Chemistry
- Many anthropogenic and natural sources; large uncertainties

Natural Methane Sources (2000s)



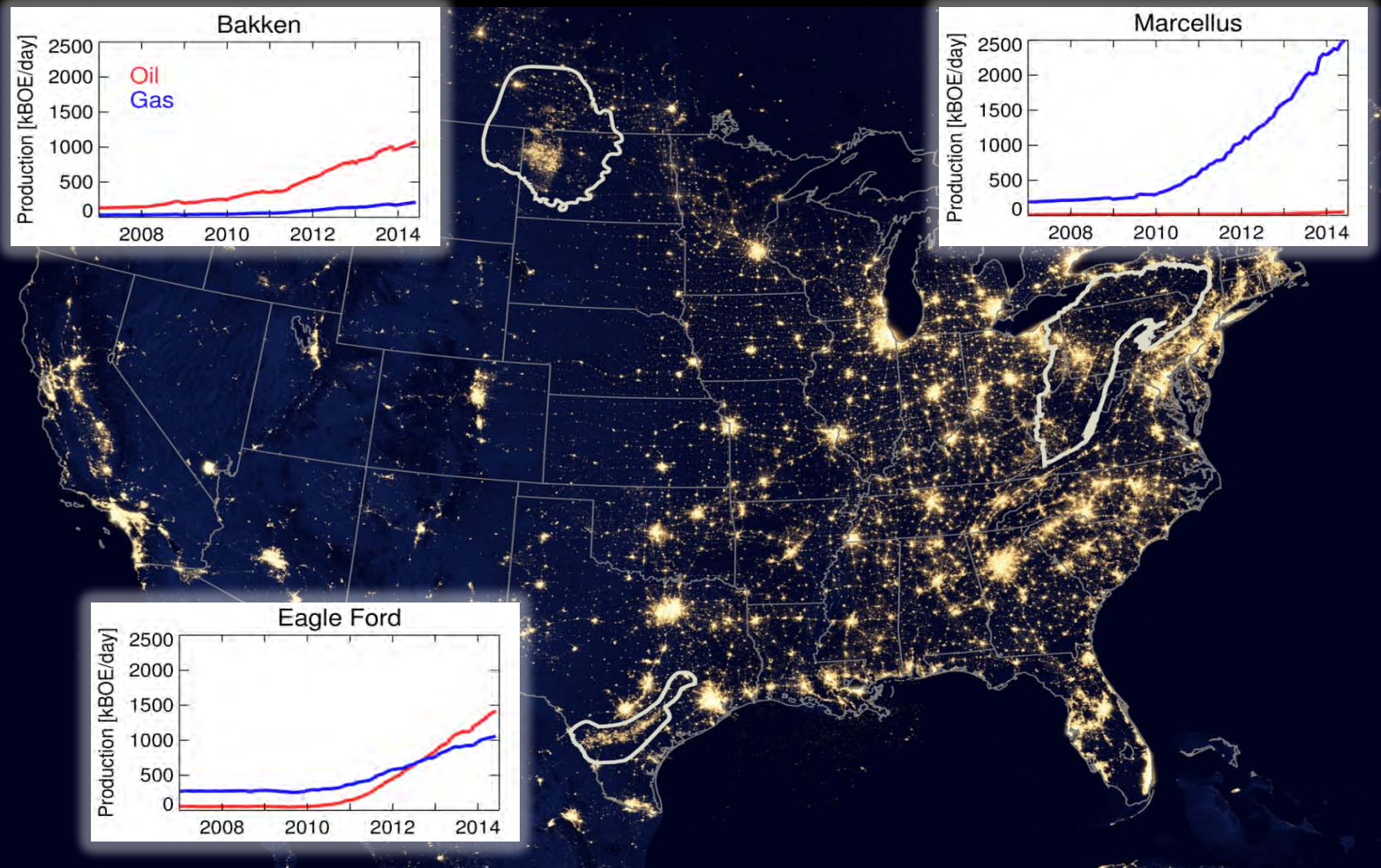
Anthropogenic Methane Sources (2000s)



Kirschke et al.,

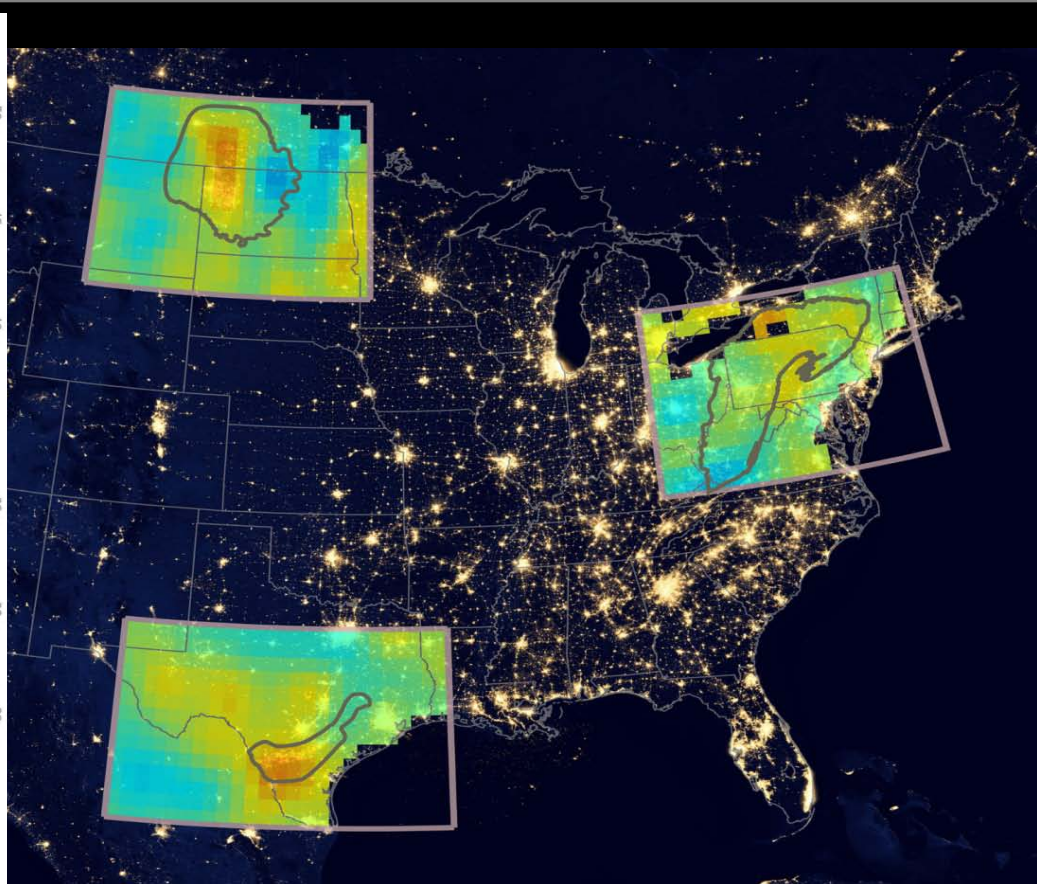
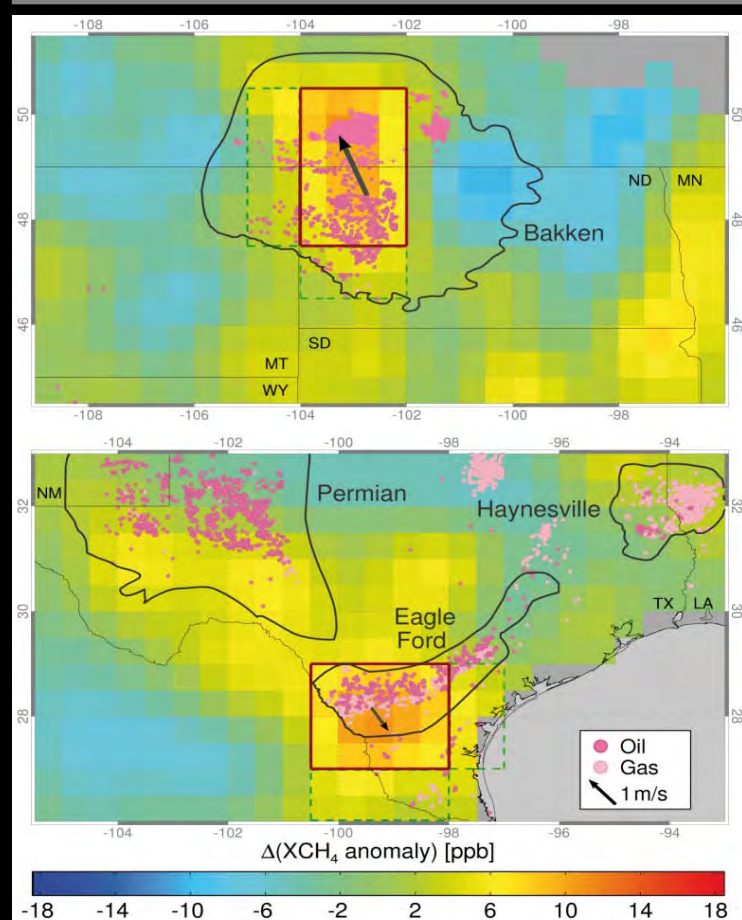


Fugitive methane emissions from oil and gas production (Schneising et al., 2014, Earth's Future)



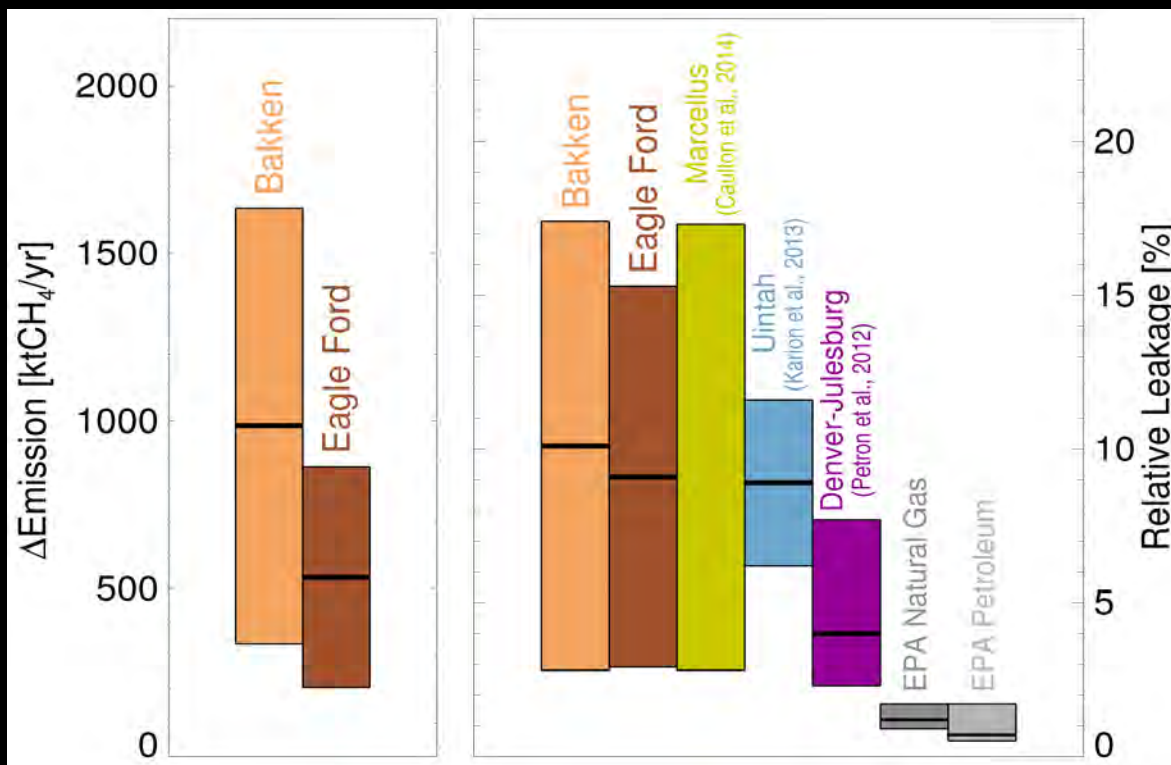
- We analyse **methane enhancements** over the fastest growing production regions in the U.S.
- Flaring in **Bakken** and **Eagle Ford** is so extensive that both regions stand out clearly in satellite measurements of nighttime lights from VIIRS onboard Suomi NPP.

Fugitive methane emissions from oil and gas production (Schneising et al., 2014, Earth's Future)



- To filter out large-scale seasonal variations or global increase, **XCH₄ anomalies** are computed by subtracting regional monthly means from the individual measurements.
- The shown **differences of the anomalies** for the period **2009-2011** relative to the period **2006-2008** highlight the changes in atmospheric methane abundance.
- Anomaly differences exhibit **increases aligning with the analysed oil and gas fields.**

Fugitive methane emissions from oil and gas production (Schneising et al., 2014, Earth's Future)



Bakken

Emission Increase:

990 ± 650 ktCH₄/yr

Leakage rate:

10.1 ± 7.3 %

Eagle Ford

Emission Increase:

530 ± 330 ktCH₄/yr

Leakage rate:

9.1 ± 6.2 %

- The **emission increase** is quantified by a mass-balance approach using the net enhancement relative to the background upwind of the prevailing wind direction and average horizontal boundary layer wind speed.
- The **leakage rate** is defined as the ratio of the emission increase between 2006-2008 and 2009-2011 divided by the production growth between these two periods.
- **Results:** Current inventories likely underestimate fugitive emissions from Bakken and Eagle Ford. Climate benefit of transition to unconventional oil and gas is questionable.

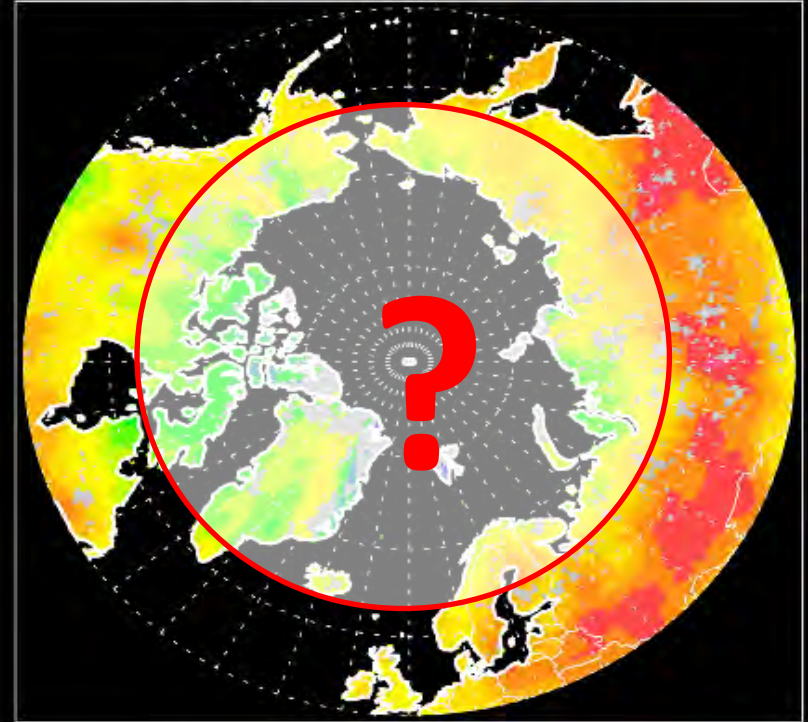
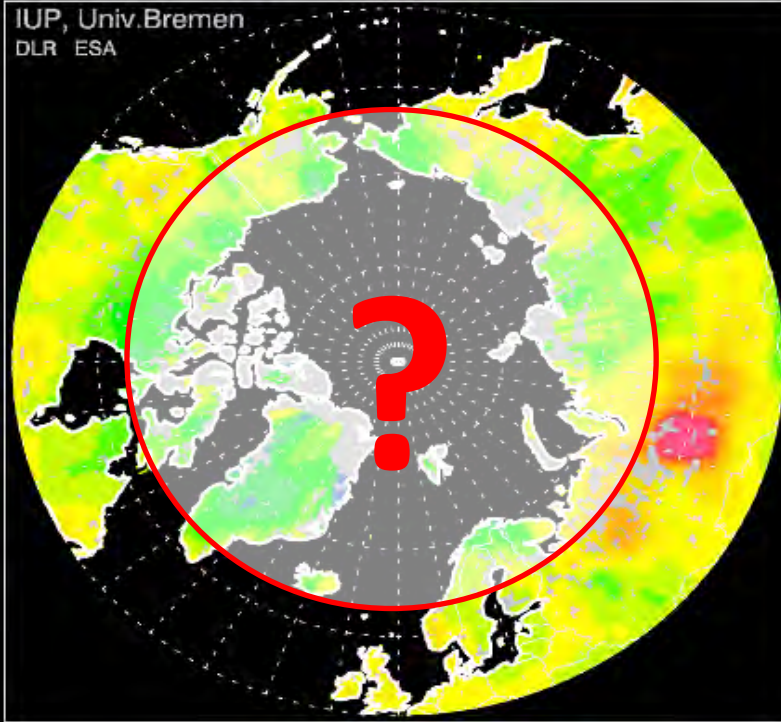
CarbonSat: Methane @ high latitudes

Methane SCIAMACHY/Envisat Northern Hemisphere

April-June 2003

July-September 2003

IUP, Univ. Bremen
DLR ESA



Number of methane molecules per billion air molecules



Highlights GHG

CarbonSat sun-glint mode allows observation of methane in vulnerable high latitude regions including Arctic sea and shelf areas



The MAMAP instrument

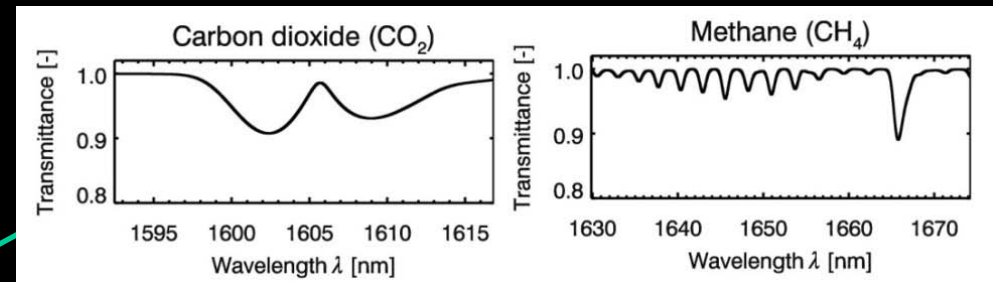


→ Methane and carbon dioxide Airborne Mapper

a passive remote sensing instrument using absorption NIR and SWIR spectroscopy

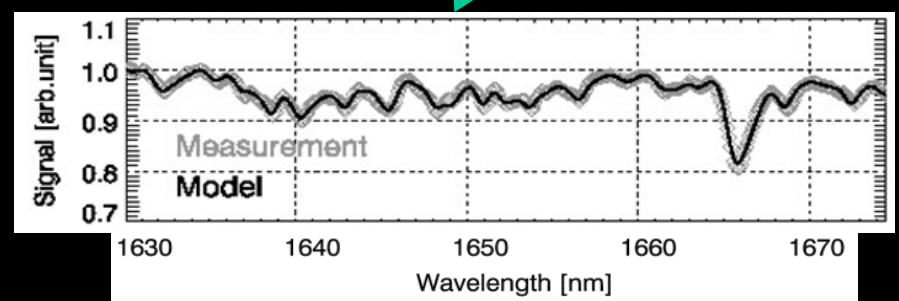
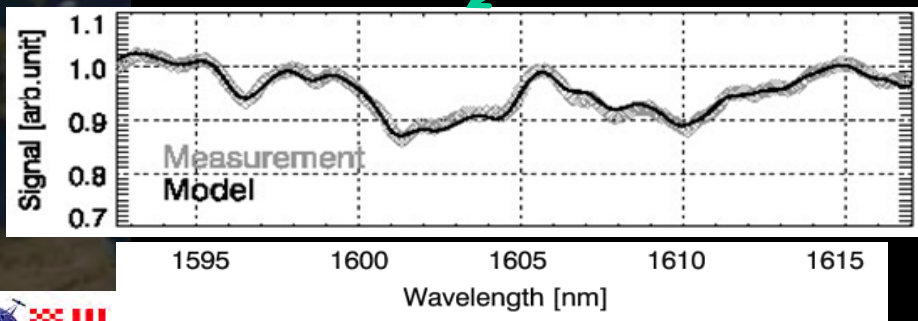


- SWIR channel
- spectral range : around 1590 nm to 1680nm
- spectral resolution: 0.9 nm



Real measurements / measured spectra

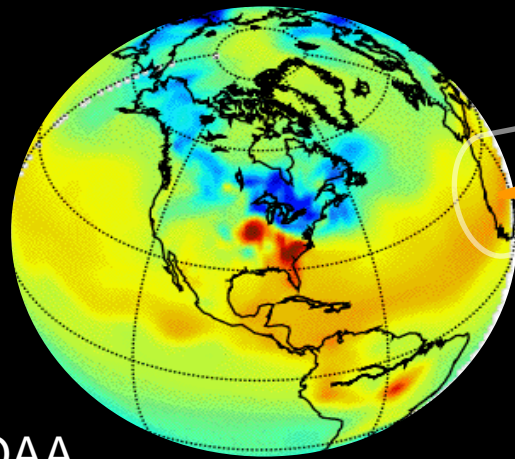
GHG



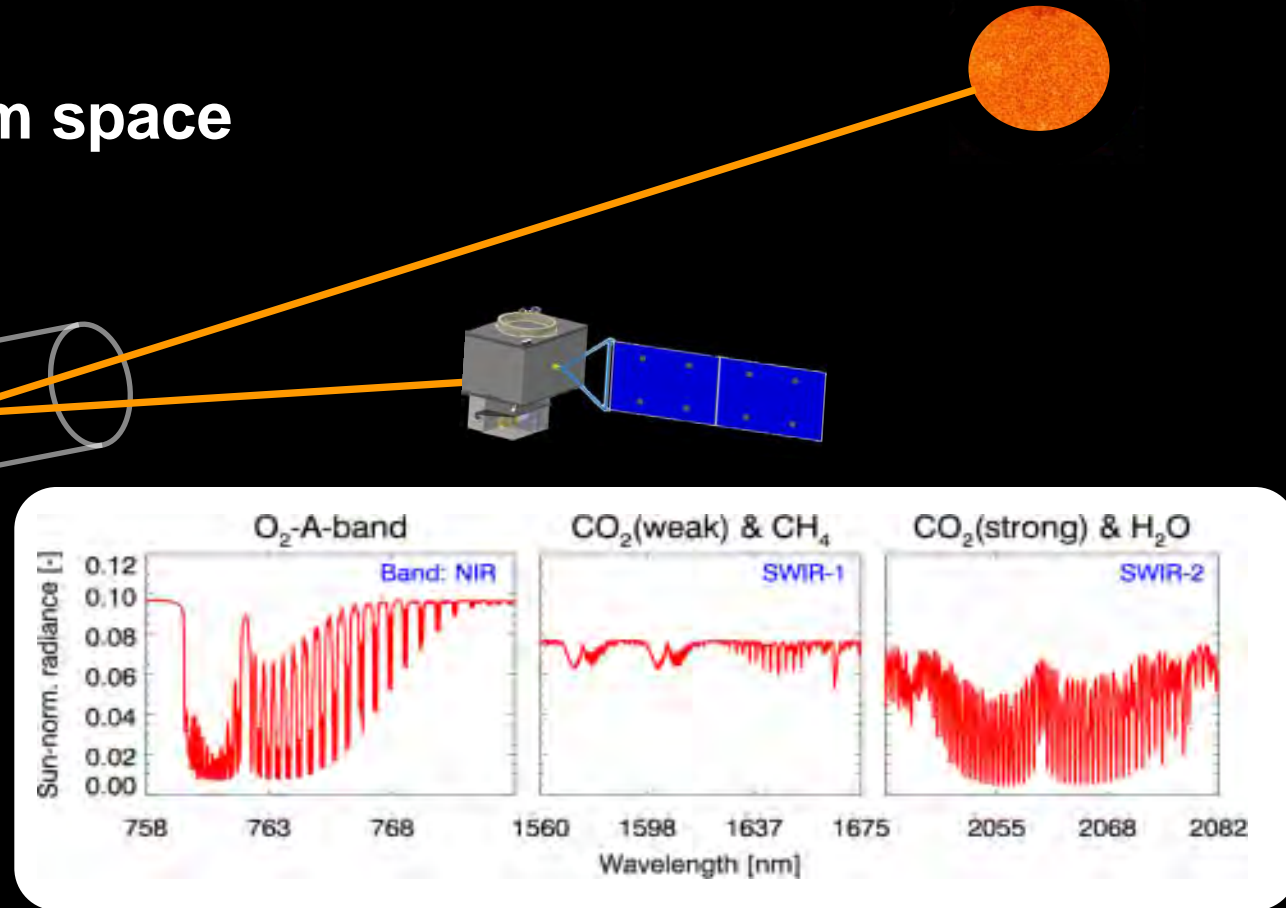
CarbonSat – ESA EE8 Candidate

CarbonSat

Global CO₂ and CH₄ from space

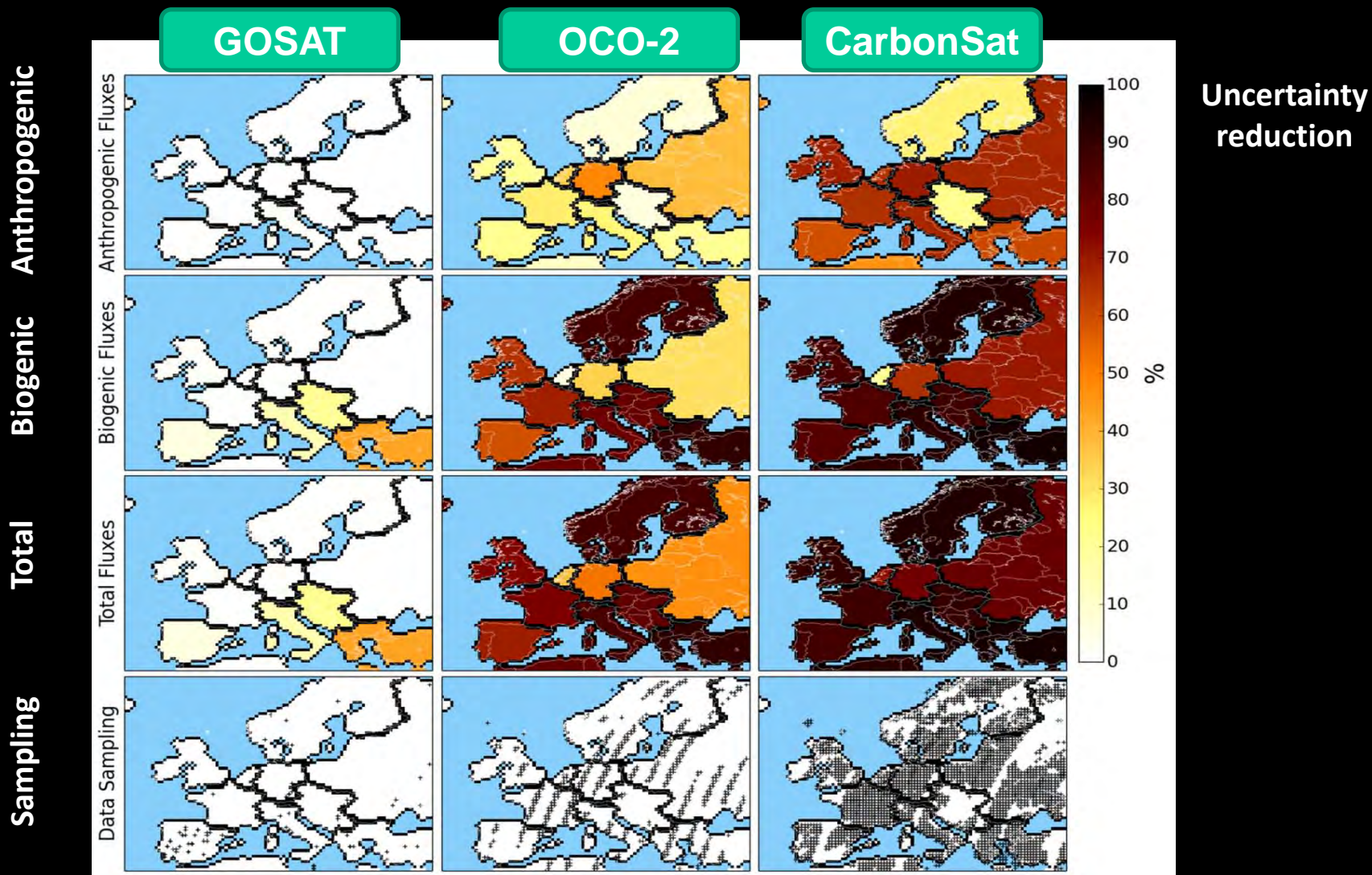


NOAA
CarbonTracker



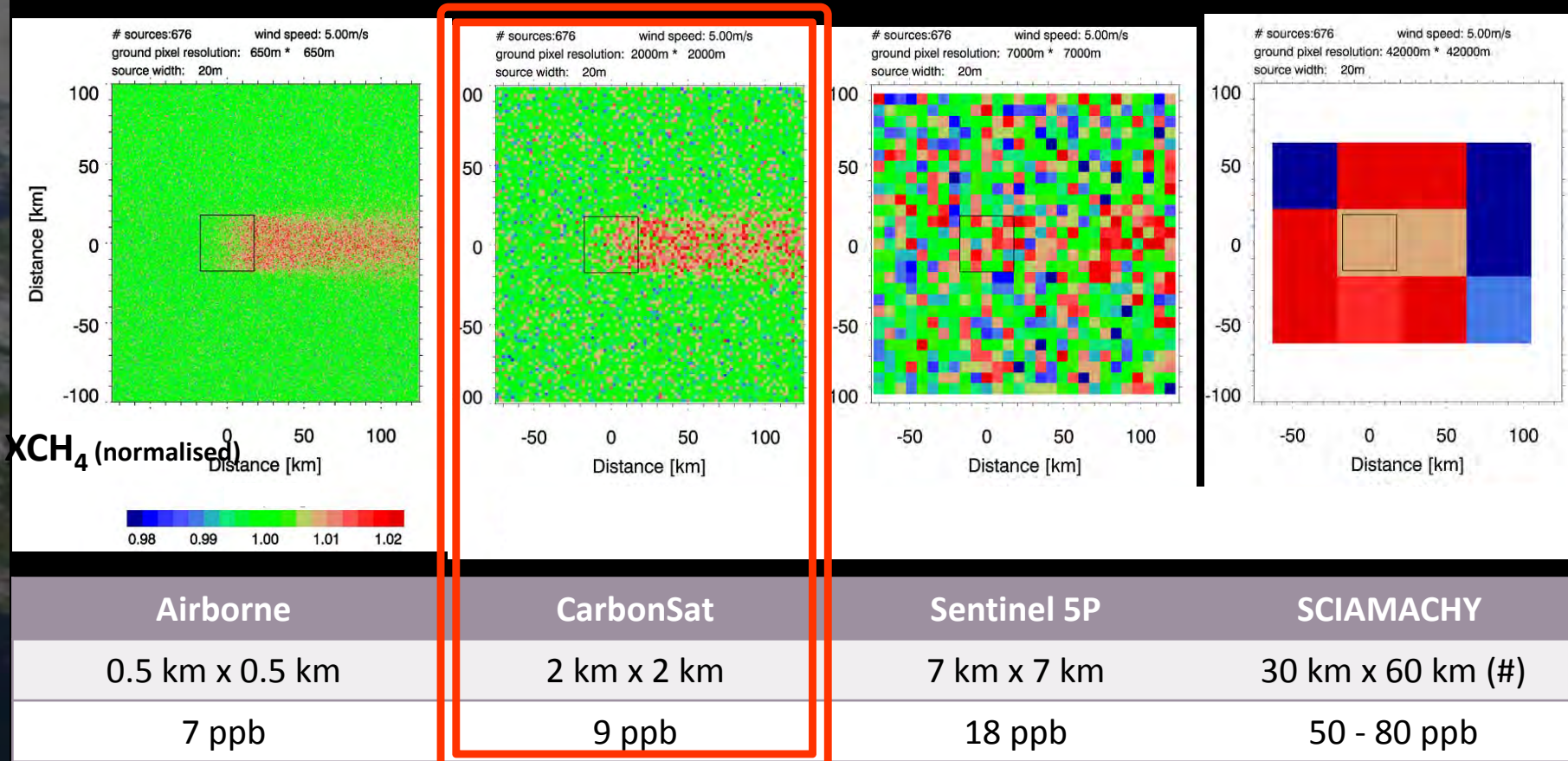
CarbonSat's unique contribution at national scales

Highlights GHG

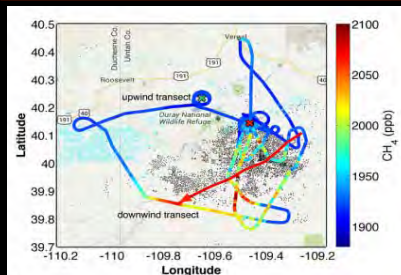


Methane Leackage from Gas Production

Simulation of XCH₄: Emission rate of = 482 ktCH₄/yr on an area of ca. 35 km x 35 km (*), 5 m/s wind speed, instrument resolution and single measurement precision as below:



(*) Similar as gas fields in Uintah county, Utah, USA (Karion et al., GRL, 2013)

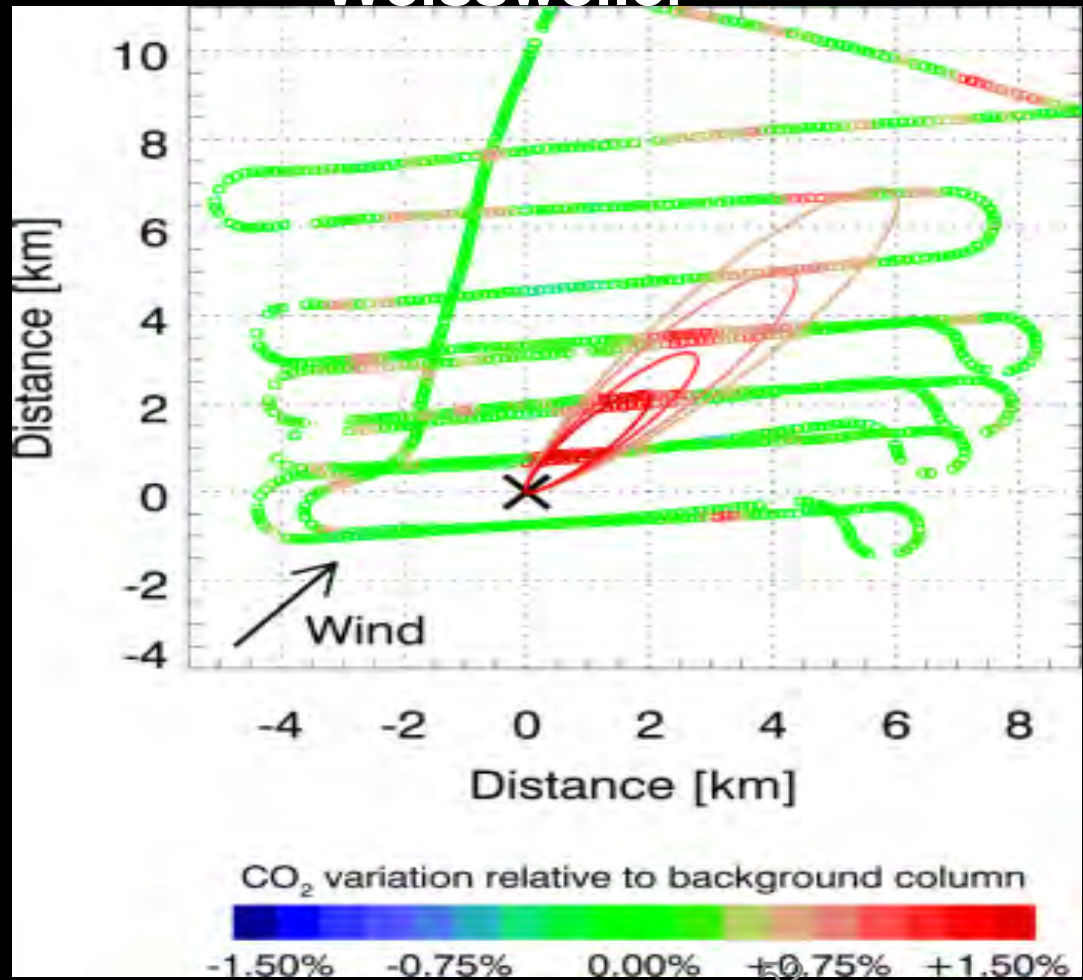
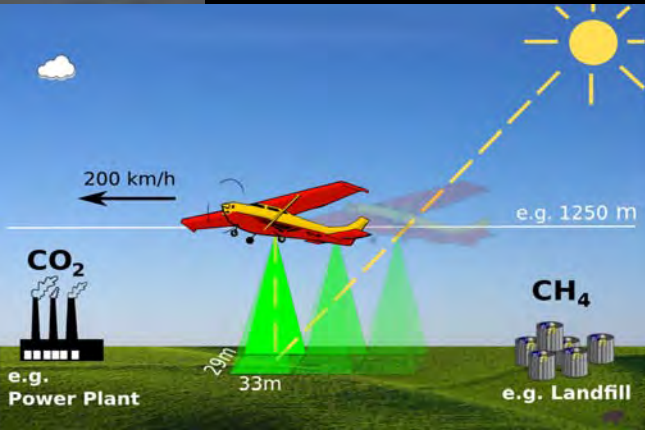


Bovensmann et al., ESA Living Planet Symposium, Edinburgh, 2013 based on Krings et al.

C-MAPExp Campaign Results: Power Plant CO₂

MAMAP Airborne remote sensing and in-situ observations on 18.8.2012:

Lignite Coal fired power plant Weissweiler

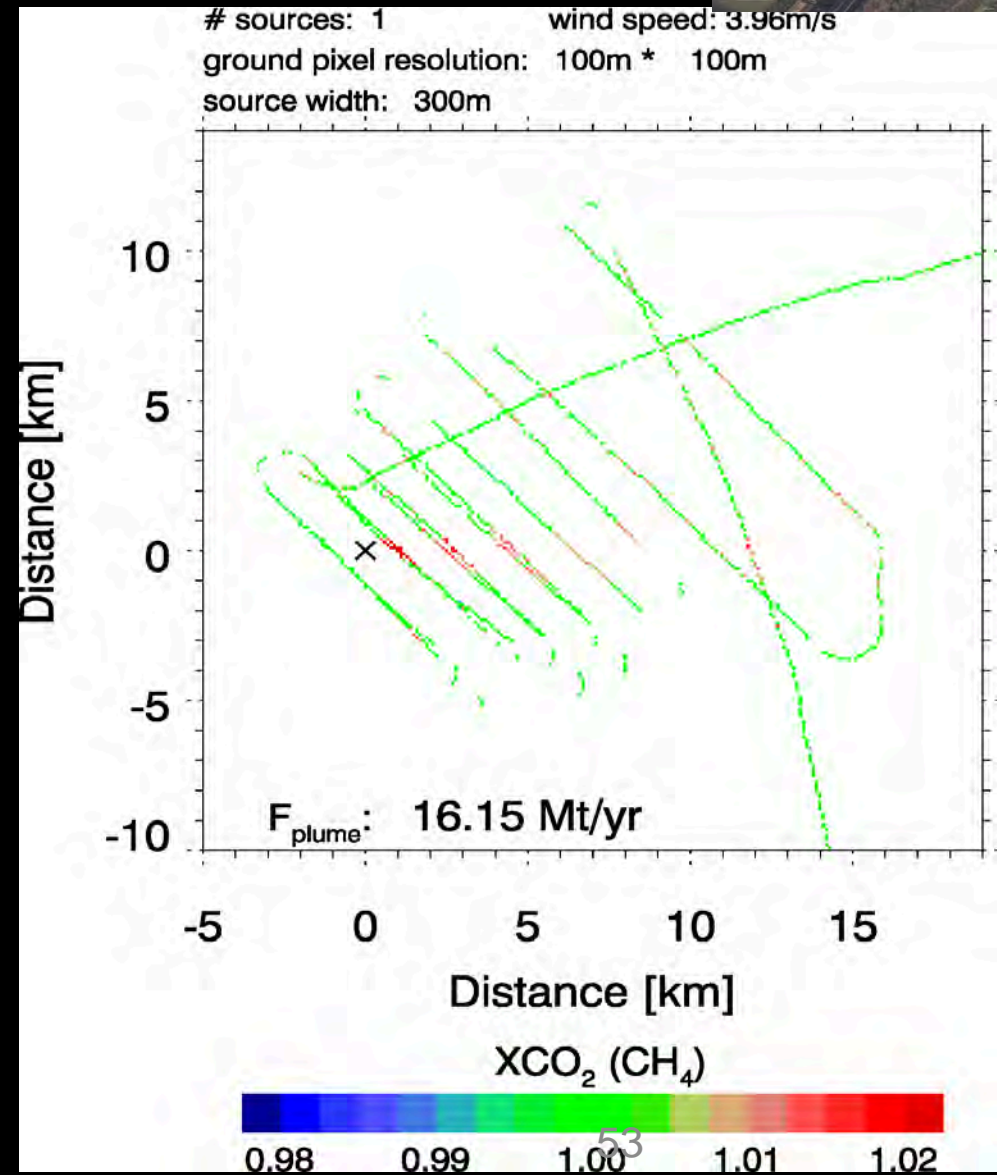


CO₂ emitting Power Plant Weissweiler



MAMAP aircraft observations:

- Remote sensing data at MAMAP resolution (approx. 100m x 100m) including plume inversion result
- Filtered for instrument inclination angle $\leq 10^\circ$
- Derived emission: 16.15 MtCO₂/yr at the time of measurements
- But what would be detected from space?



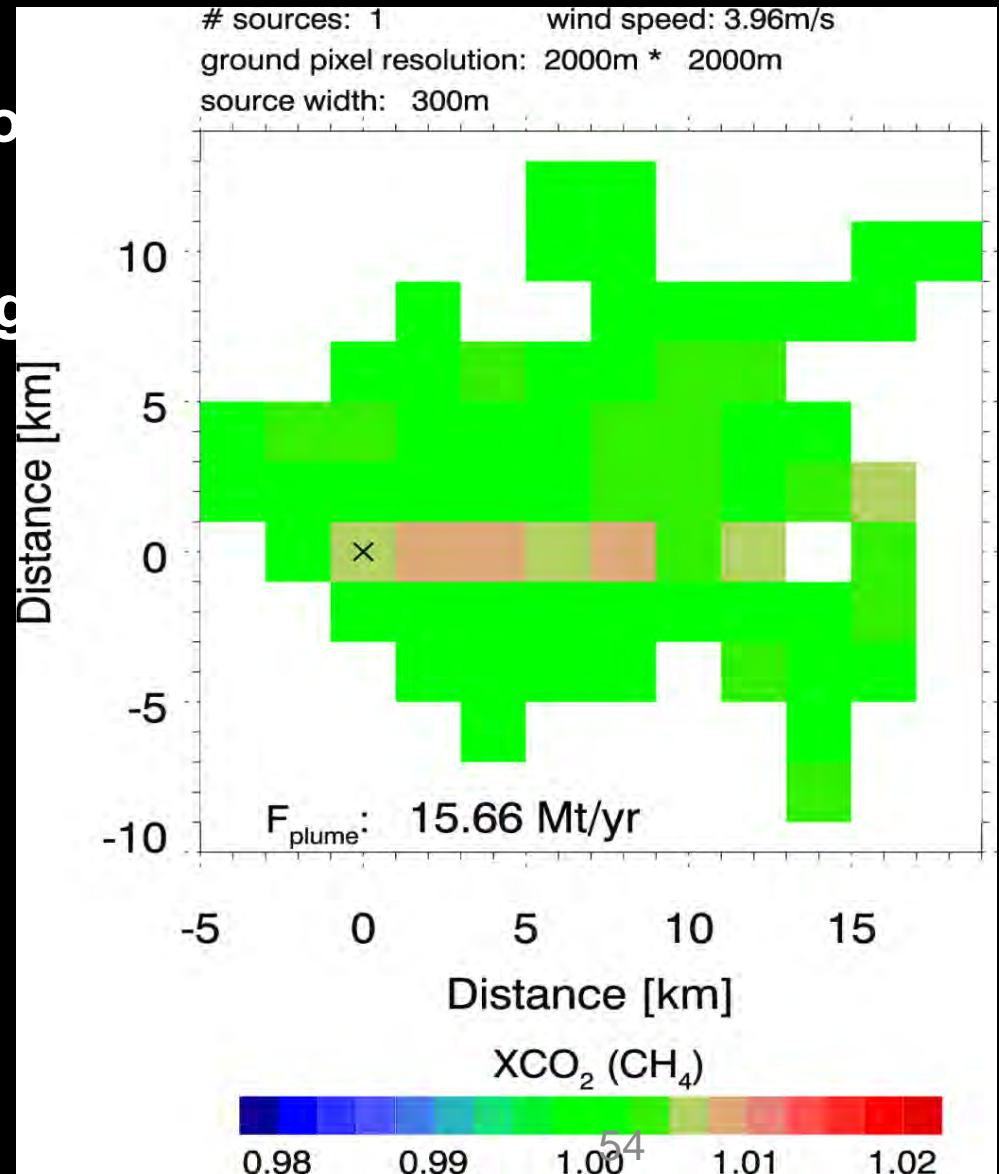
CO₂ emitting Power Plant Weissweiler



What CarbonSat will yield:

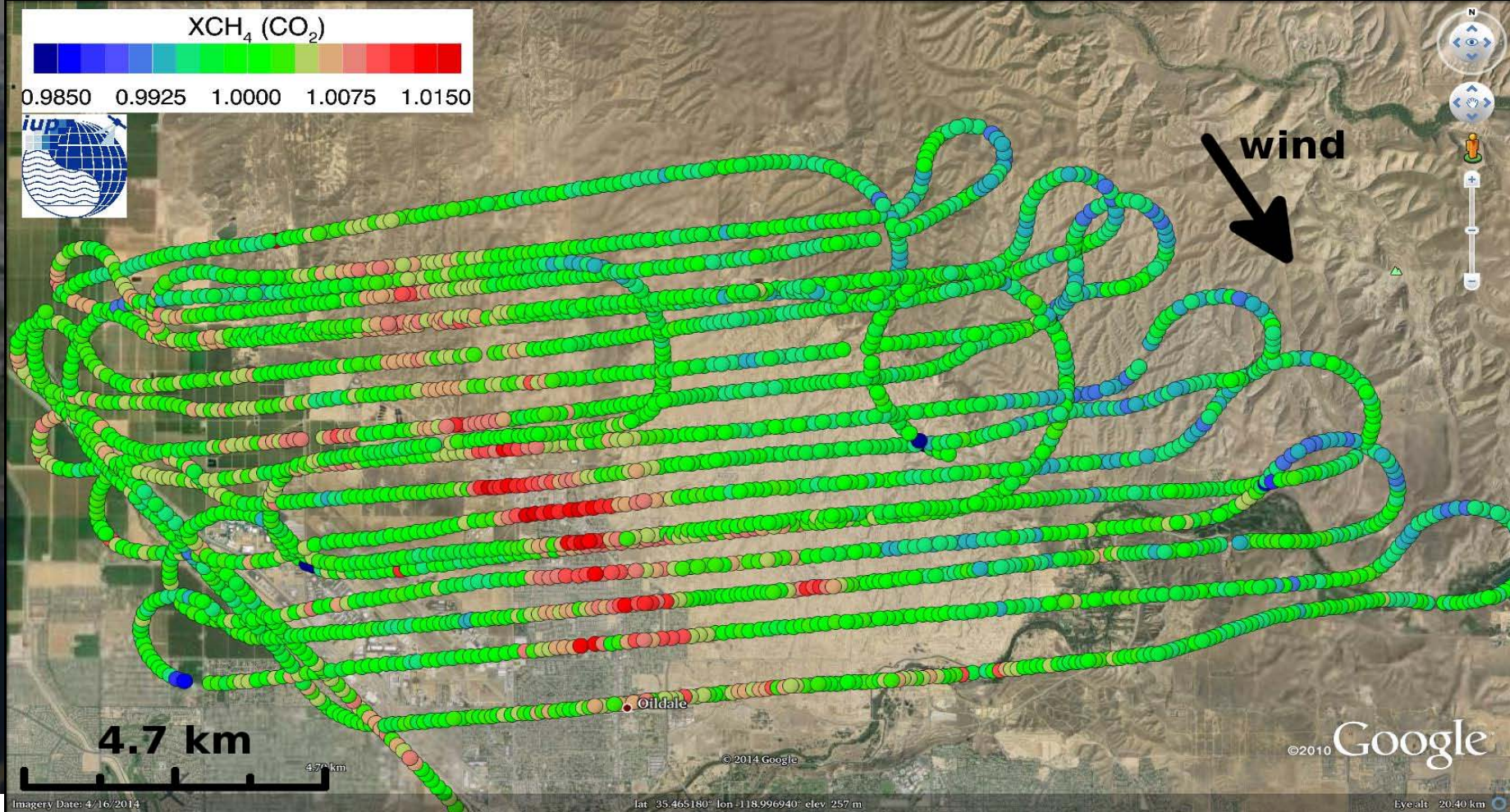
MAMAP data „converted“ to CarbonSat observations:

- Recorded remote sensing data gridded to spatial resolution of approx. 2 km x 2 km
- Including plume inversion result
- Derived emission: 15.7 MtCO₂/yr at the time of measurements



COMEX Campaign (USA) Results: Oil Field CH₄

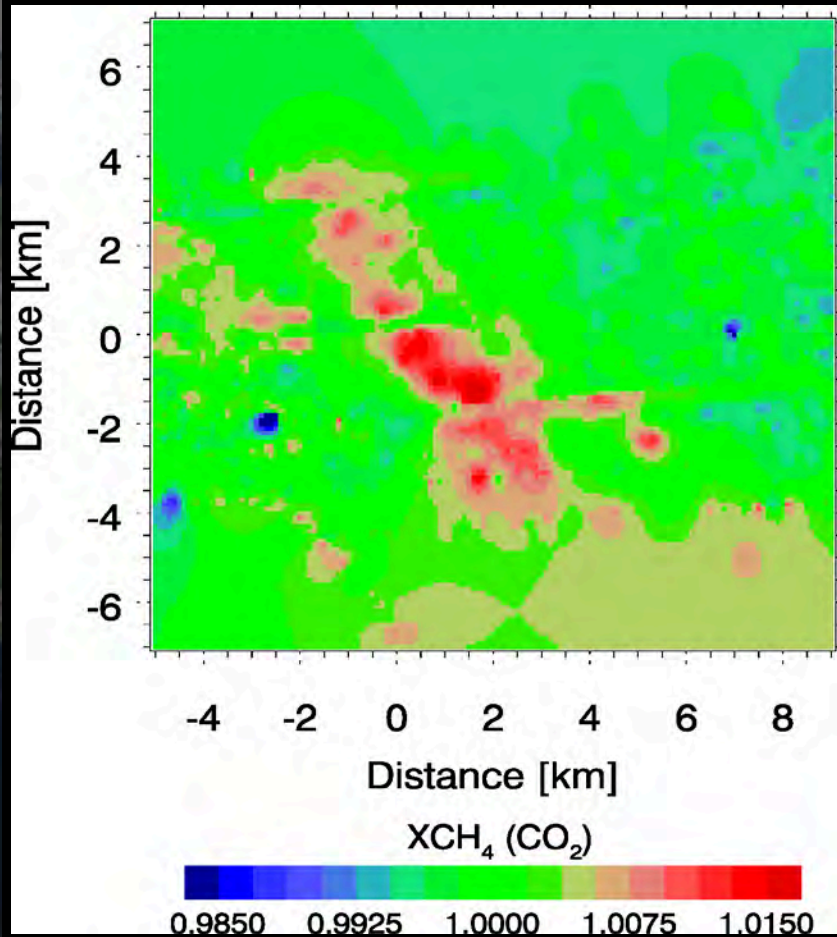
Airborne remote sensing data (MAMAP) from California, August/Sept. 2014



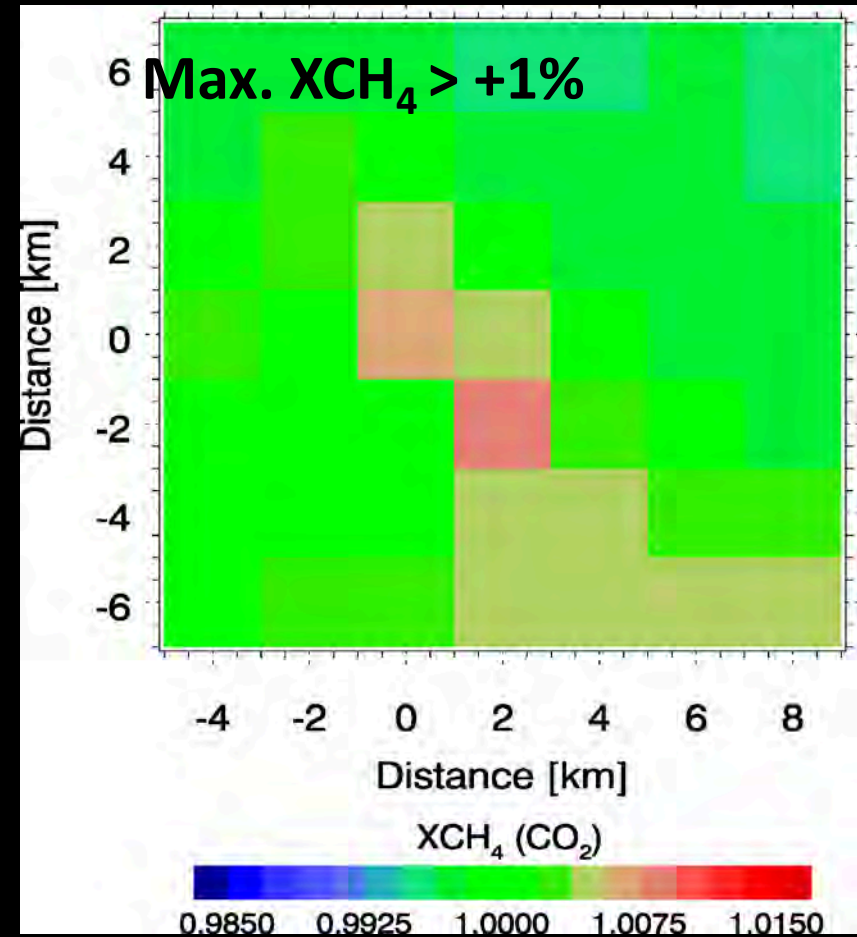
Highlights GHG

California Oil Field CH₄

MAMAP interpolated:



What CarbonSat will see at 2x2 km² resolution:



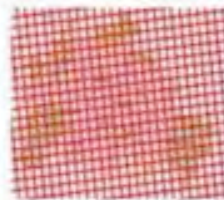
CarbonSat Constellation

Heritage from *SCIAMACHY*
60 x 30 km² Resolution

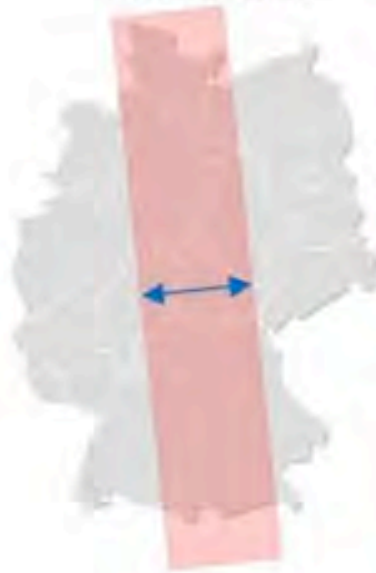


CarbonSat

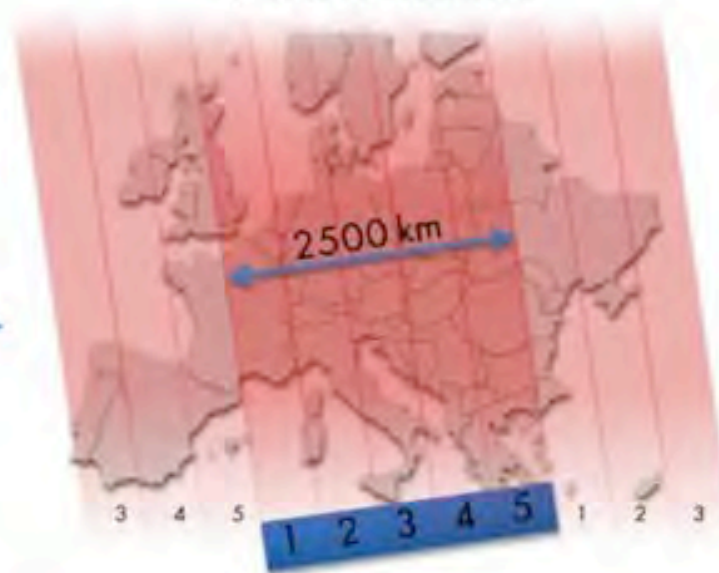
2 x 2 km² Resolution



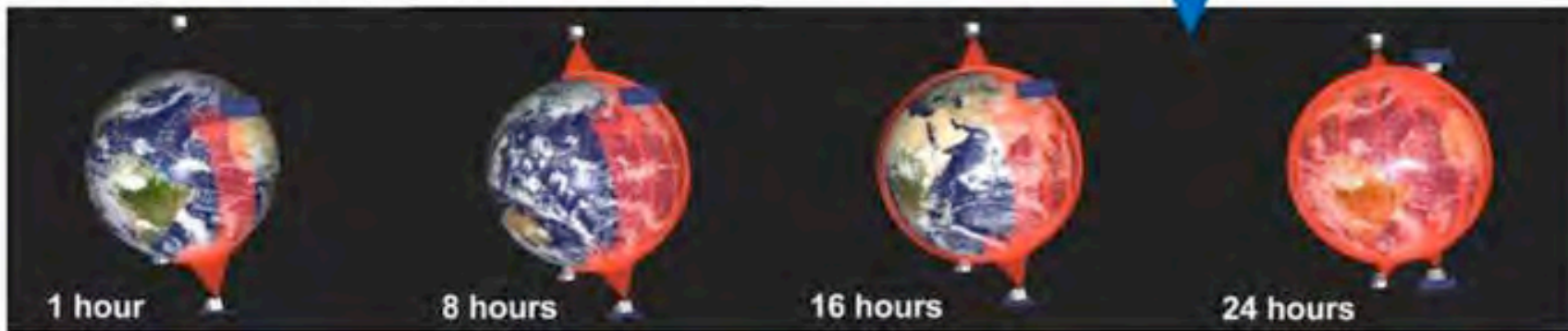
>500 km swath per
CarbonSat



Combined coverage of 5 CarbonSat's
in a constellation



Coverage of the entire earth can be achieved within 1 day

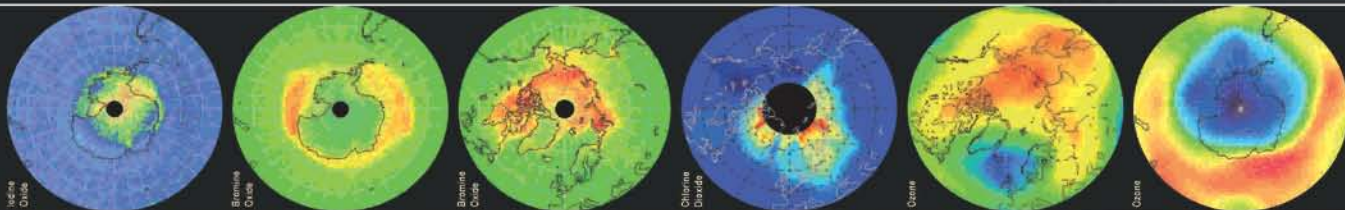
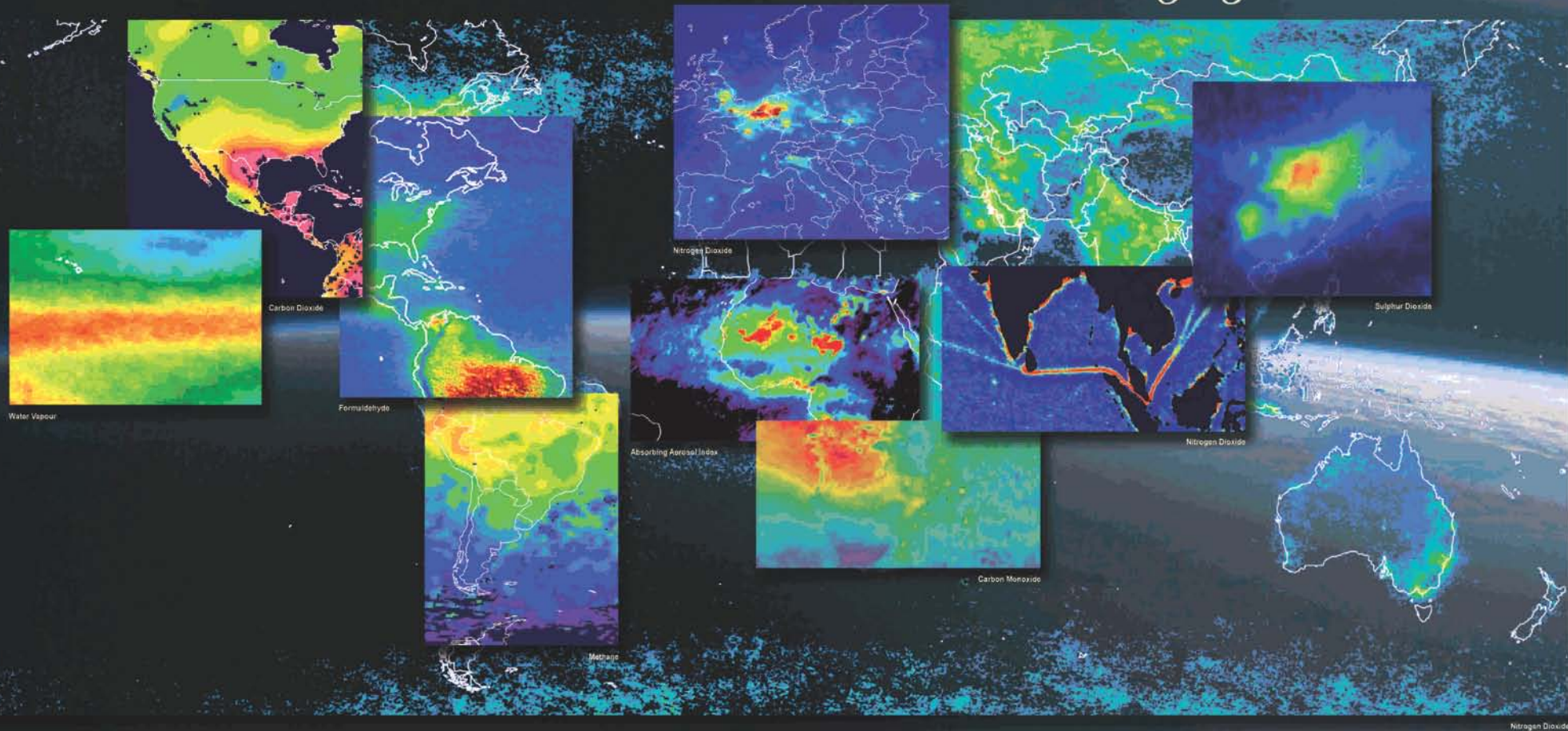


SCIAMACHY



2002-2012

hunting light and shadows



Netherlands
Space
Office



KNMI



esa

SRON
Netherlands Institute for Space Research

